FUNCTIONAL SYNAPTIC PLASTICITY IN THE DENTATE GYRUS OF THE RAT HIPPOCAMPUS

Mark Dickens Baker

A Thesis Submitted for the Degree of PhD
at the
University of St Andrews

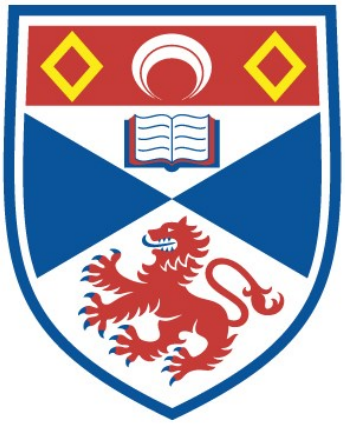

1986

FUNCTIONAL SYNAPTIC PLASTICITY IN THE DENTATE GYRUS OF THE RAT HIPPOCAMPUS.

Mark Dickens Baker

A thesis submitted in fulfilment of the requirements for the degree of Doctor of Philosophy

ProQuest LLC.
789 East Eisenhower Parkway
P.O. Box 1346
Ann Arbor, MI 48106 – 1346

I Mark Dickens Baker hereby certify that this thesis has been composed by myself, that it is a record of my own work, and that it has not been accepted in partial or complete fulfilment of any other degree or professional qualification.

Signed.....
Date..22nd October 1985

I was admitted to the Faculty of Science of the University of St. Andrews under Ordinance General No 12 on 1st October, 1981 and as a candidate for the degree of Ph.D. on 1st. October 1981.

Signed.....
Date...22nd October 1985

I hereby certify that the candidate has fulfilled the conditions of the Resolution and Regulations appropriate to the Degree of Ph.D.

Signature of Supervisor.....
Date..23rd October 1985.....

In submitting this thesis to the University of St Andrews I understand that I am giving permission for it to be made available for use in accordance with the regulations of the University Library for the time being in force, subject to any copyright vested in the work not being affected thereby. I also understand that the title and abstract will be published, and that a copy of the work may be made and supplied to any bona fide library or research worker.

Acknowledgements

I am grateful to Dr Richard Morris for the use of his lab., his encouragement and helpful discussions on experimental design. I thank Mary English for her invaluable help and advice on the histology and I am also grateful to Dr.'s David Perrett, Jim Hagan, Hugh Bostock and Professor Glen Cotrell for their interest, support and helpful critisism. I am indebted to Jim Davies and Professor Tom Sears for the use of the Sobell department word processor.

ABSTRACT

The responses of hippocampal cell fields to stimulation of afferent pathways projecting from outside and within the hippocampus have been shown to exhibit a remarkable degree of plasticity. Subsequent to conditioning stimulation of either single shocks or trains of stimuli at high frequency, the relationship between afferent stimulus and postsynaptic response can be dramatically changed. The long-term potentiation (LTP) of responses generated by stimulus trains does not appear to involve whole-neurone excitability changes, but is the result of altered synaptic effectiveness and can be localized to the region of afferent fibre termination.

In a series of acute experiments extracellular potentials generated by stimulation of the entorhinal projection to the dentate gyrus of the hippocampus in the rat, have been recorded in the dorsal hippocampus and quantified before and after conditioning stimulation. A simple computer model was developed to help explain the observed response plasticity.

Synaptic field potential LTP after afferent tetanization was explained by increased synaptic current flow, and the altered spatial distribution of the potentials by suggesting that the electrotonic properties of the granule cell dendrites are changed by repeated synaptic activation: an increase in dendritic membrane resistance being a possible mechanism.

Light-microscopic examination of the entorhinal fibres at the site of stimulation in the angular bundle after staining with solochrome cyanine, revealed heterogeneous myelination; the fibres lying dorsal and lateral to the subiculum being more heavily myelinated than those more ventro-medial. This histological inhomogeneity appeared to be confirmed by conduction velocity measurements, suggesting two functionally different groups of fibres. It has yet to be determined whether these two groups correspond to the lateral and medial perforant paths described by other workers.

TABLE OF CONTENTS

List of Figures

CHAPTER 1

INTRODUCTION

The term 'Long-term potentiation' (LTP) was coined to describe a substantial and enduring increase in the magnitude of extracellular stimulus-evoked field potentials, recorded from the dentate gyrus of the rabbit, after perforant path tetanization (Bliss and Lomo, 1973). The effect has also been called 'enhancement' (McNaughton, 1982), and is thought to be the result of a sustained increase in synaptic efficacy. Since the discovery of LTP there has been speculation as to whether such easily evoked functional plasticity is the neurophysiological basis of memory (eg Lynch and Baudry, 1984), as it appears likely that memory is a property of neural networks containing synapses capable of long-lasting modification. Whether such long-lasting changes are specific to the hippocampus, a brain structure known to be involved in the processes of learning, is unlikely since a similar phenomenon has

been observed in the neocortex (Baranyi and Feher, 1981; Bindman, Lippold and Milne, 1982).

The mechanism or mechanisms underlying the generation of long-term potentiation are only partially determined. A major problem is the inadequately understood transduction of chemical transmission to dendritic depolarization at a central synapse. For instance, it has been shown that single afferent synapses made on spinal motoneurones exhibit a very low variability of post-synaptic epsp magnitude (Jack, Redman and Wong, 1981; Redman and Walmsely, 1983), leading to the hypothesis that the contents of one synaptic vesicle can activate all available postsynaptic receptors. Some synapses made onto hippocampal neurones apparently behave in a similar way (McNaughton, Barnes and Andersen, 1981) suggesting presynaptic functional plasicity may be essentially a modulation of the probability of terminal activation, rather than the number of vesicles released per synapse. Clearly the resolution of the problem will be important in determining the degree of functional homosynaptic plasticity allowed in transmitter release.

As the experiments of Baranyi and Feher (Baranyi and Feher, 1981) suggest altered postsynaptic electro-

tonic characteristics can play an important role in determining the relationship between the input and output of a cortical nerve cell, it is possible that the electrotonic characteristics of hippocampal cells are changed after tetanic afferent activation. If this occurs in hippocampal granule cells on the induction of LTP, then this should be reflected in the dynamics of the field potentials generated on subsequent synaptic activation. Therefore, in the following series of studies, measurements of the spatial and temporal dynamics of dentate field potentials were made before and after inducing LTP in the perforant path projection to the dentate gyrus, and during paired-pulse stimulation of the perforant path. All experiments were performed in acute preparations, in order to reduce technical and methodological difficulties to a minimum, eg the behavioural state in all animals was the same - ie anaesthetised, and the electrodes could be placed accurately, without the risk of much brain movement after positioning.

CHAPTER 2

REVIEW OF HIPPCAMPAL ANATOMY AND FUNCTION

Historical Perspective

Along with the parahippocampal gyrus and the cingulate gyrus, the hippocampus forms the 'limbic lobe', a term first introduced by Paul Broca to characterize the phylogenetically primitive cortical gyri (archicortex) that ring the brain stem. McLean later renamed them the 'limbic system' (1952), encompassing the limbic lobe and related circuitry (including the amygdala, the septum, the hypothalamus, the epithalamus, the anterior thalamic nuclei and parts of the basal ganglia). In 1937 James Papez had suggested the limbic system formed a neuroanatomical substrate for emotions. Contemporary argument favoured a cortical connection with the hypothalamus, since the hypothalamus played a critical role in the expression of emotion, and emotions had to reach conciousness, thought of as a neocortical endowment. Two years later, Heinrich Kluver and Paul Bucy (Kluver and Bucy, 1939) reported

that bilateral destruction of the temporal lobe in monkeys (including the hippocampus and the amygdala), produced dramatic changes in emotional behaviour, characterized by tameness, hypersexuality and hypermetamorphosis.

Papez suggested that the cortical influence on the hypothalamus was excerted via the cingulate gyrus projecting to the hippocampus and then through the mammillary bodies. The hypothalamus then projected back to the mammillary bodies, from there to the anterior thalamus and thence to the cingulate gyrus. This group of limbic structures formed the 'Papez circuit'. Such a circuit might have the capability of self-reexcitation, as observed in the brains of cuttlefish (Young, 1938), which could have played an important role in the longevity of emotional behaviour, or perhaps in the formation of memories (Hebb, 1949).

On functional neuroanatomical grounds the concept of a limbic system as a self-contained substrate of emotion is completely discredited. Indeed the limbic lobe itself may be little more than a topological accident which contains functionally quite distinct regions. The division of the cortical mantle into neo-

cortex and archecortex may also be artificial, both neocortex and archecortex being represented in even the most primitive living vertebrates (Swanson 1983). Present knowledge suggests that the hippocampus integrates inputs from polymodal and supramodal (ie a cortical region receiving afferents from several polymodal association areas) cortical association areas (Turner, Mishkin and Knapp, 1980; Pandya, Van Hoesen and Mesulam, 1981). It may yet be shown to be the most complex supramodal association area of the brain.

Role of the Hippocampus in Memory

Human evidence

According to Squire (1983) a patient showing brain damage confined to the hippocampal formation has never been documented. The types of human amnesia available for study are therefore not optimal for the elucidation of hippocampal function. The best studied amnesic syndrome, Korsakoff's syndrome, observed in chronic alcoholics (Talland, 1965; Victor, Adams and Collins, 1971; Butters and Cermak, 1980), is caused by diencephalic dysfunction, and Mair and co-workers (Mair, Warrington and Weiskrantz, 1979) suggest the pathology may be confined to the mammillary bodies and the dorsal thalamus.

The best known amnesic is H.M., who underwent bilateral temporal lobectomy in 1953. This included the removal of the anterior two thirds of his hippocampi, during the treatment of intractable temporal lobe epilepsy (described by Scoville and Milner, 1957; Milner, 1966; Milner, 1972). H.M. shows a severely impaired memory for events which occured after the operation (anterograde amnesia), whereas his memory for

pre-operation events is normal (review: Squire, 1983). This suggests that the medial temporal region of the brain, including the hippocampus is not the site of memory storage, but presumably participates in the formation and development of memory. The observation that medial temporal dysfunction in H.M., and when induced by electro-convulsive treatment, reveals itself in rapid forgetting (as opposed to normal forgetting in Korsakoff's syndrome), is consistent with the hypothesis of hippocampal involvement in memory consolidation (Squire, 1982).

Scalp P300

This characterizable human scalp potential, with a post-stimulus maximum amplitude at around 300 msec, has been most widely studied during the 'auditory oddball' task. The subject silently counts high frequency auditory tones, which are presented serially with low frequency tones. The size of the P300 elicited is directly related to how infrequent the high tones are in the sequence. A close correspondence exists between the scalp potential and the potentials recorded within the hippocampus in patients undergoing surgical treatment for epilepsy (Halgren, Squires, Wilson, Rohrbaugh, Babb and Crandall, 1980; Halgren, Wilson, Squires,

Engel, Walter and Crandall, 1983; McCarthy, 1984). P300 probably begins after completion of perceptual recognition and categorization, and is only produced if the evoking stimulus is salient to the task.

Neurophysiological and behavioural evidence from animal experiments

Important evidence, using the techniques of electrophysiological recording and brain lesioning in animals, has been collected suggesting the involvement of the hippocampus in a variety of learning and memory functions. The investigation of learned behavioural correlates of hippocampal neural activity has been undertaken in two ways: a) the model system approach of neuronal function, and b) the analysis of perceptual and motor correlates of neuronal function.

a) The model system approach of neuronal function involves the use of predetermined conditioning paradigms, eg classical conditioning of the rabbit nictitating membrane and eyelid response to an acoustic conditioned stimulus, using a corneal air-puff as the unconditioned stimulus (Thompson, Berger, Cegavske, Patterson, Roemer, Teyler and Young, 1976).

Alternatively intrahippocampal neural activity might be recorded during operant learning (Deadwyler, West and Lynch, 1979; Rose, 1983). The model system approach runs the risk that the hippocampus is not involved in the chosen learning paradigm, and even if it is involved (see below), its involvement may be functionally redundant.

b) The analysis of perceptual and motor correlates of neuronal function is the quantification of environmental stimuli and behavioural repertoire coincident with the spontaneous activity of nerve cells (eg Rank, 1973; O'Keefe, 1976; review: O'Keefe and Nadel, 1978). The assumption is made that the perceptual and motor correlates of hippocampal activity are directly related to its memory function.

The model system approach has revealed a correlation between the rate of discharge of cells in all the hippocampal subfields and the degree of task acquisition in classical conditioning paradigms. Recently however, Thompson and his associates have shown that eyelid conditioning in the rabbit is critically dependent on the functioning of the ipsilateral cerebellum (review, Thompson, 1983), and in particular on the

integrity of the medial dentate/lateral-interpositus nuclear region. Berger and Thompson (1978a, 1978b) found that pyramidal neurons in CA3-CA1 (ie both the superior and inferior pyramidal cells) of the dorsal hippocampus show altered activity in clear correlation with learning; but the animal can still learn the conditioned response following ablation of all brain tissue above the level of the thalamus. Yet Berger (1984), has demonstrated that the hippocampus is involved in discriminative learning between two auditory tones as the rate of behavioural learning is significantly faster in animals after induction of LTP in the entorhinal-dentate projection.

Using the perceptual and motor correlates approach O'Keefe (O'Keefe, 1976), recording from the CA1 field of the hippocampus in freely moving rats habituated to a maze 'rich in spatial information', classified unit activity within the maze into the following 3 categories:

i) Place units. These were units which fired preferentially when the rat was located in a particular place in the maze.They had low (< 1 sec^{-1}) spontaneous firing rates, and high rates (around 12 sec^{-1}) when the

animal moved into the relevant area. Place units occasionally fired complex spikes (described by Ranck, 1973). Most place units had only one 'field' in the environment in which they activated, but a few had 2 or more.

ii) Displace units. These were defined as those units whose activity was related to the rat's motor behaviour regardless of the animal's position in the maze, and which fired in phase with hippocampal theta (identical to the theta units reported by Ranck, 1973). Rhythmic slow activity (RSA-theta), occurs during voluntary movement (Vanderwolf, 1969); O'Keefe emphasizing unit discharge during spatial displacement. Displace units did not show complex spiking.

iii) Misplace units. Misplace units were complex spike cells which fired when an animal sniffed in a place, either because it found something new, or failed to find something which was usually there.

(NB The complex spike cells are probably pyramidal cells (Fox and Ranck, 1975), and the theta cells inhibitory interneurones (Schwarzkroin and Andersen, 1978)

giving rise to synchronous, phasic, IPSP's in pyramidal cells and dentate granule cells.)

O'Keefe proposed that the hippocampus was involved in the formation of a central representation of the environment, the 'map' being constructed during exploration. Later work has revealed that a place cell can fire 'in register' with a suspected reward site in a four arm maze. This occurs in the absence of previously available distributed environmental cues, ie the animal is relying on 'spatial' memory only. For example a place cell may always fire in the arm 90° to the left of the arm suspected of containing food (O'Keefe, 1983), suggesting that the hippocampal 'map' is being rotated to match the environment.

Whishaw and Vanderwolf (1973) reported increases in RSA-theta in the hippocampus when a rat initiates movement. Morris and Hagan (1983), have shown that the wave-period length immediately before and after jumping is inversely related to the height of the jump, and the wave-period immediately after the initiation of the jump is directly related to the weight carried by the rat. It is therefore possible that the hippocampus is involved in motor programming , and is attempting, in

this situation, to update the central representation of the animal's spatial position.

Brain lesioning

Lesioning the hippocampus and adjoining structures suggests mediotemporal involvement in learning. Monkeys are less able to remember stimulus-reward associations after amygdalo-hippocampal and selective hippocampal resection (Mahut, Moss and Zola-Morgan, 1981; Mahut, Zola-Morgan and Moss, 1982). Similarly rats show impaired performances in radial and water maze tasks after hippocampal, fimbria-fornix and entorhinal lesions (Morris, Garrard and Woodhouse, 1980; Handelman and Olton, 1981; Morris, Garrard, Rawlins and O'Keefe, 1982; Olton, 1983).

Does spatial learning involve a special class of hippocampal operations? Or does the hippocampus provide some more general type of sensory information manipulation which happens to be required during spatial problem solving? These questions presently remain unanswered, but the latter is probably true. This is because an animal with a bilaterally lesioned hippocampus still manages to perform a spatial maze, and the hippocampus is involved in other 'types' of learning (eg Berger, 1984).

A Summary of Hippocampal Anatomy with Special Reference to the Dentate, in the Rat

The hippocampal formation is an infolding of cortical mantle, an S-shaped structure lying medial to the temporal cortex, the dorsal hippocampus lying directly below the corpus callosum. The dorso-medial end abuts on the contralateral formation and is connected to the septal area by the fimbria-fornix. The ventro-lateral end approaches the amygdala. The structure has been widely studied by anatomists for many years (eg Edinger, 1908; Lorente de No, 1934).

The hippocampal formation is divided into 4 major anatomical regions; the entorhinal area, the subicular complex, Ammon's horn and the dentate gyrus, their internal topographical relationships being most easily appreciated in 'unfolded' maps of the formation (Swanson and Cowan, 1977; Swanson, Wyss and Cowan, 1978) and similarly their relation to the rest of the cortex (Swanson, 1983). Figure 2-1.

Figure 2-1. The drawing shows the cortical mantle of a rat, including the hippoc ampus, unfolded in order to compare the relative sizes and arrangement of the various regions (adapted from Swanson, 1983).

DG. Dentate gyrus.

RI. Regio inferior of Ammons horn, ie CA4 and CA3.

RS. Regio superior of Ammons horn, ie CA1 and CA2.

PRE. Presubiculum.

PA. Parasubiculum.

ENTm. Medial entorhinal area.

ENTl. Lateral entorhinal area.

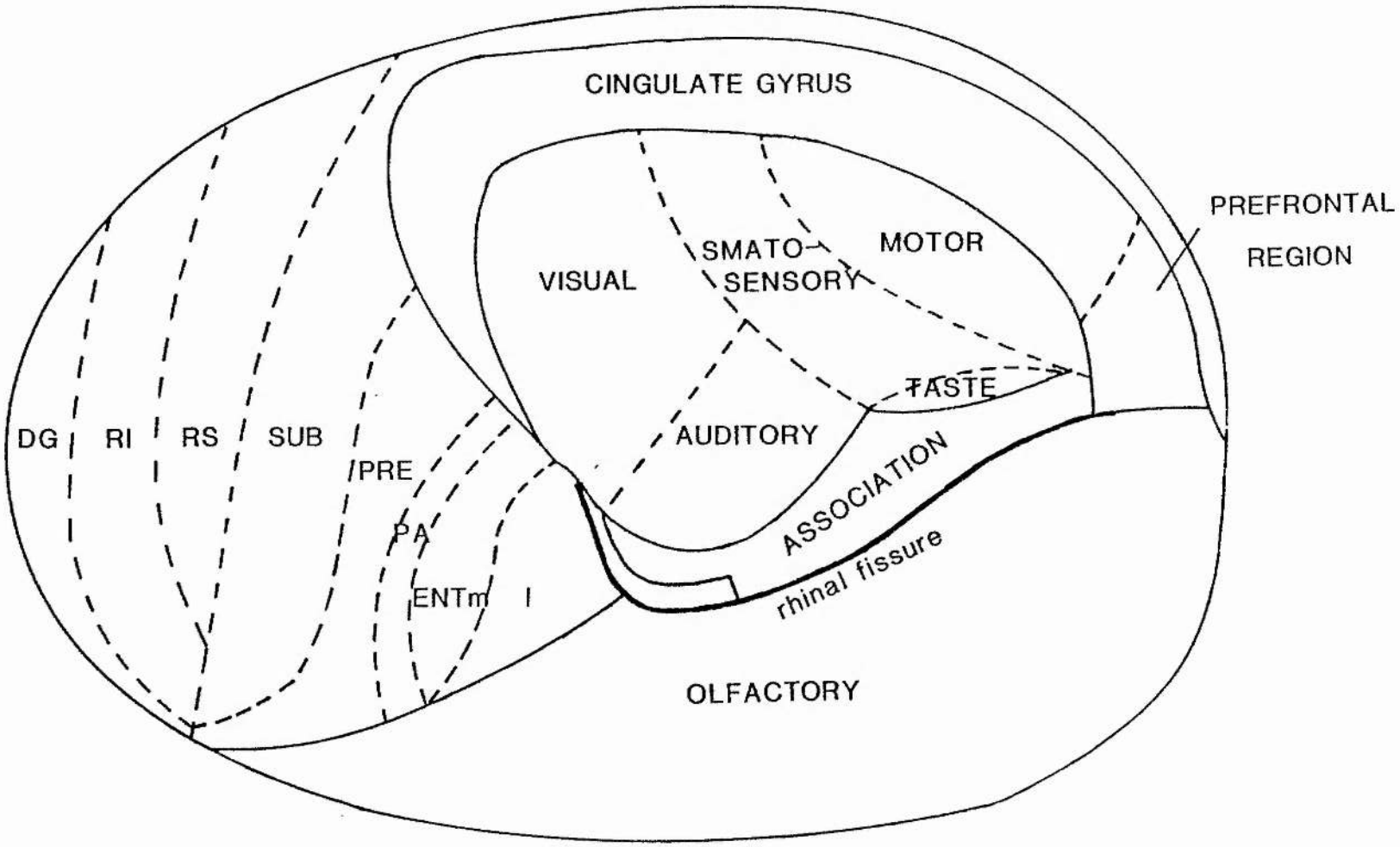
CINGULATE GYRUS
PREFRONTAL
REGION
VISUAL
SMATO-
SENSORY
MOTOR
TASTE
AUDITORY
ASSOCIATION
rhinal fissure
DG
RI
RS
SUB
PRE
PA
ENTm
I
OLFACTORY

The anatomy of the dentate gyrus

The most ventral part of the fascia dentata which abuts on the amygdala is designated the temporal tip. The antero dorsal pole is called the septal tip, figure 2-2.

In sections perpendicular to this axis, the horse-shoe shaped fascia dentata displays two blades of granule cells, the medial and the lateral crus, joined at the dentate crest. In the dorsal hippocampus the two blades become almost horizontal, the medial blade lying ventral (lower) to the lateral (upper). Hjorth-Simonsen and Zimmer (1975) refer to the blades as free and hidden, the free blade (medial) being covered with pia.

Major cell types

The major cell types are the pyramidal cells of Ammon's horn and the granule cells of the dentate gyrus. Afferent nerve fibres, organized in surface parallel bands, terminate in well defined laminae within the molecular layers of Ammon's horn and the dentate.

Figure 2-2. Drawing of the right dentate gyrus of the rat, disected free from the rest of the brain. Inset brain is in the same orientation as the enlarged dentate gyrus. Magnificat ion is about 20 (adapted from Hjorth-Simmonsen, 1972).

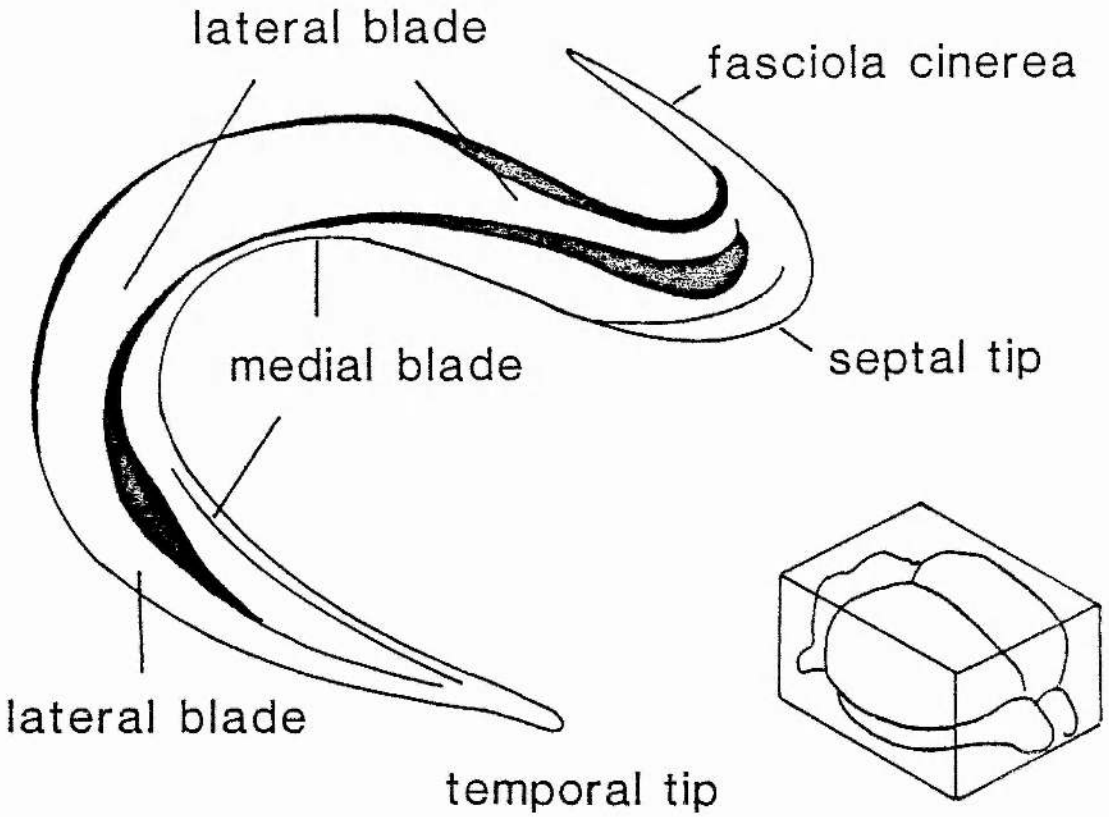
lateral blade
fasciola cinerea
medial blade
septal tip
lateral blade
temporal tip

Pyramidal cells

The Ammon's horn pyramidal cells are bipolar neurones, having a soma approximately 20 um in diameter, supporting a complex dendritic tree. The tree comprises of many basal dendrites (about 150 um long), and several primary apical dendrites, which radiate from the cell layer towards the hippocampal fissure, stretching over 400 um, branching at the distal ends. The pyramidal cells form a band of cells, running in an arc from CA4, next to the dentate gyrus, to CA1, adjacent to the presubiculum. Cells in fields CA3-CA1 make a topographically organised projection to the lateral septal nuclei, via the fimbria-fornix (Swanson and Cowan, 1977). Ammon's horn projects extensively to the cortex, CA1, CA2 and CA3 all send axons to the subiculum, and some to the pre and para subiculum, the entorhinal, perirhinal, retrosplenal and cingulate areas (Swanson and Cowan, 1977). CA3 pyramidal cells give rise to axon collaterals (Schaffer collaterals), which terminate in the stratum radiatum and oriens of field CA1 (Hjorth-Simonsen, 1973).

Granule cells

A dentate granule cell has a soma about 10 um in diameter, and unipolar dendritic tree which projects radially away from the hilus for more than 300 um. The granule cell bodies form a tightly packed lamina which follows the contours of the ventricular surface of the gyrus, such that their cell membranes are touching. Their dendritic fields resemble cones, the transverse to longitudinal ratio being greater than 1:1 in the dorsal blade and slightly less than 1:1 in the ventral blade. The average granule cell supports 2.23 1st order dendrites, the field extending to between 5 and 7 orders (Desmond and Levy, 1982). The granule cell axons are known as mossy fibres, and they make huge asymmetric synapses on the basal dendrites of CA3 pyramidal cells (Blackstad and Kjaerheim, 1961).

Interneurones

In addition to pyramidal and granule cells, a number of local circuit neurones are found in the hippocampus. Some of these are designated basket cells, because their axons form basket like 'plexa' around the cell bodies of pyramidal and granule cells. Andersen and co-workers (Andersen, Eccles and Loyning,1964a), suggested that basket cells are the most likely candi-

dates for recurrent collateral interneurones mediating Renshaw type inhibition in CA1, a similar situation existing in the dentate (Andersen, Holmqvist and Voorhoeve, 1966; Douglas, Goddard and Riives, 1983). Axo-somatic connections are nearly always Gray's type II, symmetric synapses, containing flattened or pleomorphic vesicles. They are held to be inhibitory, γ-amino butyric acid (GABAergic), synapses (Gray, 1969). Axo-somatic terminals do not degenerate after hippocampal commissural transection (Blackstad, 1967), which is consistent with their proposed local circuit function.

Alger and Nicoll (1982a) provide physiological evidence for the presence of feed-forward inhibition in the CA1, mediated by molecular layer interneurones. Alger and Nicoll (1979) and Andersen, Dingledine, Gjerstad, Langmoen and Mosfeldt Laursen (1980) have shown that CA1 pyramidal cell responses to GABA iontophoresed onto the cell body include a membrane hyperpolarization, whereas iontophoresis onto the dendrites results in a depolarization. The two responses are mediated by different classes of GABA receptor, (thought to be synaptic and extrasynaptic, respectively, Alger and Nicoll, 1982b). Iontophoresis of GABA close to granule cell bodies (Assaf, Crunelli and Kelly, 1981) causes

marked membrane depolarization possibly by activation of dendritic receptors. The distribution of glutamic acid decarboxylase (GAD), and other GABA markers (review: Storm-Mathisen, 1977) in the molecular layers of both Ammon's horn and the dentate gyrus, suggests the presence of inhibitory synapses in both cellular and molecular layers.

Intrinsic connections

The synaptic connectivity suggests information flow through the hippocampal formation initiated via the perforant path projection from the entorhinal area to the dentate gyrus, the granule cells relaying to field CA3 by the mossy fibre system, CA3 connecting via collateral axons (the Schaffer collaterals) to CA1. This is known as the trisynaptic circuit and is arranged transverse to the long axis of the formation (Andersen, Bliss and Skrede, 1971; Swanson, 1982), figure 2-3. The dentate gyrus represents a relay through which information from the entorhinal cortex reaches Ammon's horn.

Fibres arising in the contralateral formation innervate via the ventral hippocampal commissure.

Figure 2-3. Diagram of major connections between regions of the hippocampus and entorhinal cortex. Arrows show direction of impulse traffic. The entorhinal cortex (ENT) is a poly-modal association area, receiving pre-processed sensory information and relaying to the dentate gyrus (DG) by the perforant path. The output projection of the dentate gyrus are the granule cell axons, synapsing onto the CA3 pyramidal cells of the regio inferior, Ammon's horn (RI). The CA3 pyramidal cells project axon collaterals to the lateral septum and to CA1 pyramidal cells (regio superior, RS), the latter being known as Schaffer collaterals. The output of the regio superior of Ammon's horn is by axon collaterals to the septum and pre- and parasubiculum, and the entorhinal cortex. The subiculum is labelled SUB.

The trisynaptic circuit is made up of the entorhinal projection to the dentate (perforant path), the dentate projection to CA3 (granule cell axons - the mossy fibres), and the CA3 projection to CA1 (Schaffer collaterals).

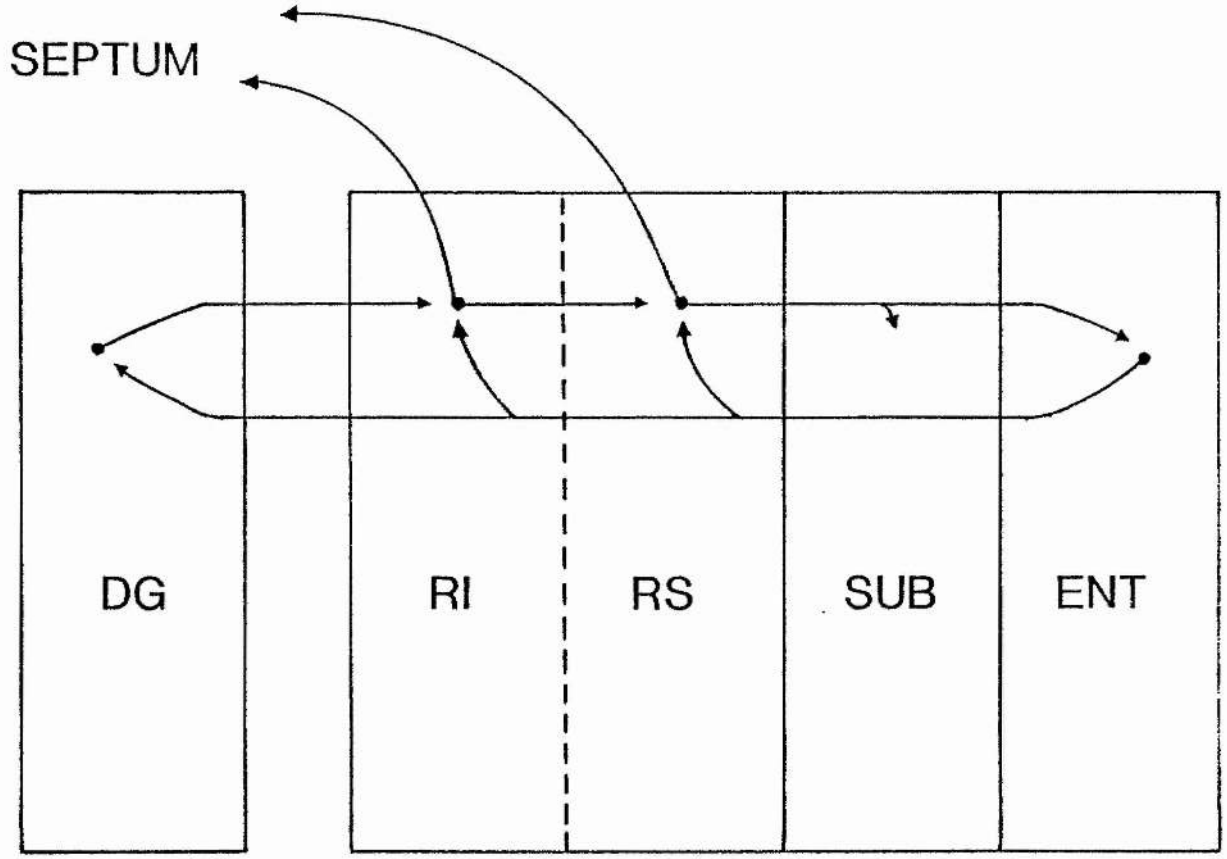
SEPTUM
DG
RI
RS
SUB
ENT

Pyramidal cells in fields CA3 and CA4 send fibres to the contralateral formation terminating in stratum oriens and radiatum of CA1-3, and the proximal 30 um of the molecular layer of the dentate, (Raisman, Cowan and Powell, 1965; Cowan, Gottlieb, Hendrickson, Price and Woolsey, 1972; Gottlieb and Cowan, 1972; 1973; Deadwyler, West, Cotman and Lynch, 1975; Laurberg, 1979; Buszaki and Eidelberg, 1982). Cells in the polymorph layer of the dentate gyrus project to the inner third molecular layer of the contralateral gyrus while CA3-CA4 pyramidal cells project ipsilaterally (associational fibres) to the same layer (Swanson et al., 1978; Swanson, Sawchenko and Cowan, 1981).

The perforant path

The major extrinsic input to the hippocampal formation is the so-called perforant path (Lorente de No, 1934), originating in the entorhinal cortex. The pathway became known as 'perforant', because the fibres penetrate all layers of the subicular and presubicular cortex en route to CA1 and the hippocampal fissure. The pathway may be divided into two different fibre systems, distinct in their origins and terminations; as shown by the Fink-Heimer silver impregnation techni-

que (Hjorth-Simonsen, 1970) and autoradiography after axonal transport of tritiated amino acids (Steward, 1976; Wyss, 1981).

a) A projection from the medial part of the entorhinal cortex, terminating in the middle of the dentate molecular layer, and in the stratum lacunosum-moleculare of CA1-CA3 known as the medial perforant path (Hjorth-Simonsen, 1972). Figure 2-4a.

b) A projection from the lateral part of the entorhinal cortex to the outer third of the dentate molecular layer and superficial stratum lacunosum-moleculare of CA3, known as the lateral perforant path (Hjorth-Simonsen, 1972). Figure 2-4b.

The two fibre systems are defined by their sites of origin in the entorhinal cortex. Intermediate perforating fibres have also been described (Hjorth-Simonsen,1972), arising immediately lateral to the medial entorhinal area and terminating between the lateral and medial fields. In fact, the anatomical evidence, (Wyss, 1981), suggests a graded entorhinal

Figure 2-4. a. The medial perforant path, originating in the medial entorhinal cortex (ENTm) and projecting to the dentate gyrus and Ammon's horn forming the medial edge of the angular bundle (shaded black). The termination sites on the middle third of the dentate granule cell dendrites and the apical dendrites of the regio superior pyramidal cells are shaded.

b. The lateral perforant path, originating in the lateral entorhinal area, forms the lateral side of the angular bundle, and projects to the outer third of the granule cell dendrites in the dentate gyrus. The terminal field and the position of the fibres in the angular bundle are shaded.

FD. Fascia dentata.

SUB. Subiculum.

Figures based on the work of Hjorth-Simonsen (1973), and Swanson (1982).

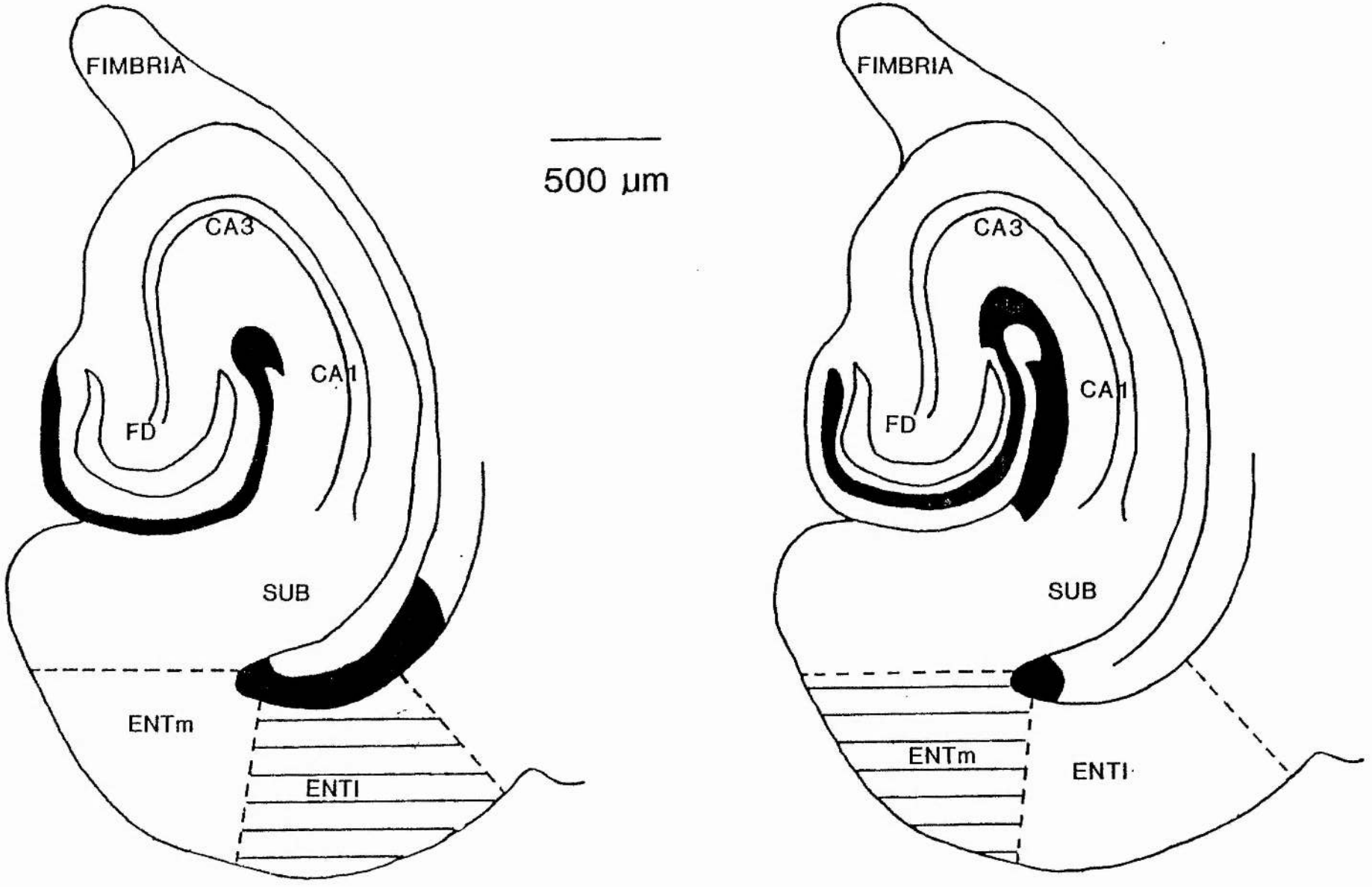

lateral perforant path

medial perforant path

projection rather than a laminated one, fibres graded in target field, along a medio-lateral cortical axis. However, it is useful to think in terms of two projections when the electrophysiological characteristics of the pathway are considered.

The origin and courses of the lateral and medial perforant paths

The perforant fibres arise between layers I-III in the entorhinal cortex (Steward, 1976; Wyss 1981). In thionin-stained material the medial zone is characterized by tightly packed, pale staining, rounded, pyramidal cells in layer II; the intermediate entorhinal area, by small, darkly staining cells, cortical layer II being divided into two cell layers, with a cell free zone between; and the lateral area by large, darkly staining pyramidal cells (Wyss, 1981).

Medial fibres pass from layers I-III, to the adjacent white matter, the angular bundle, or to a position immediately medial to it (observed in horizontal section, Hjorth-Simonsen and June, 1972). Lateral fibres from layers I-III run perpendicular to the white

matter; curving round the hippocampus and entering the angular bundle. The lateral pathway forms a sheet of steeply ascending fibres immediately lateral to field CA1 and the subiculum. Axons from both pathways leave the angular bundle and perforate the subicular and presubicular cortex continuing to CA1-CA3 and crossing the hippocampal fissure to the dentate.

Termination of the perforant path in the dentate gyrus

The medial entorhinal cortex projects ipsilaterally to both blades of the dentate, with approximately equal density, but may innervate the ventral blade more heavily. The projection displays a topographical organization, the occipital region of the medial entorhinal cortex projecting to the septal pole of the dentate gyrus, the temporal region projecting to the temporal pole of the dentate (Wyss, 1981). The lateral entorhinal projection exhibits a considerable amount of spread along the ipsilateral dentate, and does not appear to be topographically organised to the same extent. Autoradiographic label injected into a small localized region of cortex is transported over a wide area of hippocampus. The lateral entorhinal fibres preferentially innervate the dorsal blade of the den-

tate (Wyss, 1981). The sparse crossed entorhino-dentate projection shows the same dentate molecular layer projection pattern as the ipsilateral projection (Steward, 1976; Wyss, 1981), and the crossed medial entorhinal projection exhibits topographical organization.

Synaptic morphology and pharmacology of the perforant path

Perforant path fibres form asymmetric, Gray's type I synapses on the dendritic spines of granule cells (Nafstad, 1967), in the middle (medial p.p.) and the outer (lateral p.p.) thirds of the dentate molecular layer. They constitute over 85% of the total population of synapses in the dentate (Matthews, Cotman and Lynch, 1976) and upon activation give rise to depolarizing epsp's in the granule cells. If sufficient numbers of perforant path fibres are stimulated the granule cells may be excited to fire action potentials (eg. Lomo, 1971a; Assaf et al., 1981).

Nadler, Vaca, White, Lynch and Cotman (1976) found endogenous glutamate (Glu) was released in a Ca^{2+} dependent way by high $[K^+]$ in rat dentate gyrus fragments. Lesion of the perforant path reduced Glu release. Electrical stimulation and high $[K^+]$ in the ventral blade of rabbit dentate slices confirmed the release of Glu was associated with perforant path synaptic activation (White, Nadler, Hamberger, Cotman and Cummins, 1977). Stimulation of the perforant path

in vivo is associated with release of radioactive glutamate after the provision of radioactive precursor (glutamine), and the amount of radiolabelled transmitter released is directly related to the magnitude of the dentate field potential generated on stimulation (Dolphin, Errington and Bliss, 1982). Storm-Mathisen, Leknes, Bore, Vaaland, Edminson, Haug and Ottersen (1983), using a method of immunocytochemical visualization of glutamate, report that the lateral perforant path termination zone stains more heavily for glutamate-like immunoreactivity than the medial path termination zone.

Amino acid receptors of the quisqualate/kainate type mediate the excitation evoked by stimulation of the medial perforant path, the granule cells being most exquisitely sensitive to glutamate (rate of depolarization to iontophoresis of glutamate is 7 times that for quisqualate). Granule cell receptors which are most sensitive to N-methy-D-Aspartate (NMDA), are not the same as those employed by the medial perforant path in the production of epsp's (Crunelli, Forda and Kelly, 1984). It therefore appears that an amino-acid with glutamate-like immunoreactivity mediates synaptic transmission in both the lateral and medial perforant paths.

CHAPTER 3

LONG-TERM POTENTIATION

Long-term potentiation (LTP), is a dramatic form of plasticity observed in the hippocampus and one which may relate to mammalian learning mechanisms, as it is elicited by brief events and is of long duration. It has been measured as an enduring increase in the magnitude of the extracellular population spike, or increase in the magnitude of either the extracellular synaptically evoked potential or intracellular epsp, following tetanic stimulation of afferents (Bliss and Lomo, 1973; Bliss and Gardner-Medwin, 1973; Review: Teyler, Goddard, Lynch and Andersen, 1982). LTP has been demonstrated in all the pathways of the hippocampal trisynaptic circuit, and has been measured lasting for 2 months in chronically implanted rats (Douglas and Goddard, 1975).

Immediately after tetanic afferent activation in the dentate, post-tetanic potentiation (PTP, or frequency potentiation) is present, and is accounted for in terms of facilitated transmitter release or increased probability of terminal activation (Bliss and Lomo, 1973; see also Hirst, Redman and Wong, 1981). When the afferent tetanus is of sufficient intensity, LTP is revealed as an apparently non-decremental increase in synaptic efficacy, after the decay of PTP. From an analysis of perforant path synaptic potentials McNaughton (1982, 1983) has suggested that the PTP lasts about 10 minutes. Its decay is a series of superimposed exponential functions , the time constant of the longest-lasting process being < 240 seconds.

The inducing frequency of stimulation for LTP may be anything between about 10 and 400 Hz, around 100 stimuli normally being applied in a train (Teyler et al., 1982). The tetanizing train intensity must be above a certain threshold to be effective, usually near the intensity for the induction of granule cell population discharge (McNaughton, Douglas and Goddard, 1978; McNaughton, 1982), although discharge of the cells is not necessary for eliciting LTP. Using subthreshold test stimuli it has been shown that PTP of the synaptic wave can be produced at much lower stimulus intensities than LTP (McNaughton et al., 1978). This implies that

the simultaneous co-operation of afferents is necessary for the induction of LTP. McNaughton suggests that PTP may be further subdivided into three components, namely facilitation, augmentation and potentiation, each process having a progressively longer time constant, all increasing the amount of transmitter released per afferent impulse (McNaughton, 1983). However it is clear that the longevity of the processes hypothesised cannot account for the durability of the measured increases in transmitter release after tetanus (Dolphin et al., 1982).

The relationship between synaptic wave and spike potentiation is apparently not a simple one. For example, the population spike can be potentiated without parallel potentiation of the synaptic wave; significant potentiation of the dentate population spike has been recorded in conjunction with no potentiation of the synaptic wave (Bliss and Lomo, 1973). This either means there are two essentially independent potentiating mechanisms, one giving rise to population spike potentiation and one to synaptic potential potentiation, with different time courses; or that the extracellular synaptic potential amplitude may not be an accurate reflection of synaptic current flow.

Specificity of LTP

Reports of the synaptic specificity (ie homosynaptic vs. heterosynaptic) of LTP are contradictory. One problem may be that the synapses in different hippocampal subfields potentiate in different ways. Another may be the electrical isolation of potentiated synaptic regions from the soma in pyramidal cells, so that local changes in the post-synaptic membrane characteristics cannot be recorded.

Andersen, Sundberg, Sveen and Wigstrom (1977) stimulating in the oriens and radiatum fibres of field CA1, in the slice, found that the input/output curves for the population spike relative to the size of the presynaptic compound action potential, changed in the tetanized line, but not in the non-tetanized. Intrasomatic recording in CA1 revealed no prolonged somatic excitability changes, including membrane potential and resistance after the induction of LTP (Andersen et al., 1977; Andersen, 1978). Widespread effects of afferent tetanization in field CA1 have been observed (Lynch, Gribkoff and Deadwyler, 1976; Lynch, Dunwiddie and Gribkoff, 1977), including a reduction of dendritic responsiveness to iontophoresed glutamate,

and 'heterosynaptic depression' of synaptically evoked population spikes.

Importantly Yamamoto and Chujo (1978), report non-specificity of LTP in the mossy fibre - CA3 projection, after dividing the dentate gyrus in a slice, and stimulating the mossy fibres from the segments separately. Mossy fibres synapse only onto the basal dendrites of CA3 pyramidal cells, and we might presume terminal field overlap between mossy fibres from both segments of dentate gyrus.

It is difficult to selectively activate the medial and lateral perforant paths in vivo, especially when tetanizing at high intensity, as the pathways lie adjacent in the angular bundle. Harris, Lasher and Sherwood (1978) reported transient heterosynaptic potentiation in the dentate and McNaughton (1983) found either path may exhibit LTP without the other pathway being affected. However Abraham and Goddard (1983) have convincingly demonstrated a long-lasting heterosynaptic depression of the amplitude of the hilar recorded extracellular synaptic potential in both lateral and medial perforant paths after tetanic activation of the other, which the present author takes

as important evidence for the heterosynaptic effect of afferent tetanization.

Therefore, it appears that LTP is restricted to the locality of afferent termination, ie to a region of dendritic tree. It is unclear exactly how localized the region is, but it does not seem to involve the soma (at least in CA1). It is possible that untetanized afferents synapsing within the locality also show potentiation. Concurrent with potentiation in one region of the dendrites, a suppression of the ability of other inputs to discharge the cell may be observed (Lynch et al., 1977), but has perhaps little to do with LTP - such observations may be explained by suggesting that tetanic activation of afferents, particularly at lower frequencies, eg 10-20 Hz, gives rise to a reduction of somatic excitability but also to a relatively specific increase in synaptic efficacy in the termination zone, sufficient to overcome the reduced somatic excitability. Fricke and Prince (1984) report a Ca^{2+} dependent increase in somatic gK^{+}, leading to membrane hyperpolarization. This results in a depression of somatic excitability after sustained spiking activity which would inevitably accompany low frequency tetani.

Modulation of LTP

The generation of LTP is apparently under heterosynaptic control, by ascending and local, pharmacologically distinct brain systems, employing serotonin (5-hydroxytryptamine, 5-HT), noradrenaline (NA) and ɣ-aminobutyric acid (GABA). All three transmitters inhibit the spontaneous discharge of hippocampal neurones when applied iontophoretically. 5-HT containing neurones in the median raphe nuclei of the brain stem project rostrally to the hippocampus, neocortex and caudate nucleus, and dorsally to the cerebellum. NA releasing neurones are found in the locus coeruleus, another brain stem nucleus, projecting rostrally via the dorsal noradrenergic bundle, to the pons, thalamus, neocortex and hippocampal formation, and dorsally to the cerebellum.

The response of the granule cells in the hippocampal slice to the iontophoresis of 5-HT is similar to that for GABA (Assaf et al., 1981). Receptor activation is associated with increased membrane conductance (specific to Cl^- ions), and depolarization. The action of NA on CA1 pyramidal cells is the induction of a moderate hyperpolarization with no associated membrane

conductance change (Segal, 1980; 1981) - although Herrling (1981) reports NA causes prolonged increases in the input resistance of hippocampal pyramidal cells, similar to the action of acetylcholine in the cortex (Krnjevic, Pumain and Renaud, 1971). Douglas (1978) found that a brief tetanus in the commissural input to the dentate which immediately preceded or overlapped a high-frequency train to the perforant path prevented the induction of LTP. As has been discussed previously, commissural fibres make excitatory synapses on the contralateral granule cells and inhibitory interneurones (see McNaughton, 1983). It has also been demonstrated that selective pharmacological antagonists of GABA, picrotoxin, bicuculline and penicillin, enhance the production of synaptic wave LTP in the CA1 region of the hippocampal slice (Wigstrom and Gustafsson, 1983). It is likely that the effect of GABA on LTP is mediated postsynaptically, as inhibitory interneurones appear to be involved in the modulation of LTP (Douglas, McNaughton and Goddard, 1983), providing evidence for a major role for the postsynaptic neurone in the expression of LTP. Laroche and Bloch (1981) have shown that medial reticular formation stimulation soon after a tetanization of the perforant path, enhances the magnitude of the population cell discharge, over and above that increase due to perforant path tetanization alone. Bliss et al. (1983) provide evidence for

monoamine modulation of LTP in noradrenaline (< 7.5 % normal hippocampal NA content) and 5-HT (28 % average residual hippocampal 5-HT content) depleted rats. The LTP induced by perforant path tetanization is substantially reduced in magnitude in depleted animals compared with controls, the greatest effect being due to 5-HT depletion.

A 5-HT mediated presynaptic facilitation has been described in the sea hare, Aplysia (Brunelli, Castellucci and Kandel, 1976; Shimahara and Tauc, 1977; Siegelbaum, Camardo and Kandel, 1982), and it is possible 5-HT and NA have a presynaptic action modulating transmitter release from the perforant path; however, only a weak projection of both NA and 5-HT fibres reaches the dentate molecular layer - the majority of fibres terminate in the hilus (Loy, Koziell, Lindsey and Moor, 1980; Bliss, Goddard and Riives, 1983).

One explanation of the effect of monoamine depletion on LTP is that monoamine containing fibres are responsible for the tonic inhibition of contralateral CA4 cells and therefore, once that tonic inhibition is removed, the commissural fibres raise the activity of local inhibitory interneurones, and increase the GABA

mediated inhibition on the granule cells (Bliss et al., 1983). Stimulation of the dorsal noradrenergic bundle increases the dentate population spike evoked by perforant path stimulation, the effect being maximal about 50 msec after ascending fibre stimulation (Assaf, Mason and Miller, 1979). Iontophoresis of NA onto the granule cells in a hippocampal slice causes a potentiation of the population spike after perforant path stimulation, which outlasts drug application by several minutes (Harley and Neuman, 1980).

Therefore the action of NA may be directly on the granule cells, mediated by a β-receptor associated with adenylate-cyclase, as is the case for hippocampal pyramidal cells (Segal and Bloom, 1974a, 1974b), and other cortical cells (Stone, Taylor and Bloom, 1975). A second-messenger system would explain the long latency of the maximal effect of dorsal noradrenergic bundle stimulation in the dentate, and the longevity of effect after NA iontophoresis. c-AMP, produced by adenylate-cyclase is associated with protein-kinase activation (Review: Cohen, 1982) and the phosphorylation of membrane proteins (Greengard, 1976).

Possible mechanisms of LTP

The several mechanisms which have been proposed as underlying LTP, are presented below.

A prolonged increase in transmitter release

Evidence from the dentate gyrus in vivo (Dolphin et al., 1982), suggests that after tetanization of the perforant path, there is a prolonged increase of glutamate release per afferent impulse. Release of radioactive transmitter in the stratum radiatum of CA1 in hippocampal slices is significantly increased after tetanization (Skrede and Malthe-Sorenssen, 1981). The effect lasts > 1 hr. This is possibly due to:

i) Increase in the probability of vesicle release due to elevated presynaptic Ca^{2+}.

ii) Increased transmitter mobilisation, and an increase of the number of vesicles per synapse.

iii) The release of transmitter from previously unproductive pre-synaptic terminals (Hirst et al., 1981).

There does not appear to be a change in the number

of afferent fibres activated after a tetanus which could explain the increase in release (Andersen, 1978).

A problem in the interpretation of such release experiments is that the dynamics of transmitter production and release is known in insufficient detail. The presynaptic terminals must be preloaded with radioactive transmitter given in the form of a precursor. It may be that tetanization results in an increase in the probability of release of newly synthesised transmitter. Subsequent to a tetanus, the rate of radioactive transmitter release could be increased preferentially. Such a situation has been described by Zimmermann, in the cholinergic synapses of the torpedo fish electric-organ (Review: Zimmermann, Stadler and Whittaker, 1981). Therefore the results may be at least partly artifactual. However, taken with the data on PTP of the extracellular synaptic potential, it is very likely that increased transmitter release plays some part in the response to perforant path tetanus.

Recently, synaptic transmission onto spinal motoneurones has been shown to occur with an incredibly low variability of epsp amplitude in single synapses (Jack et al., 1981; Redman and Walmsley, 1983). The variability of transmission is best described by a binomial

distribution, the synapse either being 'on ' or 'off'; the probability that a synapse will release transmitter after afferent stimulation being less than 1. The maximum conductance change at such a synapse would depend on the number of receptors on the postsynaptic membrane, and not on the number of transmitter quanta liberated, as one vesicle may be enough to saturate all the receptors. Facilitated transmitter release in this situation would either be redundant (points i and ii above) or indicative of increased numbers of activated synapses (point iii). Alternatively, if the postsynaptic spine neck provided a high enough impedance to current flow into a dendritic shaft (Koch and Poggio, 1983), then neither increased transmitter release or increased numbers of postsynaptic receptors could account for LTP (see section following on increased receptors).

Stochastic variation in the size of the intracellularly recorded epsp's in both these cases would therefore be a product of their compound nature; 1 afferent making several contacts. McNaughton et al. (1980), report a few such low variability epsp's when recording from granule cells while stimulating the perforant path in a hippocampal slice.

An increase in the number of receptors

Experiments relating glutamate binding to hippocampal membranes have been performed in the CA1 field only. Baudry and Lynch (1979), reported that low levels of Ca^{2+} (10 uM) produce a substantial increase in the number, but not the affinity of Na^{+} -independent glutamate binding sites in purified hippocampal membranes. It is also difficult to elicit LTP in a medium which contains lower than physiological levels of Ca^{2+} (Dunwiddie and Lynch, 1979).

Turner, Baimbridge and Miller (1982) have reported that brief exposure of hippocampal slices to high extracellular [Ca^{2+}] alone, results in the induction of LTP of the extracellular synaptic and spike potentials evoked by Schaffer-commissural fibre stimulation. Further evidence reinforced the theory that postsynaptic Ca^{2+} influx was necessary to elicit LTP, as intracellular injection of EGTA (ethylene glycol-(bis-aminoethyl ether)-tetraacetic acid), prevents its induction, presumably by chelating Ca^{2+} (Lynch, Kelso, Barrionuevo and Schottler, 1983).

Browning, Dunwiddie, Bennett, Gispen and Lynch (1979) found protein phosphorylation in synaptic fractions of CA1 subsequent to the induction of LTP, the effect being Ca^{2+} dependent. The phosphorylated protein, molecular weight 40 K daltons, was at first thought to be a plasma membrane protein, but was later identified as the α-subunit of the enzyme pyruvate dehydrogenase, PDH. This led to the hypothesis that periods of intense synaptic activity can alter mitochondrial function, and in particular, reduce their sequestration of Ca^{2+} from the postsynaptic cytoplasm. Electron transport would cease during inhibition of pyruvate oxidation. Thus local cytoplasmic accumulations of Ca^{2+} might occur. However, it is not clear whether the increased protein phosphorylation is a consequence of inhibition of PDH activity by the tetanus directly, or a consequence of enhanced ATP production during tetanization, resulting in feed-back inhibition of PDH by ATP.

Baudry, Arst, Oliver and Lynch (1981) report that the development of Na^+-independent ^3H-glutamate binding sites in neonatal rat hippocampus is paralleled by the tissues ability to show LTP which is only reliably obtained 9 days post-partum. Post-natal development of Na^+-independent glutamate binding is therefore coinci-

dent with synapse formation; these binding sites may therefore be synaptic receptors. The binding site of ^{3}H-glutamate is apparently located postsynaptically (Baudry and Lynch, 1981), and Na^{+} entry into hippocampal slices is elevated in the presence of agonists specific for this binding site (Baudry, Kramer, Fagni, Recasens and Lynch, 1983).

Lynch and Baudry (1984), suggest that LTP is caused by a Ca^{2+} dependent increase in the number of glutamate receptors, mediated by a proteinase (calpain I), acting on a structural membrane protein, fodrin. The proposed membrane alterations would lead to the exposure of previously unused receptors (associated, presumably, with ionophores). Although the increase in ^{3}H-glutamate binding in hippocampal slice membranes after tetanization has been blocked by leupeptin (a tripeptide, proteinase inhibitor), there is no evidence that leupeptin inhibits the production of LTP. The structural membrane changes brought about by proteinase activity are also proposed as the explanation of ultrastructural changes reported in the postsynaptic locality after high frequency activation (discussed in detail below). Sastry and Goh (1984) however claim that low frequency (20 Hz) stimulation of the Schaffer collaterals causes an increase in the intracellular

[Ca^{2+}], associated with a depression of the evoked population spike. This depression could be inhibited by verapamil (1 uM) which blocks Ca^{2+} currents. "Tremendous" increases in the binding of ^{3}H-glutamate occurred only after low frequency stimulation, and was significantly depressed by verapamil. In contrast, high frequency stimulation (400 Hz) elicited LTP, which was insensitive to verapamil, and not associated with increased membrane binding of ^{3}H-glutamate. It is therefore unclear whether LTP is associated with increases in glutamate receptors.

It has yet to be shown whether the stimulation associated increased binding of ^{3}H-glutamate is caused by the accumulation of functional receptors, and if the receptors are functional, whether they are synaptic or extrasynaptic.

Unexplained evidence from Lynch, Gribkoff and Deadwyler (1976) on the effect of iontophoresis of glutamate onto CA1 pyramidal cells, showed that the induction of LTP was accompanied by a reduction of dendritic responsiveness to glutamate. The decay of the effect was apparently related to the decay of LTP, and so unlikely to be simple receptor desensitization.

The Lynch and Baudry theory cannot, at the present time, be properly tested, as it is impossible to record the intracellular voltage changes taking place in the dendrites on activation of a single synapse. Even if there were an increased number of functional receptors, they might not have a significant effect on the amount of current entering the dendrites on synaptic activation, if the spine neck axial resistance were sufficiently high. With a high resistance spine neck, variations in the amount of transmitter released, or in the number of receptors, could not significantly affect the dendritic shaft voltage transient on synaptic activation. This is because the reversal potential would be rapidly reached for the ion species involved, and current would cease to flow across the post-synaptic membrane.

Neuroanatomical modifications

Fifkova and Van Harreveld (1975) reported that tetanic stimulation of the perforant path in the mouse causes swelling of the dendritic spines in the dentate gyrus. As the current flow down a spine into a dendritic shaft is dependent on the axial resistance of the spine neck, current flow would increase if the spine neck widened (Rall, 1970; Koch and Poggio, 1983).

Spine morphology may be under the control of Ca^{2+} activated contractile proteins, including actin (Fifkova and Delany, 1982). Desmond and Levy (1981) also reported spine swelling after the induction of LTP, but in conjunction with lengthened postsynaptic densities. They found a reduction of the number of synapses in the activated dendritic zone. Outside the zone there seemed to be a reduction in size, but an increase in number of spines. Lee and co-workers (Lee, Schottler, Oliver and Lynch, 1980; Lee, Oliver, Schottler and Lynch, 1981) did not find changes in spine morphology in CA1 after establishment of LTP in vivo or in vitro. However, they found an increase in the number of dendritic shaft synapses.

The anatomical data on LTP is more confusing than helpful in elucidating mechanisms. Swelling of spines may well be a secondary consequence of transmitter release or dendritic membrane characteristics. It will be necessary to determine adequate conditions of fixation as well as experimental procedures before conclusions can be made (Teyler et al., 1982).

Altered postsynaptic excitability

As has been discussed above, LTP is unlikely to be caused by a cell-wide increase in excitability. However, intrasomatic recording only measures changes in the soma and adjoining portions of the dendritic tree. It is possible that local postsynaptic membrane changes occur in the dendrites near activated synapses.

Decreased local circuit inhibition

In field CA1, after induction of LTP in the stratum radiatum, orthodromically evoked intracellular ipsp's were slightly reduced in amplitude, but prolonged, whereas antidromicaly evoked ipsp's (Renshaw type inhibition) were unaffected (Haas and Rose, 1980). Yamamoto and Chujo (1978), reported a depression of ipsp amplitude recorded in CA3 pyramidal cells on activation of the mossy fibres after tetanization. They suggested this may play a major part in the induction of LTP. How such a decrease in ipsp amplitude might come about is not known, but increases and decreases in intracellularly recorded epsp's and ipsp's could have as much to do with the properties of the post-synaptic membrane as the amount of transmitter released. Changes in the sizes of ipsp's may therefore be a consequence of the induction of LTP. It has been

shown, for instance, that the affinity of GABA receptors in the CNS for GABA is modulated by a junctional membrane protein, GABA-modulin (Toffano, Guidotti and Costa, 1978; Costa, 1981). This protein acts by inhibiting c-AMP dependent and independent protein kinases which increase the affinity of the GABA receptor for GABA. One could hypothesise that subsequent to the generation of LTP, the GABA receptor has a decreased affinity for GABA. The prolonged duration of ipsp's can be explained by an increase in the number of action potentials in the bursts fired by interneurones after tetanization of afferents (Andersen et al., 1964a; Andersen, Eccles and Loyning, 1964b).

Evidence for mechanisms of LTP from pharmacological blockade studies

The experiments reported below were all performed in the hippocampal slice, on the Schaffer collateral-commissural input to CA1.

Powerful evidence for the post-synaptic control of the generation of LTP was provided by the blockade of glutamate-like receptors by D,L-2-amino-4-phosphobutyrate (APB) (Dunwiddie, Madison and Lynch, 1978). During the action of the drug,

tetanization of the Schaffer collaterals did not result in the induction of LTP, revealed after the APB was removed. Collingridge, Keh and McLennan (1983) showed that D,L-2-amino-5-phosphovalerate (APV), almost exclusively antagonising the NMDA class of receptor, while not preventing normal synaptic transmission, blocked the production of population spike LTP. Harris, et al. (1984), confirmed that NMDA receptors, antagonised by 2-amino-5-phosphonopentanoate (AP5) and 2-amino-7-phosphonoheptanoate (AP7), have to be activated to induce LTP of the population spike. LTP is also blocked, in a dose dependent way, by PCP (Phencyclidine, 'Angel dust') and cyclazocine, at concentrations which do not affect normal synaptic transmission (Stringer, Hackett and Guyenet, 1984). PCP can also eliminate previously established LTP. PCP binds to a specific receptor, which is concentrated in synaptosomal fractions of rat brain, especially in the cerebral cortex, the corpus striatum (Vincent, Kartalovski, Geneste, Kamenka and Lazdunski, 1979) and the hippocampus (Zukin and Zukin, 1979). Kujtan and Carlen (1982) have shown that 2 uM PCP increases the input resistance and the threshold for spiking in CA1 pyramidal cells. PCP might be binding to a receptor normally occupied by an endogenous LTP modulating compound and Lacey and Henderson (1983) have shown PCP blocks NMDA receptor mediated depolarizations. Alternatively, the

lack of reversibility of the effect on LTP by PCP and cyclazocine might mean a non-specific membrane interaction.

Trifluoperazine, a tranquillizer which binds calmodulin and blocks its activity, inhibits the Ca^{2+} dependent phosphorylation of proteins, among them a 40 K dalton molecule, and inhibits the production of LTP in the slice (Finn, Browning and Lynch, 1980).

Summary of LTP

Hippocampal LTP is an increase in the efficacy of synaptic transmission, resulting from high frequency afferent activation. Depending on the tetanizing stimulation parameters used, it can last for considerable periods of time (months, in vivo).

This increased efficacy is paralleled by elevated levels of transmitter release in the fibre terminal field, although exactly how long this elevation lasts is unknown. Whether it reflects a naturally occurring process, or is only a product of non-physiological stimulation, is also unknown. It is conceivable that elevated transmitter release at a single synapse would have no effect on the magnitude of the resulting intracellular epsp, as all receptors might usually be saturated, or the impedance of a dendritic spine may effectively limit the amount of current which can flow into a dendritic branch. However the evidence for increased transmitter release playing some part in the response to afferent tetanization is persuasive.

High frequency afferent activation also causes postsynaptic changes which are probably Ca^{2+} dependent (although not blocked by verapamil) triggered by NMDA receptor activation and modulated by noradrenaline, 5-HT and GABA. These postsynaptic changes must be localized within a small region of dendritic tree, and probably do not involve the soma. An increase in the number of receptors has been postulated, although the evidence is inconclusive and contradictory. Morphological changes have been reported in afferent terminal fields, but they may be due to fixation methods and or be secondary consequences of electrochemical events.

CHAPTER 4

FIELD POTENTIAL GENERATION AND COMPUTER MODELS

A description of field potential generation

Field potentials are generated within a volume conductor when a neural element carries a non-uniform membrane potential. Non-uniformity of membrane potential results in current flow within the element, and necessarily current flow in the volume conductor. Such a situation is induced by transmembrane current flow, eg on synaptic activation.

A point at which positive current flows into an element is known as a current sink, and where current flows out of an element, a current source. As the resistance of the extracellular fluid is non-zero the current flowing through it is associated with an extracellular potential field - the current flowing between any two adjacent points being directly proportional to the potential difference between the points.

If the membrane of an element is at any time uniformly polarized or depolarized, there will be no resulting longitudinal current flow, and therefore no field potential.

The spatial orientation and microscopic organisation of the elements giving rise to the field potentials is crucial, as current flow in a volume conductor will add linearly and algebraically at every point in space. Cancellation of fields can thus take place (see Brindley, 1974).

If the duration of a current sink and source is brief compared to the time constant of the membrane, almost all the local outward current will be capacitative and therefore essentially independent of the membrane resistance. If the duration of the sink and source is of the same order of magnitude as the membrane time constant, or of longer duration, then this will not be the case. The activation of a localized population of perforant synapses on granule cells falls into this second category. The time constant of a granule cell membrane has been measured as lying between 11.0 and 16.21 msec (Durand, Carlen, Gurevich and Kunov, 1983).

The potential divider effect

General references to this effect include Rall and Shepherd (1968) and Hubbard, Llinas and Quastel (1969). Extracellular current is generated by a non-uniform membrane potential, current flowing between a source and sink, longitudinally, adjacent to the neural element. This is the primary extracellular current. Current also flows throughout the volume conductor, following combinations of anatomical resistances. This is known as secondary extracellular current, figure 4-1a. Field potentials are recorded relative to an indifferent electrode, which lies somewhere on the secondary extracellular current path. The indifferent electrode is therefore at some potential, which is a constant fraction of the potential difference between both ends of the primary current path. The fraction is given by the ratio of resistances in the volume conductor between the indifferent electrode and both ends of the primary current path.

Dentate field potentials

Classically, when a neurone fires an action potential, positive current enters across the membrane in

the form of Na^+ ions, and rapidly depolarizes the cell. On synaptic activation of a cell, it is the initial segment of the axon which is first depolarized to threshold, the action potential being propagated back into the soma and forward down the axon. This positive inward current in the soma is associated with outward current in the dendrites, and the axon distal to the initial segment. Repolarization of the cell body rapidly follows the depolarization, as K^+ ions exit the cytoplasm, through voltage dependent channels in the cell membrane down their electrochemical gradient. Thus the membrane potential is restored. There is a simultaneous influx of positive current in the dendrites, to make up the circuit. In the dentate gyrus, where the cell bodies form a discrete layer and many granule cells are activated in synchrony, the granule cell population spike is recorded negative at the cell layer or in the hilus and positive in the molecular layer. The potential reverses along the extracellular resistance lying parallel with the soma-dendritic axis (Rz in figure 4-1). On synaptic activation, positive current enters the dendrites via ion-species specific channels (in the case of the perforant path/granule cell synapses, probably carried by Na^+ ions), associated with postsynaptic receptors. Current simultaneously flows across the adjacent dendritic membrane and from

Figure 4-1. a. Diagram of the potential divide in the dorsal blade of the dentate gyrus. Current is set flowing on synaptic activation (Iin and Iout), across the membrane of the granule cell dendrites and soma. Rz is the extracellular resistance perpendicular to the plane of the cell layer. R1 connects the hippocampal fissure with the indifferent, and R2 connects the hilus with the indifferent. The extracellular potentials are recorded (at the potentiometer) between the indifferent and any point along Rz.

b. diagrammatic granule cells (shaded black), and the types of potential recorded at the distal and proximal dendrites, with a skull indifferent. The cell on the left is receiving synaptic input, while the cell on the right is discharging an action potential.

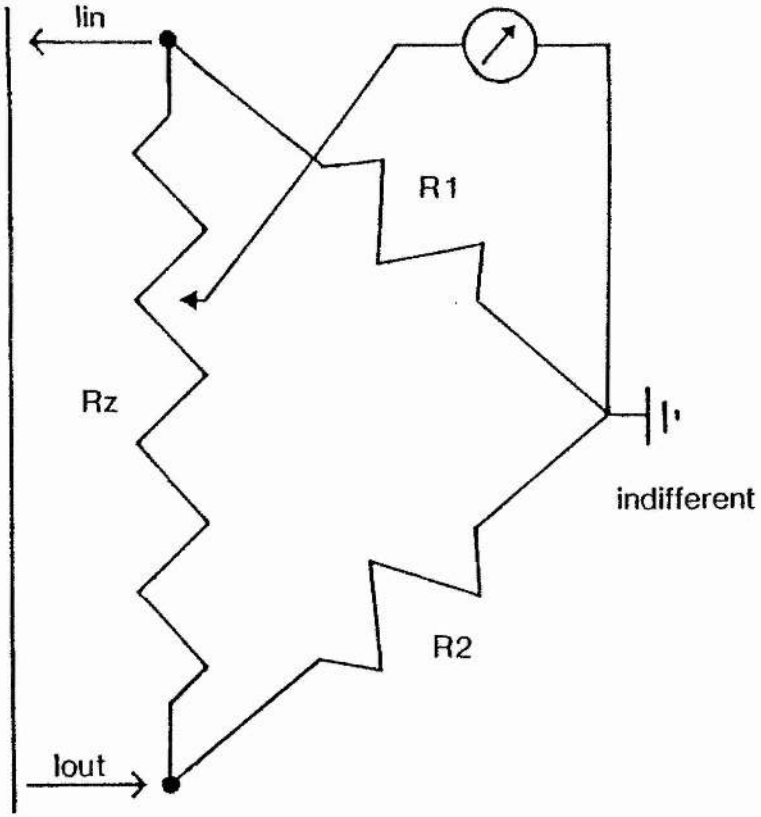

a

potential divide

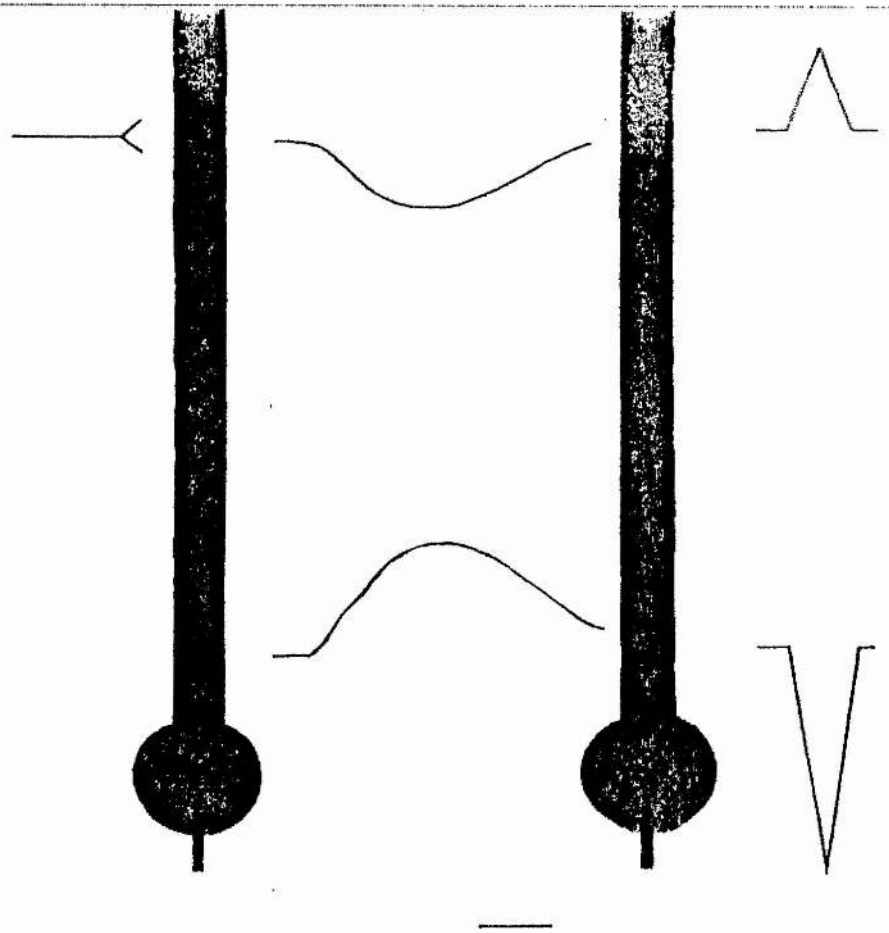

b

synaptic wave

population spike

calibration 2 msec 1 msec (positive up)

the cell body. This gives rise to a negative potential at the level of the synapses, which reverses in the molecular layer, giving a positive potential at the cell body layer. Figures 4-1 and 4-2.

In the dorsal hippocampus, the dorsal blade of the dentate gyrus is approximately horizontal, the granule cells oriented vertically. The dendrites form a discrete molecular layer dorsal to the cell bodies, an arrangement designated 'open field' (Lorente de No, 1947). As the radius of the neuronal population, is much greater than the length of a neural element, (ie the soma and dendrites) the relationship between the field potential and the current source density (CSD) in such a population of neurones (with no concurrent synaptic activity in vertically adjacent cell fields) is given by;

1) $$\sigma_z \frac{\partial^2 V}{\partial z^2} = - Im$$

(Nicholson and Freeman, 1975).

Where σ_z is the conductivity of the brain along the z axis, and V is the potential at any point along it.

Figure 4-2. A. Simultaneous recordings made in the molecular layer (upper trace) and the hilus (lower trace), on suprathreshold activation of the granule cells by stimulation of the perforant path. Population spike is marked with an asterisk. Note reversed polarity of the spike at the two recording sites. Calibration, upp er trace 2mV/4msec; lower trace 4mV/4msec.

B. Simultaneous recordings made in the molecular layer (upper trace) and hilus (lower trace) of a 'population epsp', generated on activation of the dorsal edge of the angular bundle (medial perforant path, McNaughton and Barnes, 1977) ie between 2.2 and 2.5 mm below brain surface.

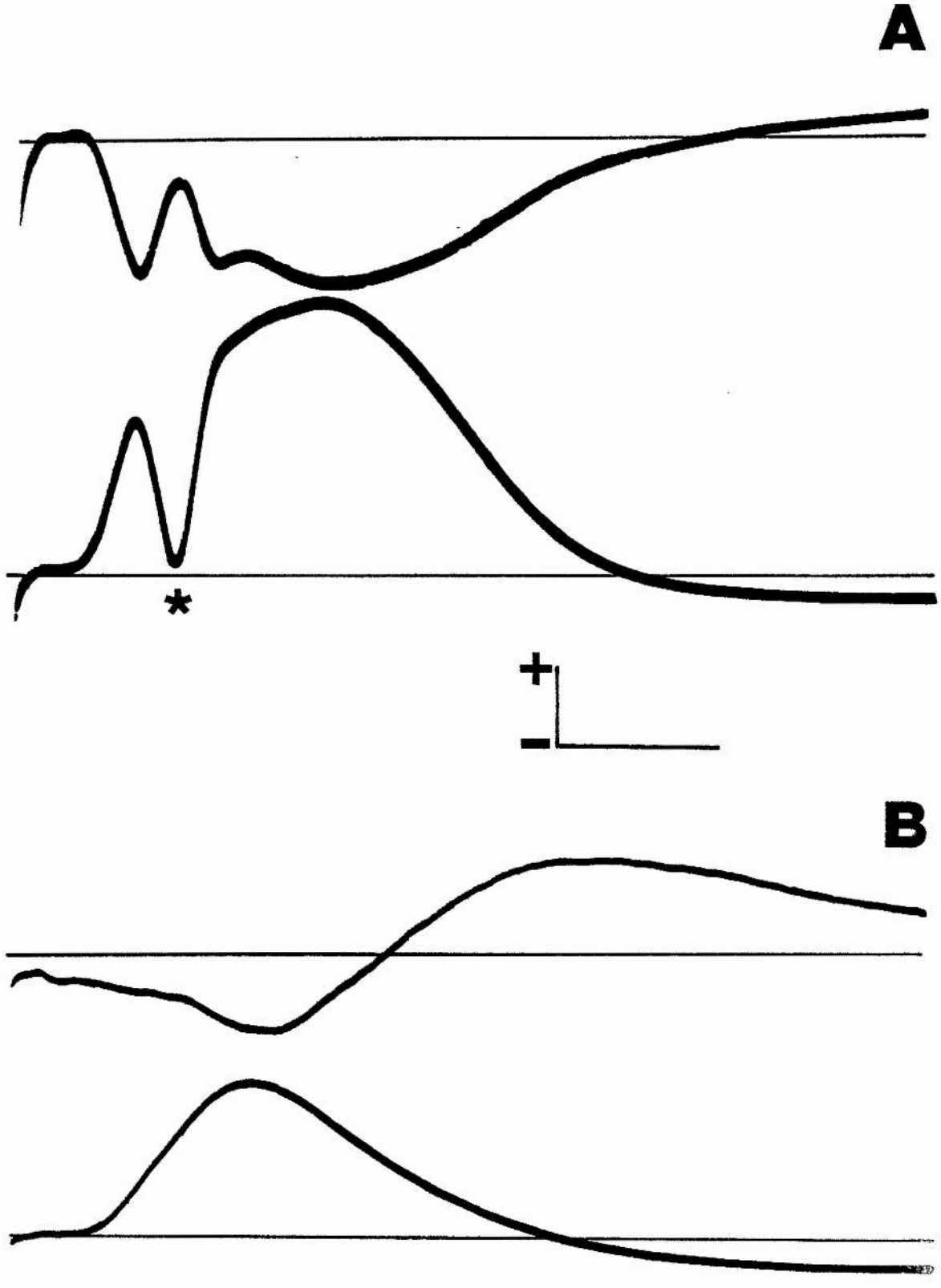
A
*
+
-
B

The first differential of the potential along the z axis multiplied by the conductivity of the brain in the z direction, gives the current flow longitudinally along the axis (Iz current). The second differential gives the change of the longitudinal current with distance ie, the transmembrane current per unit length.

Relationship between the field potential and the intradendritic voltage

In a situation where there is little secondary current, the primary current flowing adjacent to a differentially polarized neural elemental is approximately equal to the intra-elemental current, but in the opposite direction. In the dentate, after synaptic activation, the Iz current must be approximately equal to the intradendritic current flow, but in the opposite direction. Therefore, the rate of change in extracellular voltage along the z axis must be approximately proportional to minus the rate of change in intradendritic voltage at any point along the axis. This may be expressed thus;

$$2) \qquad \frac{\delta V_o}{\delta z} = -\left(r_o \; / \; r_{in} \right) * \frac{\delta V_{in}}{\delta z}$$

Where V_o is the rate of change of voltage outside the

dendrites, V_{in} is the rate of change of voltage inside the dendrites, and r_o and r_{in} are the resistances to current flow outside and inside the dendrites respectively (Rall and Shepherd, 1968) along the z axis.

In the simple case where total intradendritic axial resistance (r_{in}) is constant throughout the length of the tree and where there is a negligible radial component to the extracellular synaptic current, the extracellular potential profile is a mirror image of the intradendritic potential profile, scaled by the ratio of extracellular and intracellular resistances (assuming no concurrent synaptic activity in vertically adjacent cell fields). It is therefore clear that whatever processes alter intracellular potential distribution, will also cause corresponding changes to the field potential. The four factors which may alter the current flow inside such an dendritic tree are the internal axial resistance per unit length of dendrite (r_{in}), the resistance of a unit length of membrane to current flow across it (r_m), the resistance of the extracellular fluid per unit length (r_o), and the capacitance of the membrane per unit length (c_m). Together these properties determine the electrotonic structure of this or any other element.

Quantification of the extracellular evoked potentials in the dentate

Activation of the perforant path results in near synchronous activation of synapses in the dentate molecular layer. The magnitude of the resulting potential is proportional to the stimulus intensity, and therefore the number of afferent fibres activated (Bliss and Lomo, 1973; McNaughton et al., 1978). Low intensity stimuli evoke potentials which have been quantified by maximum amplitude measurement (McNaughton, 1982). Higher stimulus intensities evoke a population spike which is superimposed on the synaptic wave. When recording close to the cell body layer, the population spike appears as a negative going fast potential. It has been quantified in the following 2 ways. Firstly by maximum amplitude measurement, ie measuring the potential difference between the onset of the negative spike potential to its peak (Bliss and Gardner-Medwin, 1973; Lomo, 1971b); and secondly by the more sophisticated technique of computing the gradient of the line which bridges the pre and post-spike positive potential peaks. The spike amplitude is calculated as the potential difference between the peak of the spike and the voltage of the bridging line at the same latency (Douglas et al., 1982). The positive sec-

tion of the evoked potential preceding the negative spike potential, on the suprathreshold potential, is taken to be generated by synaptic current flow. It is commonly measured as a voltage at a fixed latency after stimulation, (Bliss and Gardner-Medwin, 1973; Douglas et al., 1982), or as the slope between two points of different latencies (Bliss et al., 1983).

Cable theory

The electrotonic properties of a nerve cell are the foundation on which the integration of all its synaptic currents and active responses rest. Rall's 1959 application of cable theory to spinal motoneurones was an attempt to describe the spread of current from a neurone soma into a branching dendritic tree. Modifications of the theory provided a biophysical description of the flow of intracellular current from a dendritic site to the soma (eg Rall and Rinzel, 1973), leading to a highly successful quantitative model which provided a solution to the problem of how synaptic events occurring on distal dendritic branches could affect the initial segment and soma (Rall, 1969). Similar theoretical descriptions of motoneurones, cortical cells and invertebrate cells are now numerous, eg the use of Rall's application of cable theory (Burke

and Ten Bruggencate, 1971; Jack and Redman, 1971; Iansek and Redman, 1973; Barrett and Crill, 1974; Christensen and Teubl, 1979; Turner and Schwartzkroin, 1980; Durand et al., 1983), and modelling the electrotonic structure as a set of isopotential compartments linked by ohmic resistances. In this type of model each compartment correspondins to a single region of the cell, and the more compartments there are the closer is the approximation to cable theory (Rall, 1962; Perkel and Mulloney , 1978; Perkel, Mulloney and Budelli, 1981; Edwards and Mulloney, 1984).

Application to dentate field potentials

The dorsal blade of the dentate gyrus in the dorsal hippocampus is formed of tightly packed, unipolar, granule cells. The terminal regions of entorhinal afferents are confined to the outer and middle thirds of the molecular layer, the lateral and medial entorhinal projections respectively. Radial extracellular current flow generated on synchronous synaptic activation will be negligible within an active zone, as the sheet of cells, is many times wider and longer than it is deep (around 400 um - from the tip of the dendrites to axons). Thus Nichloson and Freeman's approximation of zero radial current will apply (equation 1). As the

granule cell molecular layer abuts the hippocampal fissure and the 3rd ventricle, one might suggest that the resistance between the indifferent on the skull and the molecular layer is substantially less than the resistance from the skull to the hilus. This ratio lies in the region of between 1:3 and 1:4, figure (4-3).

Computer models

Equations and terms

Variables

x = segment number (segment units)
l = length of cable (segment units)
I = membrane current (arbitrary units)
r_m = membrane resistance per segment (arbitrary units)
r_a = internal axial resistance per segment (arbitrary units)
r_o = external axial resistance per segment (arbitrary units)

subscripts

in = segment receiving input current
o = segment immediately adjacent to current input segment

Constants

λ = cable length constant (segment units)

I_{in} is thus the current entering the cable and I_o is the current exiting the cable at the immediately adjacent segment. I_x is the current exiting the cable at any other segment defined by the number x.

Figure 4-3. Diagram of the potential profile recorded across the upper blade of the dentate by a Na^+-acetate filled glass microelectrode. Vertical steps taken are 50 um. Stimulation of the lateral perforant path (L), and medial perforant path (M) (McNaughton and Barnes, 1977). The average amplitude of 5 synaptic potentials is plotted, measured at 3 msec post-stimulus latency (M), and 5.5 msec post-stimulus latency (L). Baseline potential was taken at 1.8 msec post-stimulus latency.

The ratios of the potential generated at either side of the molecular layer, is between 1:3 and 1:4. Arrow signifies region of intense multiple-unit discharge. The diagrammatic granule cell receives lateral entorhinal input, and medial entorhinal input.

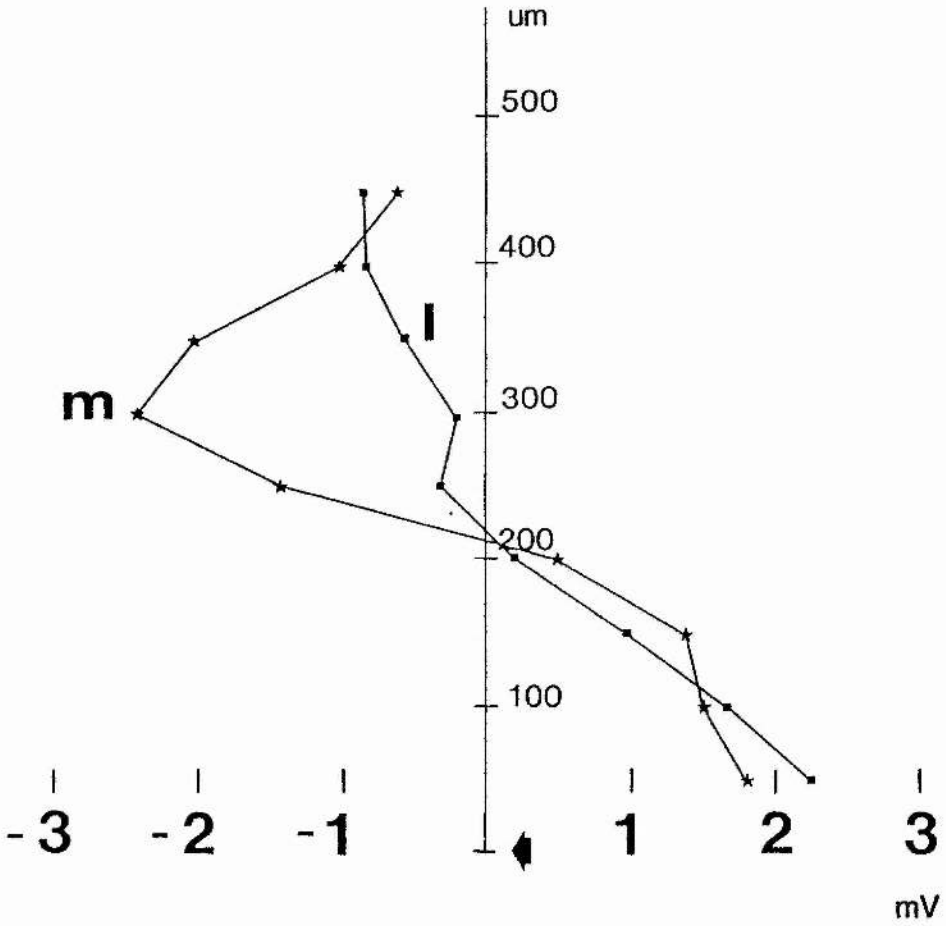
um
500
400
300
200
100
m
l
-3
-2
-1
1
2
3
mV

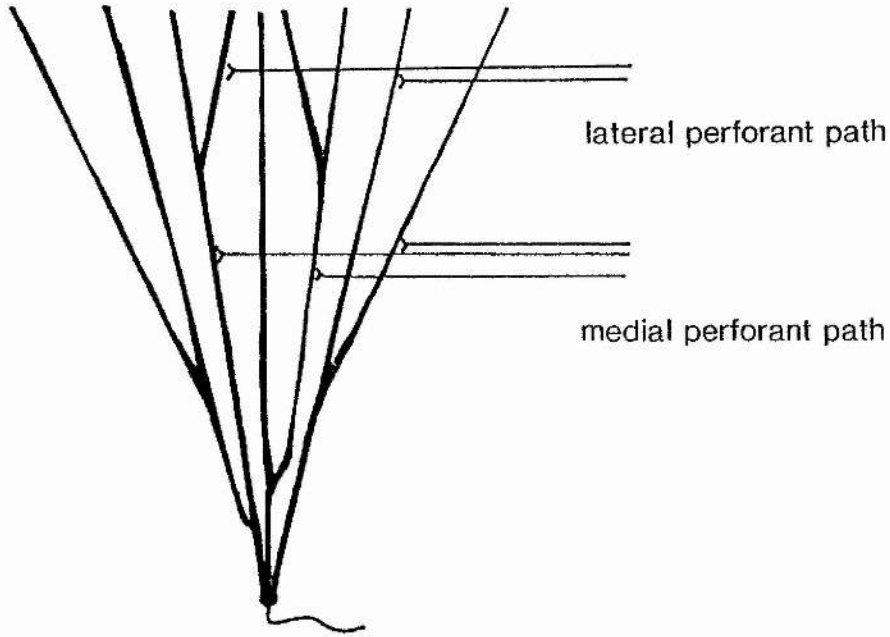
lateral perforant path
medial perforant path

Equations

semi-infinite cable, derived from Hodgkin and Rushton (1946)

3) $I_x = I_o * e^{-x/\lambda}$

4) $I_x = -(I_{in} / \lambda) * e^{-x/\lambda}$

sealed cable, derived from Rall (1959)

5) $I_x = I_o * (\cosh [(x - x_o)/\lambda] / \cosh (l / \lambda))$

6) $I_o = -I_{in} / (\lambda + x)$

As a first approximation, the dendrites of the granule cells are assumed to be non-branching and non-tapering, ie λ is constant throughout the tree As the granule cells are packed tightly into lamina, with almost totally overlapping dendritic fields, the current flow on synchronous synaptic activation would be approximated by the current flow induced in a series of parallel cables, with the correct electrotonic characteristics. It is assumed that a single afferent synapses onto all dendrites at the same electrotonic distance from the soma. Thus a granule cell dendritic tree is represented as a single cable, receiving synaptic input at specific localities along its length, figure 4-4. Durand et al. (1983) have measured the dendritic electrotonic length as 1.1 λ . The figure of

Figure 4-4A. Cable structure, such as a dendrite, with a synapse located at one end. r_{Sy} represents the internal resistance of the synapses - modulated by changes in the number of conducting ionophores in the postsynaptic membrane. The emf in the circuit is generated by the transmembrane electrochemical gradient for the ion species employed. V1, V2 and V3 are values of potential in the extracellular fluid generated on synaptic activation.

Figure 4-4B. diagrammatic representation of a dendritic cable with lumped somatic impedance. Ignoring capacitance in dc conditions, the soma is represented by a resistance R_S. The arrow represents the point of current entry.

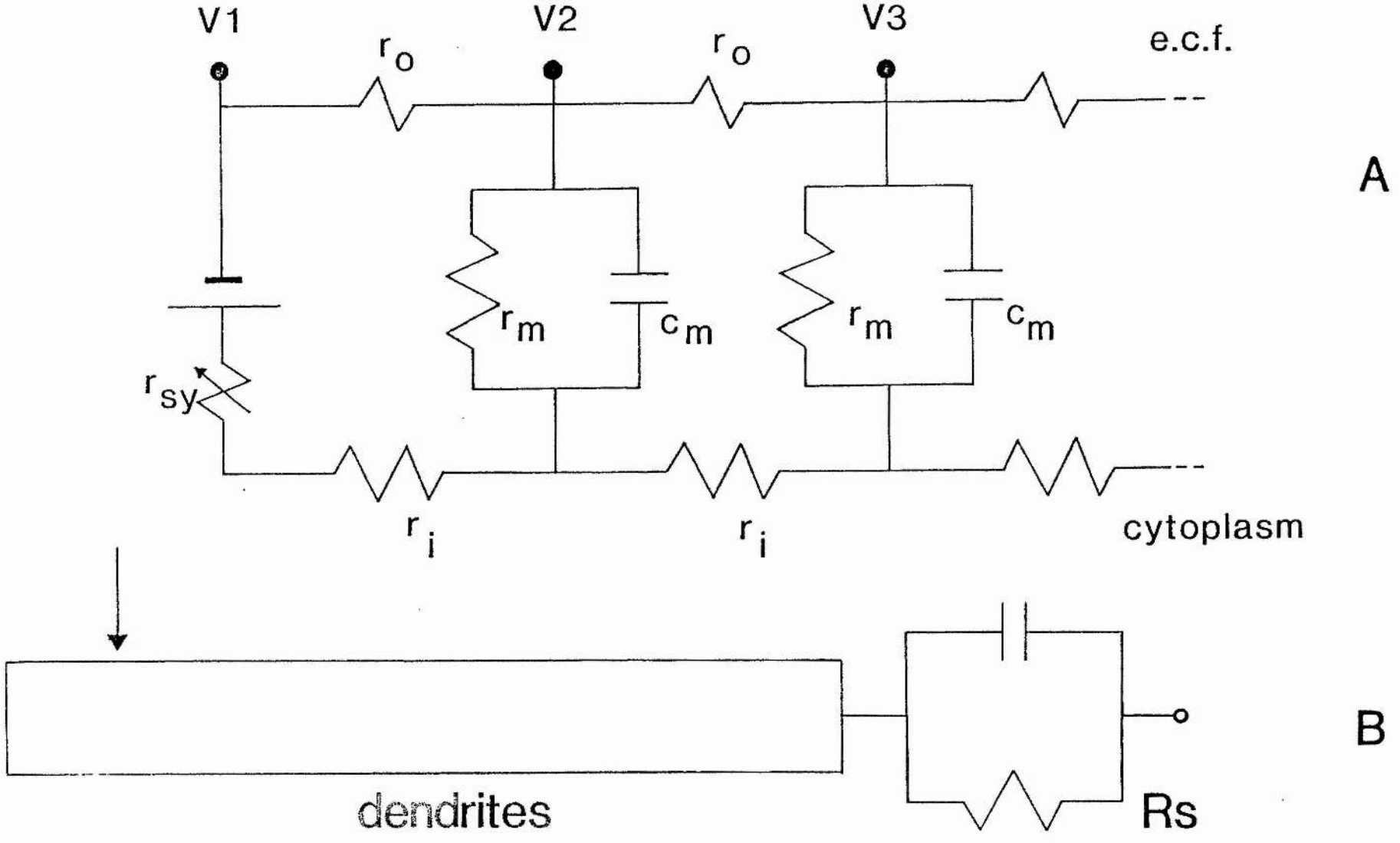
V1
V2
V3
r_o
r_o
e.c.f.
A
r_m
c_m
r_m
c_m
r_{sy}
r_i
r_i
cytoplasm
dendrites
Rs
B

1 λ has been used in the model, and is compared with leakier dendrites 5 λ long, for reasons clarified below.

For the purposes of computation a cable is considered to be divided into a series of segments . A segment is assumed to have a spatially uniform membrane potential. Two types of dendritic cable have been used. Firstly a sealed cable, assuming no axial current flow out of the dendrites at both the distal and somatic ends. Secondly a cable with low axial resistance at the soma end has been used. Here the soma end resistance is equal to that of an infinitely extended cable, while the distal end is sealed as before. This is referred to as a semi-infinite cable.

Where the distance between the point of current input into the cable and the sealed end is $\ll \lambda$, transmembrane voltage decrement with distance between the input segment and the seal is ignored in an approximation of I_o. In the semi-infinite cable a good approximation of I_o in the segments immediately adjacent to the input segment (on both sides) is given by, equation 6, where x is the number of segments between the current input segment and the sealed end. Where both ends of the cable are sealed, and the distances to the ends are both $\ll \lambda$, then equation 7 can be derived.

7) $I_o = - I_{in} / (1 - 1)$

Modelling synaptic activation of the lateral and medial entorhinal projections to the dorsal blade dentate granule cells

A granule cell dendritic tree is represented as a cable 30 segments long , the soma as 2 segments and the axon initial segment as 1 segment (together representing R_S, ie the total resistance to current flow out of the proximal end of the cable including axial and membrane resistances). In order that the positive and negative voltage maxima of the resultant field potential be fully contained within the 'observed' length of cable, when it is treated as semi-infinite, the transmembrane current at the 3 soma - axonal segments is made to account for that source current not exiting the dendritic cable, thus total inward and outward membrane current over the 33 segments is equal. A field potential profile may therefore be generated from the transmembrane current by a process of double integration using an integrating polynomial (eg the trapezoidal rule). The zero point of the first integral is that point where inward and outward transmembrane currents, along the z-axis, are equal on both sides. This gives the Iz - the extracellular axial current flowing adjacent to the cable as shown in figures 4-8 and 4-9. The second integral waveform is

considered a dipole, the terminating potentials at both ends determining the potential of the indifferent.

Lateral

Activation of the outer third of the granule cell dendrites was modelled by sink current entering the distal 11 segments of the cable. Sequential computation of the source current complementing each point sink was carried out in both directions and the current summed algebraically.

Using a normally distributed sink current, $\sigma = 1.8 * x$, the resultant sink/source is similar in profile to the sink/source distribution reported by Jeffreys (1979, his figure 1e) on transmembrane current analysis in the hippocampal slice. The results for R_s = infinity, ie a sealed ended cable, are given in figures 4-5 and 4-7. Where the somatic and axonal conductance is equal to that provided by an infinite cylindrical extension, with the same electrotonic characteristics as the dendritic cable, the situation can be modelled as a semi-infinite cable, figure 4-5.

Figure 4-5. Lateral perforant path activation.

a. Transmembrane current and corresponding field potential profile in a uniform finite cable 1 λ long. Current and voltage profiles generated with r_m set to r_m^* 1, r_m^* 2, r_m^* 5 as above. Notice that increasing the membrane resistance proportionally reduces the synaptic current flow, and reduces the magnitude of the field potential.

b. Transmembrane current and corresponding field potential profile in a uniform semi-infinite cable - where the dendrites are exactly 1 λ long, and the resistance of the soma, R_s, is equivalent to an infinite extension of the cable. r is set to r_m^* 1, r_m^* 2 and r_m^* 5, as above. Notice that increasing r_m causes a substantial shift in the point of potential reversal.

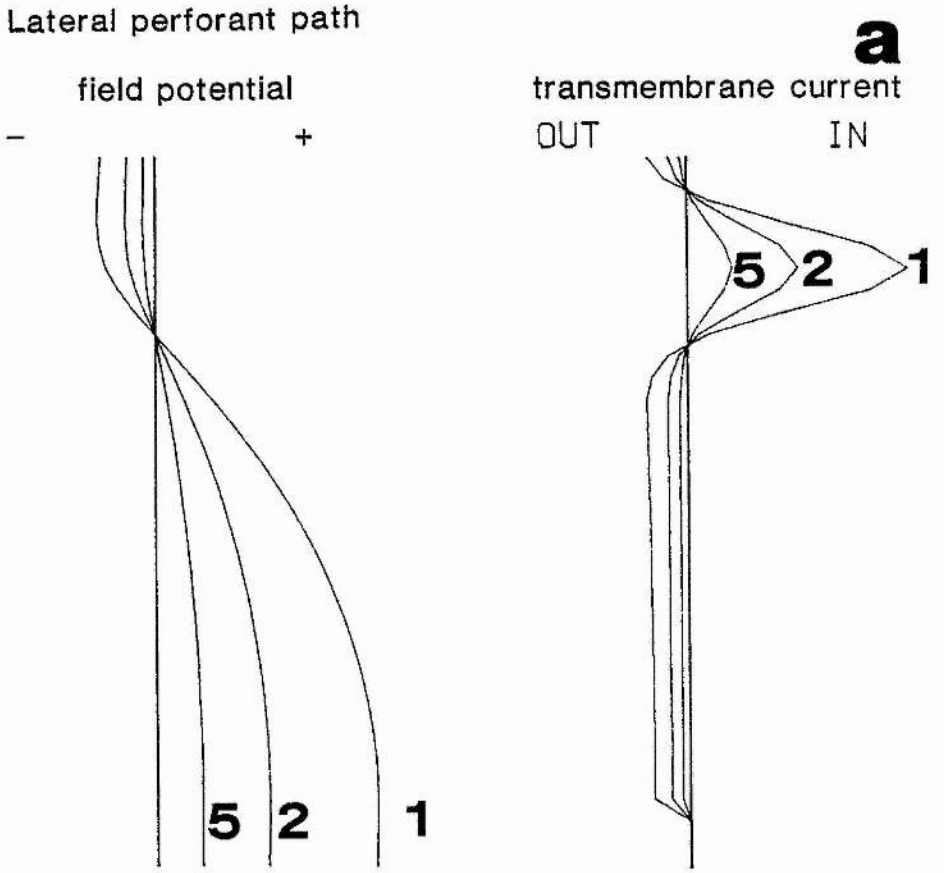

SEALED-END CABLE

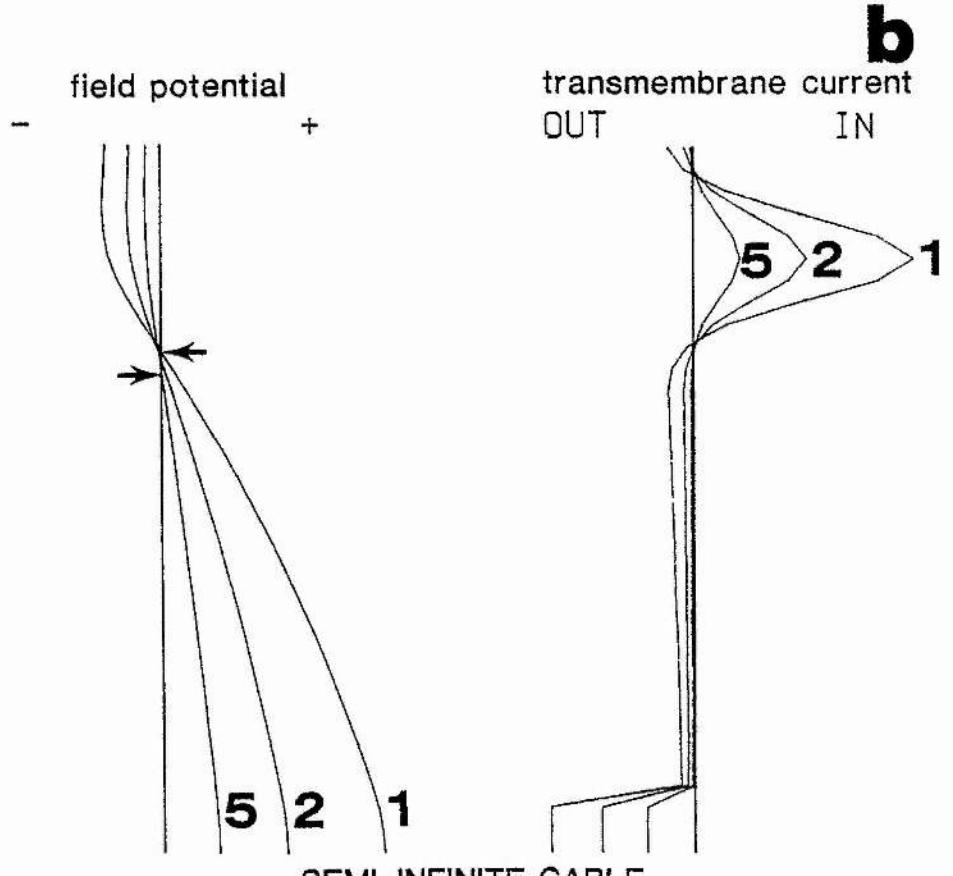

SEMI-INFINITE CABLE

Figure 4-6. Medial perforant path activation.

a. Transmembrane current and corresponding field potential (corrected for CA1 sink 2° current) in a uniform finite cable 1 λ long. r_m is set to r_m^* 1, r_m^* 2 and r_m^* 5. It is assumed that there are similar resistance changes occurring in CA1.

b. Transmembrane current and the corresponding field-potential in a uniform semi-infinite cable - where the dendrites are exactly 1 λ long and the resistance of the soma, R_s, is equivalent to an infinite extension of the cable. r_m is set to r_m^* 1, r_m^* 2, r_m^* 5 as above.

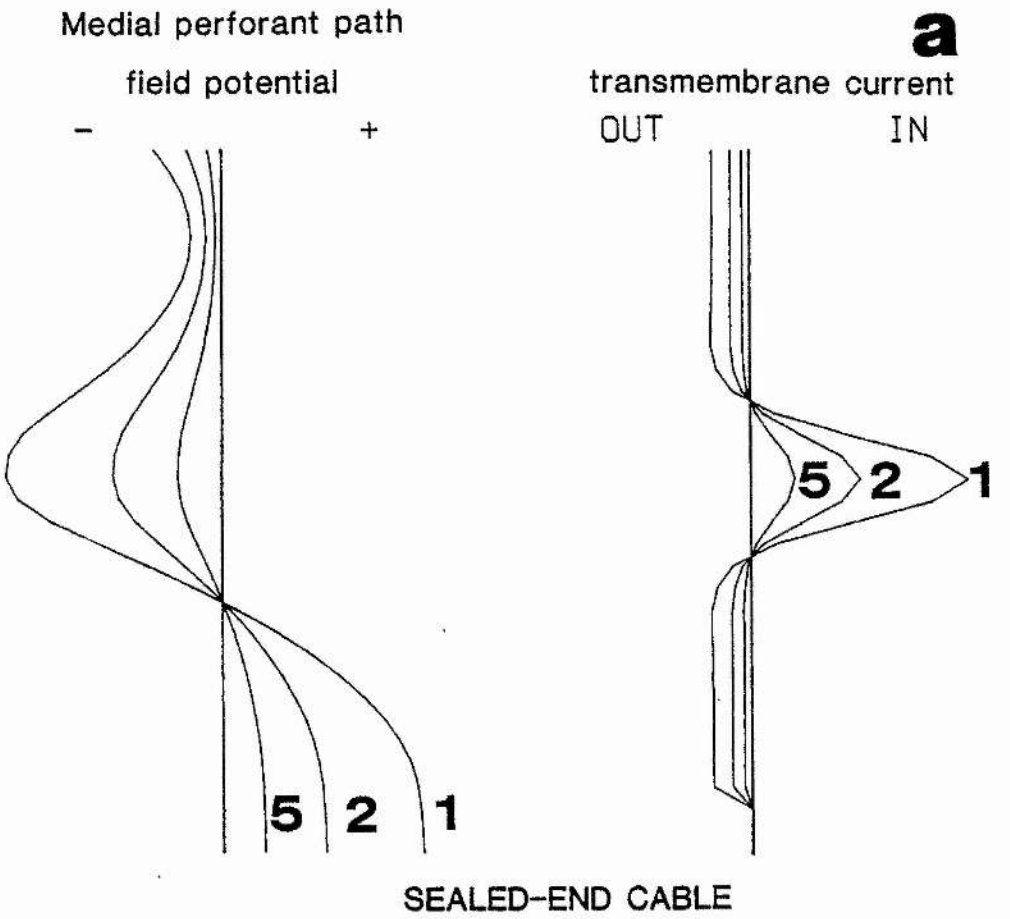
Medial perforant path
field potential
a
transmembrane current
OUT
IN
5
2
1
SEALED-END CABLE
b
field potential
transmembrane current
OUT
IN
5
2
1
SEMI-INFINITE CABLE

Medial

Activation of the middle third of the granule cell dendrites was modelled by sink current entering from segment 11 to segment 21 of the equivalent cable with a sink current intensity distribution as above. The results for R_s = infinity are given in figure 4-6. The medial entorhinal cortex in the rat not only projects to the dentate , but also to the CA1-CA2 pyramidal cells, (Steward, 1976; Wyss, 1981), which lie dorsal to the upper blade of the dentate. Therefore the secondary current of a simultaneous sink beyond the distal end of the equivalent cable must be allowed for when estimating the resulting field potential. This has the effect of attenuating the magnitude of the current flowing towards the sink on the dendritic cable, from the distal end, as current summates linearly.

The assumption is made in the estimate of the medial entorhinal projection field potential that reciprocity exists between the magnitude of the 2° current associated with synaptic activation in regio-superior and the Iz current (see below) of the dentate induced by activation of synapses on granule cells. In other words, the number of active synapses in the dentate and CA1 are assumed to proportionally co-vary. This seems reasonable as changes in the

Figure 4-7. Lateral perforant path activation.

a. Transmembrane current and the corresponding field potential generated in a finite, sealed ended cable. The cable is 5 λ long. If one compares with figure 4-4, the most marked difference is the proportion of current exiting the cable close to the sink region. This is therefore a better approximation of the granule cells than the finite cable only 1 λ long.

b. Close up of field potential.

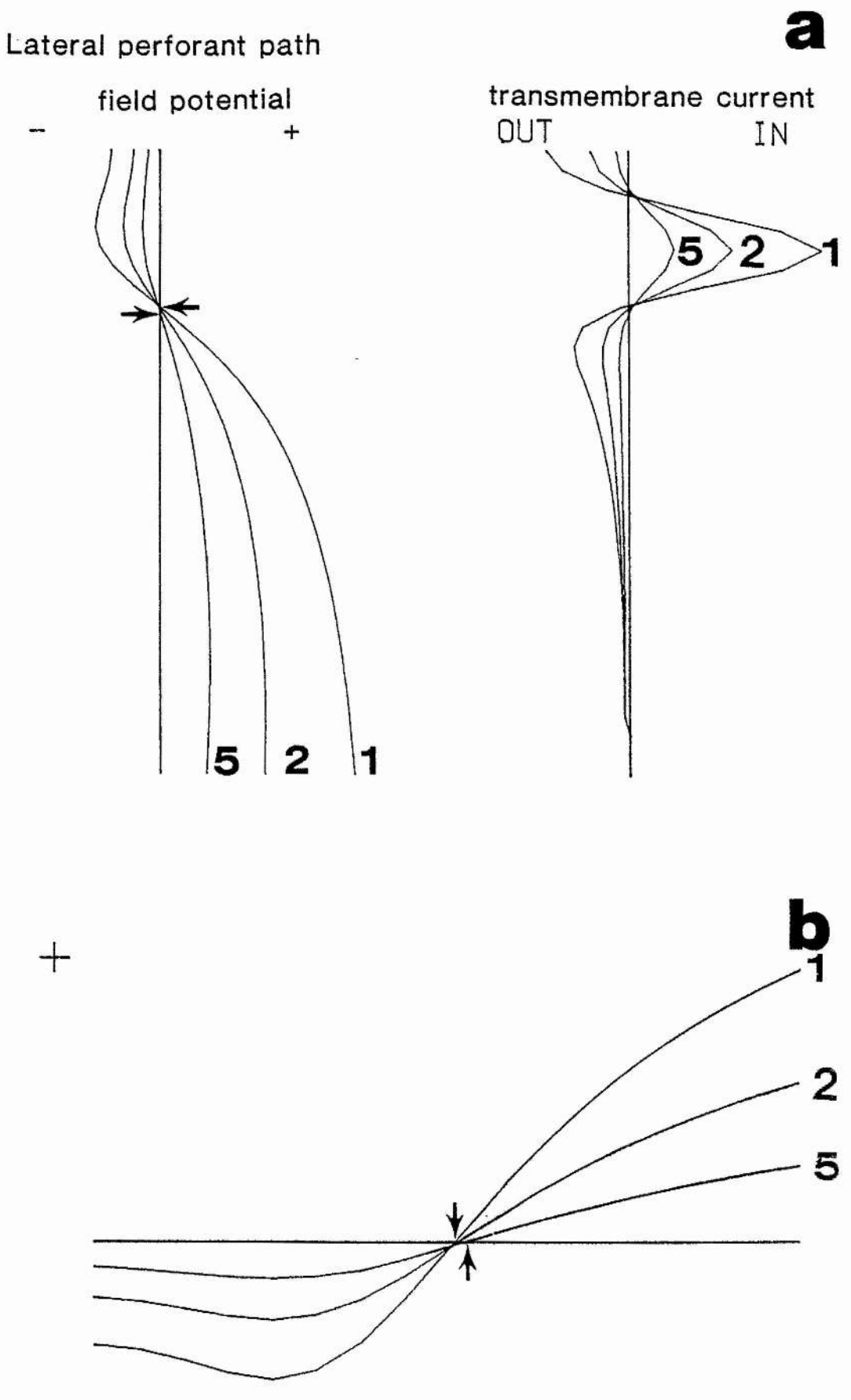
Lateral perforant path
a
field potential
−
+
5
2
1
transmembrane current
OUT
IN
5
2
1
b
1
2
5

Figure 4-8. Diagram of the transformation between transmembrane current (Im) and field potential profile (Vz) in a population of parallel cylindrical elements. The final potential is divided so that the integral of the potential = 0.

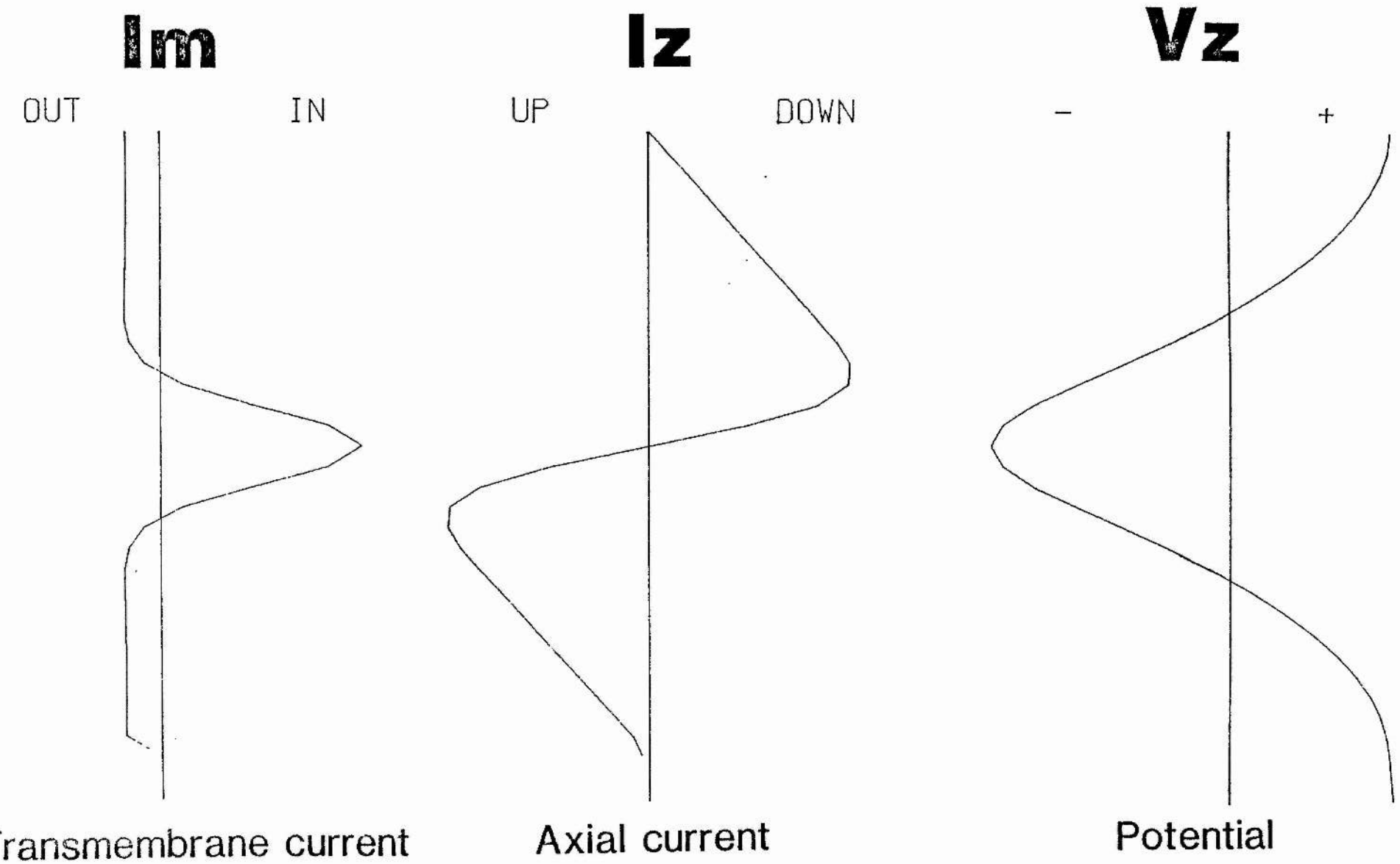
Im
OUT
IN
Transmembrane current
Iz
UP
DOWN
Axial current
Vz
−
+
Potential

Figure 4-9. Similar diagram to fig. 4-8, except here the axial current (Iz) is corrected for the presence of another sink adjacent to the distal end of the cable. The corresponding field potential profile is divided in a 1:4 ratio.

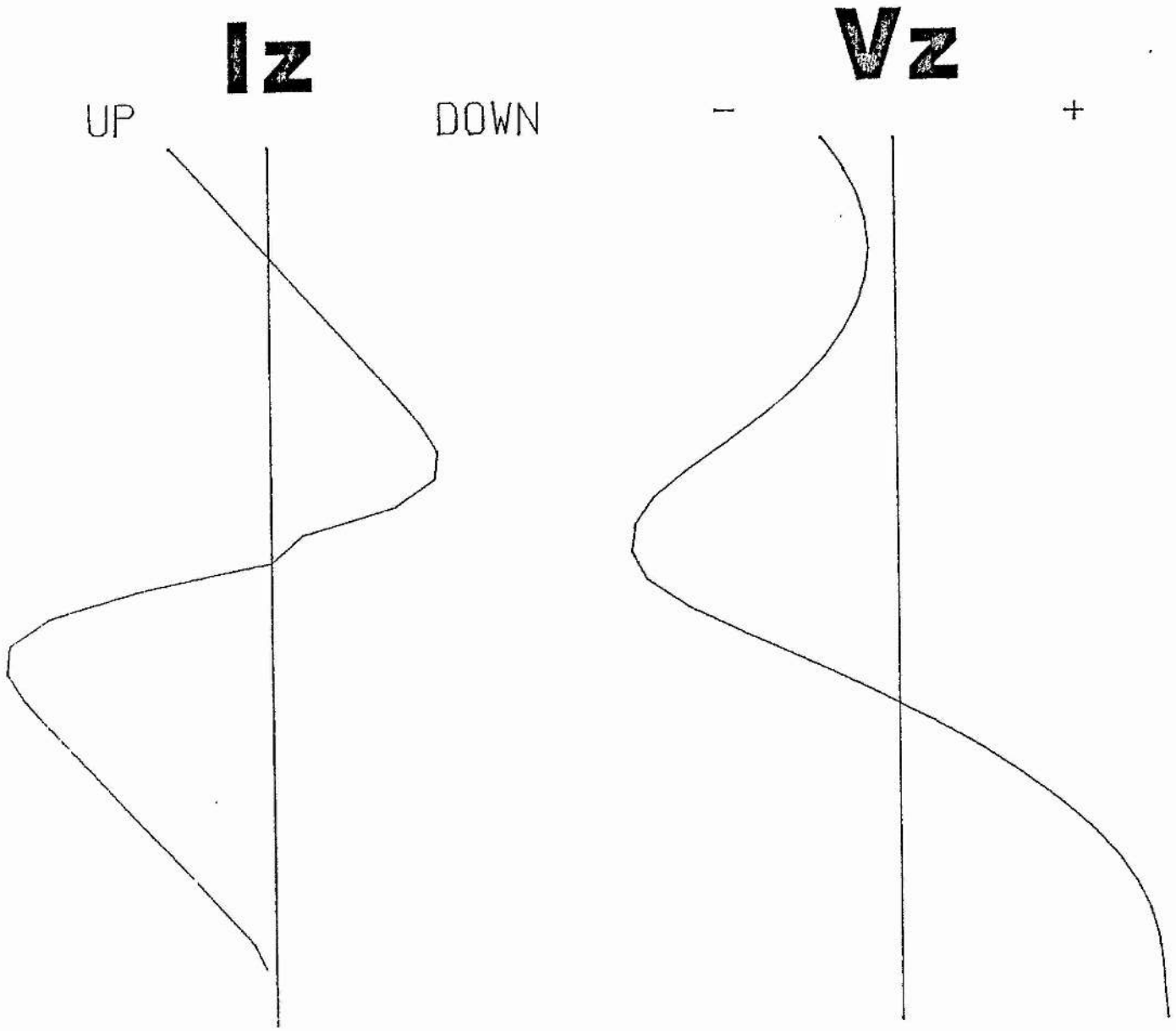
Iz
UP
DOWN
Vz
−
+
Corrected axial current
Potential

activity of both subsets of projecting fibres will co-vary on non-specific electrical stimulation in the region of the angular bundle. The effect of the CA1 sink has been demonstrated by suction removal of regio superior in the rabbit, Lomo (1968, his figures 3 and 12).

Variables in the model

Input conductance

Changes in the evoked release of transmitter, the numbers of synapses activated or the number of open ion channels will modify the input conductance of the receptive dendritic membrane in the target region. Input conductance changes can be modelled by varying the sink intensity.

Membrane resistance

Increases or decreases in membrane resistance will change; a) The length constant, λ, of the cable and b) the total amount of current flow. The length constant is proportional to the $\sqrt{r_m}$. Therefore as r_m increases, λ increases; eg r_m increasing by a factor of 2 means λ increases by a factor of 1.4.

At each point along a dendrite or equivalent cable, the steady state transmembrane current follows Ohm's law, ie current is inversely proportional to membrane resistance. Per 10 um segment of granule cell dendrite or equivalent cable the membrane resistance, r_m , is about 1000 times greater than r_a , the core resistance (calculated from Durand et al., 1983). r_a has therefore been ignored for the purposes of scaling the total current flow with membrane resistance, figure 4-4, resulting in an inverse relation between the total current flow and the membrane resistance.

Assuming that the extracellular conductivity of the brain remains constant the relative changes in both input conductance and membrane resistance give rise to waveforms which can be compared directly.

Shortcomings of the model

Non-linear membrane current/voltage relationship

Excitable membranes do not behave as simple resistance-capacitance networks. They incorporate voltage sensitive conductances, so the relationship between transmembrane voltage and current is non-linear. In

general, depolarization of a cell causes a reduction in the membrane resistance. The model does not account for differential depolarization within the dendritic tree and if there was substantial non-linear behaviour, one would expect a differential lengthening in the electrotonic length near the synaptic region, ie the distal dendrites, being predominantly affected. In simple terms, the distal dendrites would be made leakier to current. Hence, modelling the granule cells as a series of cables of longer than 1.1λ, eg 5λ, is an informative comparison.

Current transients

The model is based on equations describing current flow under dc conditions. Synaptic current flow becomes less dependent on the membrane resistance as the duration of synaptic conductance increase is reduced and the current becomes progressively more capacitative. The attenuaton of current flow along a cable is also frequency dependent, because the transverse impedance is less when current flow is transitory. This will mean that the synaptic/soma attenuation factor is greater when current flow is transitory, than in the steady state. A transmembrane voltage profile set up in an infinite cylindrical ele-

ment by a localized current transient, is described by a Δ function (Jack, Noble and Tsein, 1983, p46, 77, 164-167).

Improved model

Durand et al. (1983), have shown that the dendritic branching power of the granule cell is 1.56 (given by $d_1^n = d_2^n + d_3^n$, where d_1 is the parent dendrite diameter, d_2 and d_3 being the daughter dendrite diameters and n the branching power) , and is constant throughout the tree. The dendrites can thus be electrotonically represented as a continuous cable. As Desmond and Levy (1982) found that the dendritic branching ratio is close to 2 (ie a parent dendrite gives rise to around two daughter dendrites), the two major insufficiencies of the first model, ie the increasing surface area of the dendritic tree with distance from the soma, and the increasing total dendritic axial resistance with distance from the soma, can be overcome.

The cable representing the dendrites is divided into 3 segments, each representing orders of dendritic branching, and each having a length equal to the anatomical length of the corresponding order of dendrites.

Only 3 orders of branching are represented because, on average, the dendritic tree has two major regions of branching, at about 60 um and 180 um from the cell body. The first order dendrites are so short (on average only 9 um) they can be ignored. The ratio of the number of dendrites before and after both major branch points is close to 1:2. Each cable segment has slightly different electrotonic properties from its neighbours, characterised by a long length constant at the soma end, and a short length constant at the distal end; ie the distal dendrites are significantly more leaky to current than the proximal.

Taking the branching ratio to be 2, with non tapering dendrites the axial resistance to current flow, r_a, across the dendritic tree will not increase, before and after branch points. Conversely, the membrane resistance per unit length of dendritic tree will decrease in the ratio 1 : .7, as the area of membrane per unit length increases. Therefore, assuming the intradendritic axial resistance to current flow is much greater than the extracellular resistance the ratio of λ before and after a branch point is 1 : .83. This is because;

$$\frac{\lambda_{after}}{\lambda_{before}} = \frac{\sqrt{.7}}{1} = .83$$

The total electrotonic length of the dendrites must be made to equal 1.1λ , the length measured by Durand et al. (1983). This is diagrammatically expressed in figure 4-10. The resistance at the soma end of the dendrites is best thought of as being infinite (ie a sealed end), as the mossy fibres are only about 1 um in diameter. When there is no concurrent synaptic activation in vertically adjacent cell fields, eg on activation of lateral perforant path fibres, the intracellular potential profile generated by current entering this model dendritic tree can be scaled by the ratio of extracellular and intradendritic resistances at all points along the dendrites, giving a field potential profile for steady state conditions.

Results

The results from the uniform cables may be summarised as follows:

Figure 4-10. Model of a granule cell dendritic tree. The dendritic tree orders of branching refers to the order of the dendrites observed at the appropriate distances away from the granule cell body. Although the order of branching given for the distal section is 5<, fifth order and above are not always attained by a dendrite. The first order dendrites are ignored because of their short lengths. The two major branching regions are modelled as changes in the characteristics of the cable. The lengths of the cable sections are given beneath. The total dendritic length is 1.1 λ (Durand et al., 1983). The electrotonic lengths of the cable segments become .16 λ, .42 λ and .52 λ. Notice that almost half of the electrotonic length of the cable is confined to the distal one third.

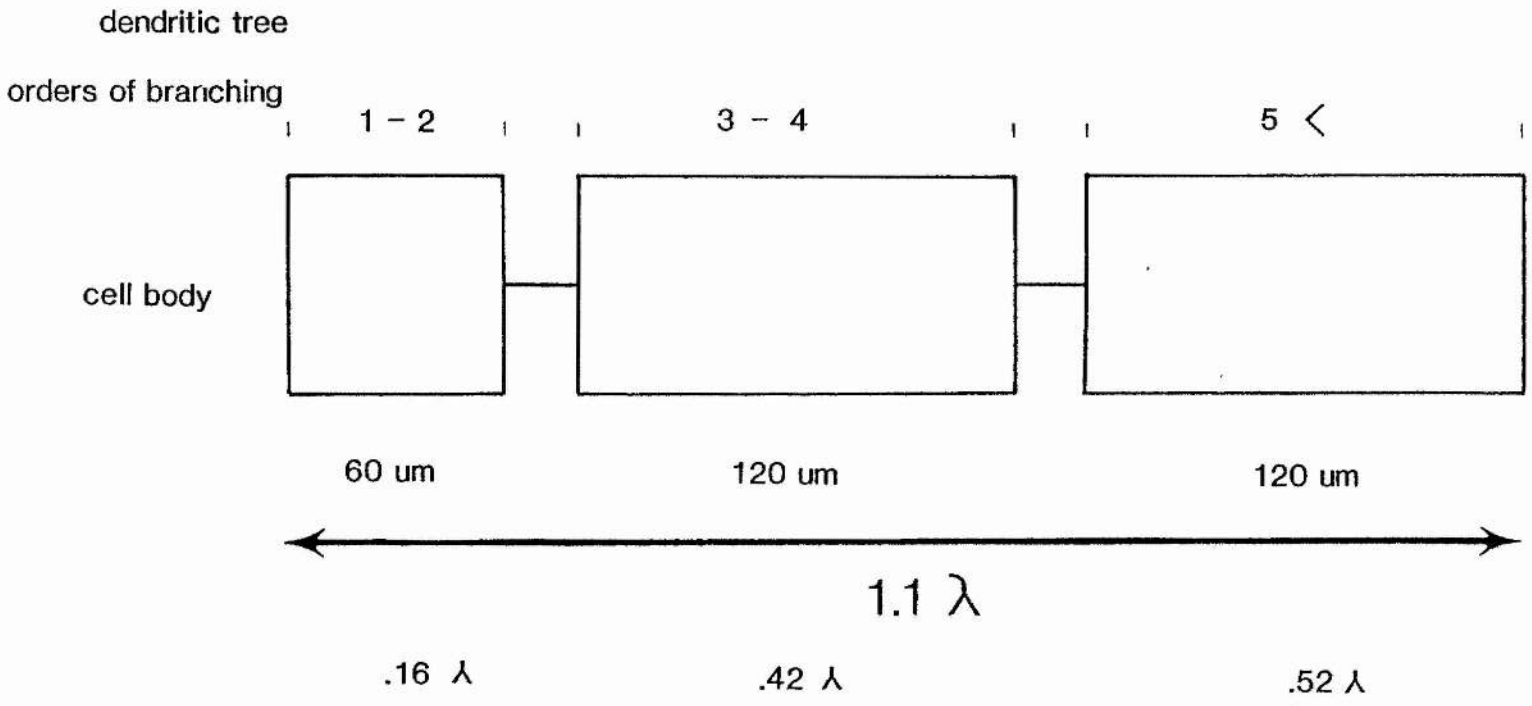
dendritic tree
orders of branching
1 – 2
3 – 4
5 <
cell body
60 um
120 um
120 um
1.1 λ
.16 λ
.42 λ
.52 λ

a) The magnitude of the extracellular dipole varies directly with the amount of current flowing on synaptic activation.

b) The amount of current flow varies inversely with the cable membrane resistance. (This generalization will also apply to transients, but the degree of proportionality will decrease with increasing transient frequency).

c) Alterations in the amount of current flow (eg on facilitation of transmitter release), without altered sink distribution (which might occur with recruitment of synapses), does not affect the position of the potential-reversal point on the z-axis.

d) Increased cable membrane resistance reduces the size of the extracellular dipole and causes the potential reversal point to approach the soma end, the amount of movement is increased by expansion of the length of cable between the synaptic region and the sealed soma end, being maximal when the somatic output impedance is equivalent to an infinitely extended cable. This is because the distribution of source current between the sink and the end of the cable is the critical factor in determining the position of the reversal point on the z-axis, the distribution being more profoundly affected

by membrane resistance changes when the impedance to current flow away from the sink is low.

Discussion

Previous theoretical discussion on the generation of evoked potentials in the dentate (McNaughton, 1980), has been based on the assumption that the potential recorded close to a region of an element with a non-uniform membrane potential, is proportional to the transmembrane current in that locality. In the case of low-resistance metal or glass electrodes penetrating the brain, potentials are recorded which are generated by current flow between differentially polarized elements and, or regions of elements. The situation is complicated further by the indifferent electrode being within the resulting potential field, on a secondary current path, and causing a potential divide. It would therefore not be true to say that the potential recorded in a volume conductor, in this way, is proportional to the local transmembrane current.

Changes in evoked potential shape, predicted by such a model with alteration of the dendritic characteristics, may provide insights to dendritic function

which is impossible or difficult to quantify intracellularly. Future difficulties may be experienced in creating an accurate model of field potential generation, which may be overwhelming. It may be useful only to apply such techniques to an in vitro preperation, such as the slice or the mini-slice.

Computer programs

Current sink at distal end of a semi-infinite cable

```
 100 DIM A(32),B(32),B1(32),B2(32)
 110 FOR J%=0 TO 32 \ A(J%)=0 \ B(J%)=0 \ NEXT J%
 120 FOR J%=0 TO 32 \ B1(J%)=0 \ B2(J%)=0 \  NEXT J%
 130 PRINT "Lambda"; INPUT W%
 140 REM CURRENT SINK \ A(5)=100 \ FOR J%=6 TO 10 \
 A(J)= A(5)*EXP(-(J%-5)**2/(2*1.8**2)) \ NEXT J%
 150 FOR J%=4 TO 0 STEP -1 \ A(J%)=A(5)*
 EXP(-(5-J%)**2/(2*1.8**2)) \ NEXT J%
 160 REGION ("UPPER",1) \ GRAPH (,,,A(),,,1) \ REM
 CALCULATION OF SOURCE CURRENT TOWARDS INFINITE
EXTENSION
 170 FOR K%=0 TO 10 \ B(K%+1)=-A(K%)/(W%+K%) \
 FOR J%=K%+2 TO 29 \
 X=J%-K% \ B(J%)=-(A(K%)/(W%+K%))*EXP(-X/W%)
 180 NEXT J% \ B(K%)=0 \ FOR J%=0 TO 29\ B1(J%)
=B(J%)+B1(J%) \ NEXT J% \  NEXT K%
 190 REM  CALCULATION OF SOURCE CURRENT TOWARDS SEALED
 END \ FOR K%=10 TO 1 STEP -1
 200 T1=-A(K%)/29 \  B2(K%-1)=T1 \ FOR J%=K%-2
TO 0 STEP -1\ L=K%+1 \  X=L-(K%-J%)
 210 B2(J%)=T1*(.5*(EXP(X/W%)+EXP(-X/W%)))/
(.5*(EXP(L/W%)+EXP(-(L/W%))))
 220 NEXT J% \ B2(K%)=0 \ FOR J%=0 TO 29 \ B1(J%)=
 B2(J%)+B1(J%) \  NEXT J% \ NEXT K%
 230 REGION ("LOWER",2) \ GRAPH(,,,B1(),,,2) \ X=0 \
FOR J%=0 TO 10 \ X=A(J%)+X \ NEXT J%
240 Y=0 \ FOR J%=0 TO 29 \ Y=B1(J%)+Y \ NEXT J%
\ Z=-(X+Y)/3
 250 PRINT "Return"; \ LINPUT R$ \ FOR J%=0 TO 29 \
 B(J%)=A(J%)+B1(J%) \ NEXT J%
 260 B(30)=Z \ B(31)=B(30) \ B(32)=B(30)
 270 GRAPH("SHADE, LINES",,,B(),,0,2) \ LABEL
 (,"Resultant sink/source") \ STOP
```

Current sink in the middle third of a double sealed-end cable.

```
 100 DIM A(32), B(32), B1(32), B2(32), B3(32), B4(32)
 110 FOR J%=0 TO 32 \ A(J%)=0 \ NEXT J% \  FOR J%=0 TO 32
 \ B1(J%)=0 \ NEXT J%
 120 FOR J%=0 TO 32 \ B2(J%)=0 \  NEXT J% \ FOR J%=0
TO 32 \ B3(J%)=0 \ NEXT J%
 130 PRINT "Lambda"; INPUT W%
 140 A(15)=100 \  FOR J%=16 TO 20 \ A(J%)=A(15)*
EXP(-(J%-15)**2/(2*1.8**2)) \ NEXT J%
 150 FOR J%=14 TO 10 STEP -1 \ A(J%)=A(15)*
EXP(-(15-J%)**2/(2*1.8**2)) \ NEXT J%
 160 REGION("UPPER",1) \ GRAPH(,,,A()) \ REM CALCULATION
 OF SOURCE CURRENT IN ONE DIRECTION
 170 FOR K%=10 TO 20 \ T=-A(K%)/29 \ B(K%+1)=T \ FOR
 J%=K%+2 TO 29 \ L=30-(K%+1) \ X=L-(J%-K%)
 180 B(J%)=T*(.5*(EXP(X/W%)+EXP(-X/W%)))/(.5*
 (EXP(L/W%)+EXP(-L/W%))) \ NEXT J%
 190 B(K%)=0 \ FOR J%=0 TO 29 \ B1(J%)=B(J%)+B1(J%) \
 NEXT J% \ NEXT K%
 200 REM CALCULATION OF SOURCE CURRENT OPPOSITE
DIRECTION \ FOR K%=20 TO 10 STEP -1
 210 T1=-A(K%)/29 \ B2(K%-1)=T1 \ FOR J%=K%-2 TO 0
STEP -1 \ L=K%+1 \ X=L-(K%-J%)
 220 B2(J%)=T1*(.5*(EXP(X/W%)+EXP(-X/W%)))/(.5*
(EXP(L/W%)+EXP(-L/W%))) \ NEXT J%
 230 B2(K%)=0 \ FOR J%=0 TO 29 \ B3(J%)=B2(J%)+B3(J%)
 \ NEXT J% \ NEXT K%
 240 FOR J%=0 TO 32 \ B2(J%)=B1(J%)+B3(J%) \ NEXT J%
 250 REGION ("LOWER",2) \ GRAPH(,,,B2(),,,2)
 260 PRINT "Return"; LINPUT R$ \ FOR J%=0 TO 32 \
 B4(J%)=A(J%)+B2(J%) \  NEXT J%
 270 GRAPH("SHADE,LINES",,,B4(),,0,2) \ LABEL
 (,"Resultant sink/source",,2) \  STOP
```

CHAPTER 5

MATERIALS AND METHODS

Experimental surgery

All experiments were acute, performed on adult male Hooded-Lister rats. Anaesthesia was induced with urethane (1.3g/kg), administered I.P., and maintained with subsidiary doses via the same route. The depth of anaesthesia was sufficient to completely abolish flexor and corneal reflexes.

Before mounting an anaesthetized animal into a stereotaxic frame, the trachaea was exposed by an incision just caudal to the larynx. The trachea was incised and cannulated with a length of resilient polythene tubing, the exposed length of tube being securely sutured to the skin of the neck, and the wound closed. This allowed the animal to breath easily throughout the experiment. Animals were held in a Kopf, Horsley-Clarke, stereotaxic with skull bregma and

lambda horizontal. The left dorsal hippocampus and the ipsilateral angular bundle were penetrated by electrodes inserted through square windows in the skull, opened using a dental drill. Care was taken not to break the dura with the drill head. Two indifferent electrodes (female Amphenol pins soldered to 10 BA steel screws), were screwed into the skull over the right side of the cerebellum and the cortex, figure 5-1. Body temperature was held between 36 and 38 C using a heated operating table and monitoring rectal temperature using a rectal thermometer (Digitron Instrumentation).

Stimulation

Stimulation was achieved using a single 110 um outer diameter stainless steel, Teflon coated wire (Medwire, Clark Electromedical), attached to a female Amphenol pin, carried on a stereotaxic manipulator. The wire was inserted into the brain after cutting the dura. All stimuli consisted of constant current, cathodal, monophasic square waves, from a Neurolog system NL 510 pulse buffer, delivered via an NL 800 stimulus isolator. The maximum stimulus current used was 350 uA, stimulus durations ranging between 3 and 100 usec, depending on the experimental arrangement.

Figure 5-1. With the skull horizontal, the animal's head is held in a steriotaxic frame and two windows (W) are opened in the skull overlying the left cortex, after removing the periosteum (P).

Two indifferent electrodes (I) are screwed into the skull over the cerebellum and the right cortex.

B. Bregma

L. Lambda

X. Saggital suture

Y. Coronal suture

Z. Lambdoidal suture

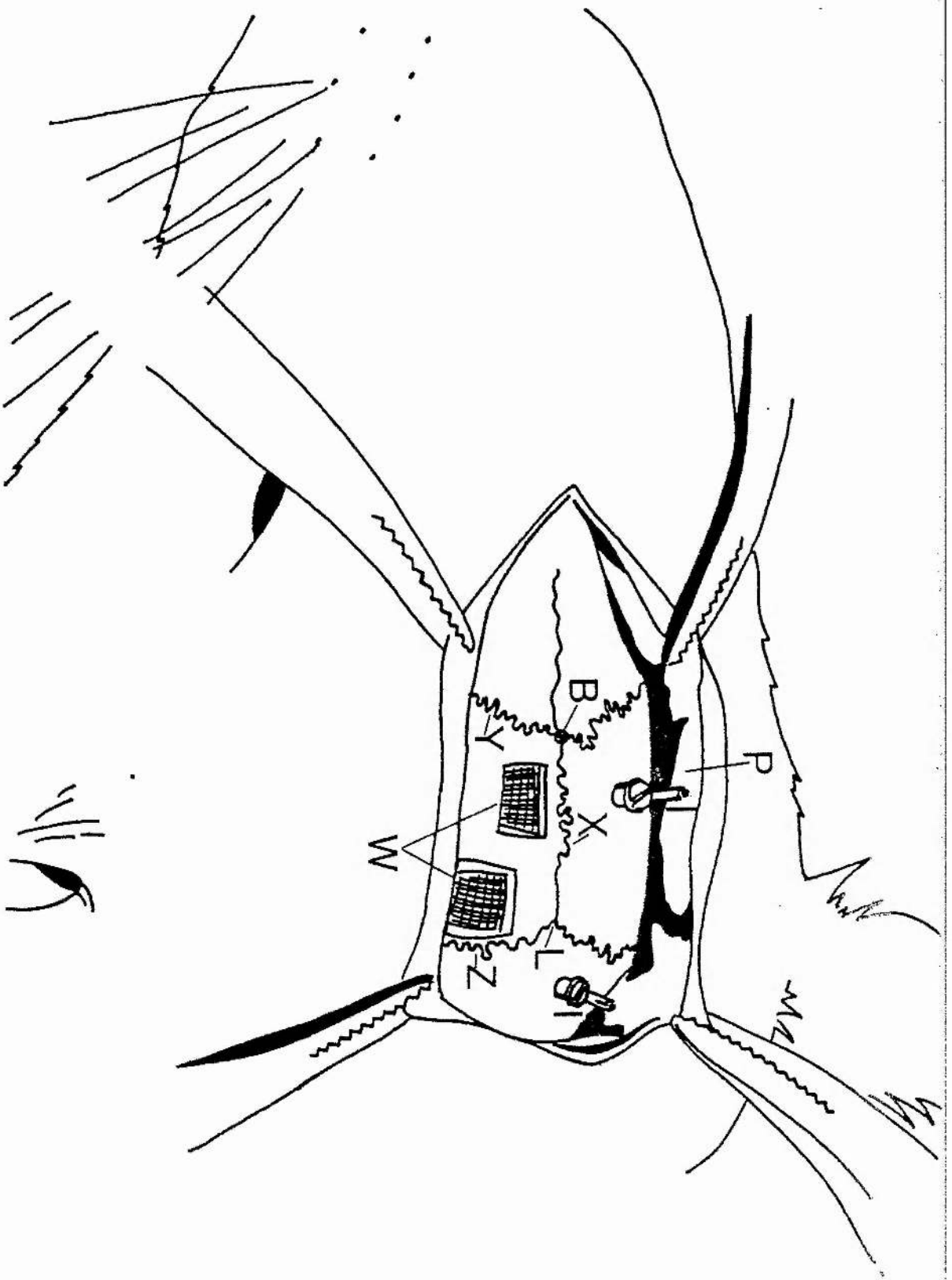
B
Y
P
X
W
L
Z

During one set of experiments (chapter 7), bipolar stimulation was achieved by using two adjacent 110 um diameter Teflon-coated wires, with tips separated by less than 1 mm.

Recording

Recordings were made either via platinum/iridium, Teflon coated wires (70 um outer diameter, Medwire, Clark Electromedical), attached to a female Amphenol pin, carried on a stereotaxic micro-manipulator; or alternatively, using conventional Na-Acetate (2 M) filled glass micro-electrodes (G.C.150T.F.-10, Clark Electromedical), with tips approx. 15 um in diameter, attached directly to a unity-gain head stage amplifier (NL 104, Neurolog system).

Amplification

Signal amplification with wire recording electrodes was by a Grass 7P511 AC EEG amplifier, with high and low frequency cut-offs set at 10 KHz and 1Hz respectively, when recording evoked population field-potentials. When recording multiple unit discharge the low frequency cut-off was set at 300 Hz. Alternatively, with glass micro-electrodes, a Neurolog

system NL 104 AC preamplifier was used with the same filter settings. Signals were displayed directly on a storage oscilloscope, from which they could be photographed.

Data collection

Potentials were not recorded until the recording and stimulating electrodes had been in position for at least 15 minutes, to allow their positions to stabilize after implantation. Evoked potential analysis was performed on-line, using a MINC 11/23 computer, the normal sampling speed being 10 KHz. Either mathematical analysis was performed immediately, or averaged waveforms could be stored on disk. Sampling was initiated by a TTL pulse, synchronous with brain stimulation, arriving at a Schmitt trigger. Computer analysis could also be performed off-line after storing evoked potentials on FM tape. In this case, the trigger pulses were simultaneously taped on another recording channel, so that both recorded evoked potentials and trigger pulses could be played back together.

Experimental procedures

After drilling out two rectangular windows in the skull over the left cortex the stimulating electrode tip was positioned 7.5 mm posterior and 4 mm lateral to skull bregma and lowered through the posterior window, till a just discernible impression was made on the intact dura. This dorso-ventral position was taken as brain surface. A similar procedure was followed with the recording electrode when using Teflon coated wire. The recording electrode penetrated the more anterior window at 3.5 mm posterior and 1.8 mm lateral to bregma (McNaughton and Barnes, 1977). When using a glass micro-electrode no brain surface measurement was made before cutting the dura, rather the electrode was lowered until the tip made electrical contact with the exposed brain surface. With the preparation grounded, the ambient electrical noise would end at this point, which was taken as brain surface. This was easily observed using the oscilloscope (cut offs set at 300 Hz and 10 KHz). The dura was broken with a bent hypodermic needle and the membrane pulled back to the window edges with iris forceps. Breaking the dura was often associated with some bleeding, which was controlled by gentle application of cold-saline soaked swabs. Bleeding was always stopped before procedures continued. This was particularly important, as oozing of

blood on the brain surface could alter the pressure on the brain, and change the excitability of the perforant path fibres during a long recording session.

The recording electrode was slowly lowered into the brain, continually monitoring for multiple unit discharge on the oscilloscpoe. The cortex is usually quiet, but when an electrode begins to penetrate the hippocampus, a rapid discharge of cells in field CA1 is recorded. This is usually around 2 mm below brain surface and it provides a clear indication of electrode tip position. The spikes observed are both single and complex, and when the electrode is approaching the CA1 cell layer are negative going. The frequency and amplitude of the discharge falls when the electrode tip passes into the stratum radiatum, spikes being recorded in the positive direction. Approaching the dentate is characterized by the appearance of smaller amplitude positive going spike discharges, with a frequency of discharge which is clearly oscillatory. On entering the dorsal blade cell layer, the spikes are of reversed polarity, ie negative. This is usually about 2.7-3.0 mm below brain surface (figure 5-2). The potentials appear to reverse polarity because of a potential-divide.

Figure 5-2. Multiple unit discharge recorded on penetrating the dorsal hippocampus by a low resistance metal electrode. On the left are the major cell types, the pyramidal cells of regio superior and the granule cells of the dentate gyrus. The distal dendrites of CA1 pyramidal cells and the dentate granule cells terminate at the hippocampal fissure which lies between the cell layers. The numerals refer to the recording sites.

i. Negative going spikes recorded near the CA1 cell layer (2 mm below cortical surface).

ii. Positive going spikes recorded on the discharge of pyramidal and granule cells in the distal dendrites of both.

iii. Typical granular cell layer/hilus recorded, negative-going spike.

Calibration: 50 uV, 4 msec

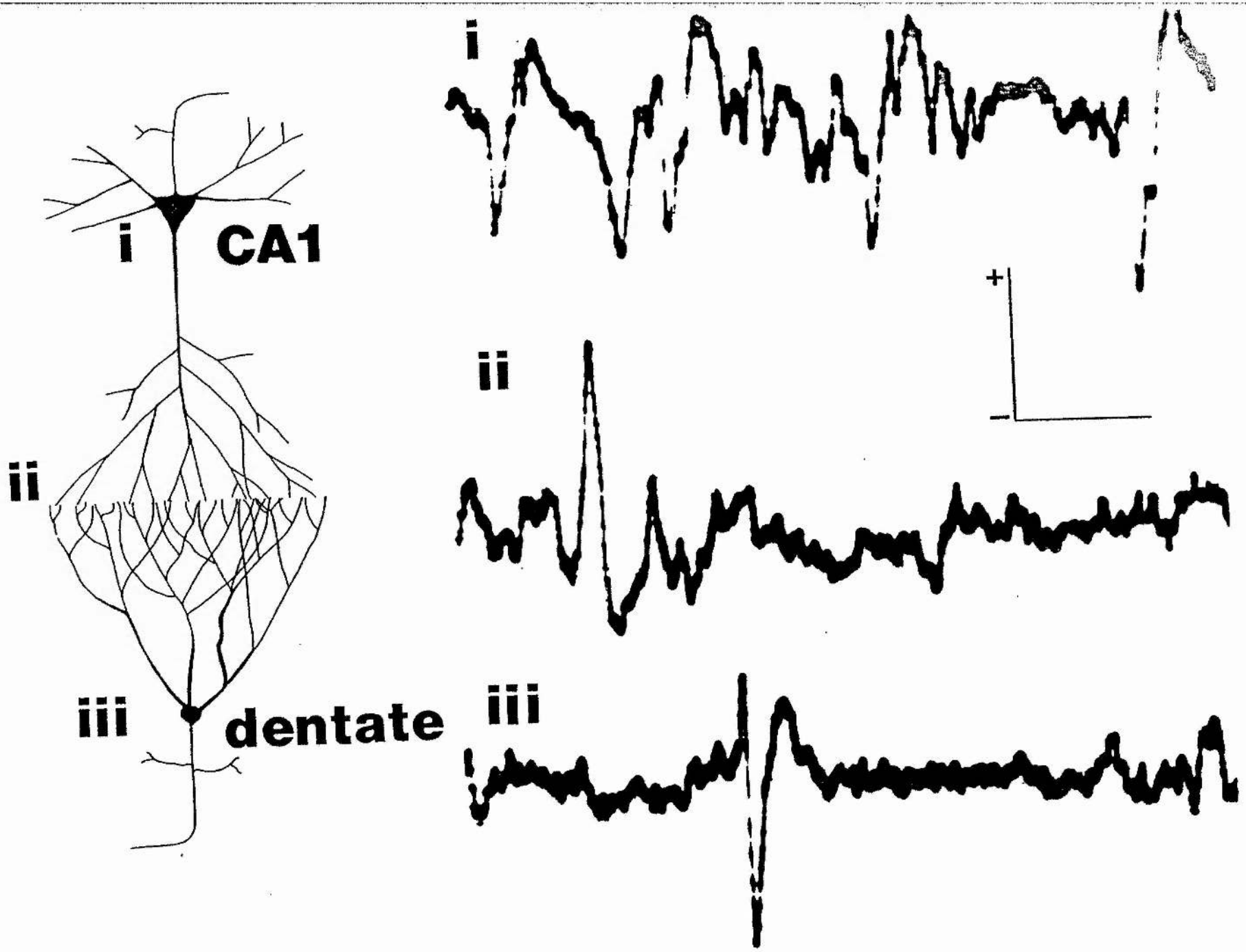
i
CA1
ii
iii
dentate
i
+
−
ii
iii

Once the recording electrode is positioned in or below the dorsal granule cell layer the stimulating electrode is lowered into the brain. Cathodal pulses at 350 uA and 100 usec duration are continually delivered at .2 Hz, as the electrode is lowered. These are the 'search' stimulation parameters, the positive output of the stimulus isolator being connected to the screw electrode over the cerebellum. As the electrode tip approaches the angular bundle, a positive going synaptic field-potential is recorded in the dentate. The optimal placement for discharging the granule cells is achieved by fine tuning the electrode tip position, using a low stimulus current. A large (> 5 mV amplitude), population spike negativity was commonly obtained with 3 V, 100 usec pulses, max. current 300 uA.

Computer analysis techniques

Differentiation

Differentiation of evoked potentials was achieved by a numerical method based on Sterling's formula. The derivative of a fourth-degree Sterling polynomial can be written as;

$$Y(k) = \frac{Y(k-2) - [8 * Y(k-1)] + [8 * Y(k+1)] - Y(k+2)}{12 * x}$$

Y(k) is any point in a 1 dimensional array Y(n), and where x = 1/f; f = frequency of sampling (La Fara, 1973). When employed in a computer program the equation appears as;

```
B(J%) = (A(J%-2) - (8 * A(J%-1)) + (8 * A(J%+1)) -
 A(J%+2) / (12 * .1)
```

Where array B(J%) is equal to d A(J%) / dt, in units per msec. Differentiation of waveforms has been useful in different branches of physiology (Linden and Snow, 1974; Coombs, Curtis and Eccles, 1957), maximum and minimum rates become maxima and minima. This helps in quantification of a dynamic function which is a composite, the components having different latencies and

durations.

Potential reversal point estimation

Using two adjacent platinum / iridium recording electrodes, one penetrating 400 um deeper into the brain than the other, it is possible to record the potentials at two points on either side of the potential reversal point, generated on synaptic activation, in the dorsal granule cell layer. The tip separation was set under a microscope, the wires and attached amphenol pins being set in dental cement up to about 4 mm from the tips. Sampling was carried out simultaneously via two A-D channels, triggered by a single TTL pulse.

As a first approximation the rate of potential change between the electrode tips is assumed to be constant ie where both recording positions lie between the dipole maximum negativity and positivity the total voltage difference between the electrode tips at any time after afferent stimulation is;

(V ventral - V dorsal)

The fractional potential difference between the most ventral electrode and the potential reversal-point is therefore given by;

$$x = \frac{V_{ventral}}{(V_{ventral} - V_{dorsal})} * 100$$

where x is the fractional percent of the total potential difference.

CHAPTER 6

OBSERVATIONS ON THE PERFORANT PATH

Introduction

Differing values of the conduction velocity of the perforant path have been reported. Gloor, Vera and Sperti (1963) give 1.5 m/sec and Lomo (1969) 3.3 m/sec. No differentiation between lateral and medial perforant paths was made in these studies. Laatsch and Cowan (1966) report that the medial perforant path fibres are unmyelinated and have diameters between .2 and .5 um. Myelinated fibres are also present in the perforant path, with diameters between .61 and .79 um (Nafstad, 1967). Tielen, Lopes da Silva and Mollevanger (1981), and Abraham and McNaughton (1984) report that the lateral entorhinal fibres conduct impulses faster than the medial entorhinal fibres, in hippocampal slices from the guinea pig and rat. Tielen et al. report conduction velocities for the medial entorhinal fibres of .19 to .44 m/sec, while the lateral entorhinal fibres showed velocities between .65 and 2.11 m/sec.

Abraham and McNaughton's measurements showed less of a difference between the two sets of fibres.

As the fibre projections can apparently be characterised by conduction velocity, it was hypothesised that the lateral entorhinal fibres would be more heavily myelinated than the medial at the level of stimulation in the angular bundle. Therefore a phospholipid stain was used to assess the degree of perforant fibre myelination and to determine the course of the myelinated fibres in the angular bundle. For the sake of clarity all following references to the medial and lateral perforat paths will follow the convention of McNaughton and Barnes (1977) and McNaughton (1980). This is namely that stimulation at the dorsal and ventral extremes of the angular bundle excite the medial and lateral perforant paths respectively. Electrophsiological and histological observations reported below support a distinction between medial and lateral entorhinal fibres in terms of conduction velocity.

Methods

The brains of 20 rats, fixed in formal saline and

embedded in gelatine, were frozen and sectioned coronally at 40 um intervals. The animals were previously involved in electrophysiological experiments, in which stimulation of both the dorsal and the ventral regions of the angular bundle took place, ie all electrode placements were functional in eliciting dentate synaptic potentials. All animals were stimulated at a dorsal site, which evoked medial perforant path potentials (McNaughton, 1980)in the dorsal ipsilateral dentate gyrus. In several animals, the electrode was advanced into the brain to a site which evoked lateral perforant path potentials. Small electrolytic lesions were made at the site of stimulation by passing anodal current (15 V, 20 Hz, 20 msec pulse duration, for 15 sec). Two staining methods were employed, the cresyl fast-violet method (CFV), and solochrome cyanine (Cox, 1982). CFV stains the nissl substance, and cell nuclei. It is an excellent method for revealing cell patterns. Solochrome cyanine is used as a myelin stain, staining myelin sheaths blue/purple. Two sequential sections out of five were saved, one being stained with solochrome cyanine and the other with CFV. Typically stained tissue was photographed, and is presented in the following series of photomicrographs.

Waveforms generated at the dorsal granular layer in the dentate were recorded on stimulation in the

Figure 6-1. Solochrome cyanine stained coronal section of cortical mantle at in the region of the entorhinal area (7.5 mm posterior to bregma), caudal to the hippocampal formation.

SB. Subiculum.

PR. Presubiculum.

PA. Parasubiculum.

LEA. Lateral entorhinal area; characterised by relatively large pyramidal cells in the outer zone of layer II, which are stained by solochrome cyanine.

IEA. Intermediate entorhinal area. Layer II is divided into two sublayers by a cell free zone; the cells do not stain with solochrome cyanine.

MEA. Medial entorhinal area. Layer II comprises tightly packed, small and rounded pyramidal cells, which are not stained with solochrome cyanine.

(Chevrons delimit cortical areas).

ab. Angular bundle - which is heavily stained with solochrome cyanine on the lateral side of the subiculum. Myelinated fibres climb over the subiculum to gather below the visual cortex, and above the dorsal surface of the subiculum.

fm. Forceps major. Fibres gather at this coronal level to project to the more rostral corpus callosum.

The asterisk marks the site of stimulation, in the dorsal region of the angular bundle which gives rise to short medial perforant path potentials in the dentate gyrus. In this region, myelinated fibres will be predominantly excited. Calibration bar is 1 mm.

1

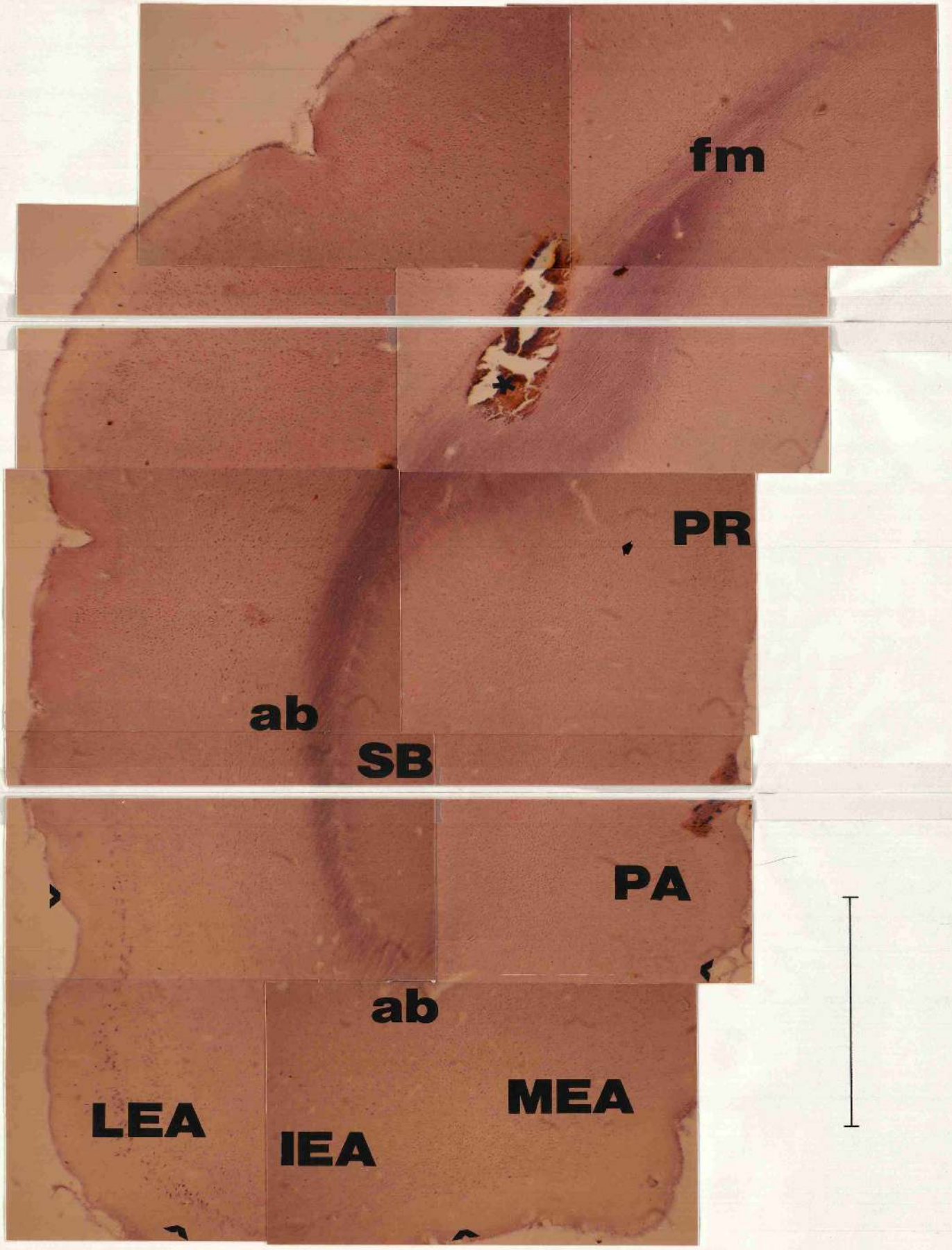

Figure 6-2. CFV stained coronal section of cortical mantle, 7.5 mm posterior to bregma.

MEA. Medial entorhinal area.

SB. Subiculum.

PA. Parasubiculum.

ab. Angular bundle.

The myelinated fibre bundle appears as a plume emerging from behind the section of subiculum.

The electrode track traverses the myelinated fibre bundle, and penetrates the non-myelinated fibres climbing the medial side of the subiculum (stimulation site is marked with an asterisk). Stimulation at this site gives rise to lateral perforant path type potentials in the dentate gyrus. An arrow is placed at a region of non-myelinated ascending fibres, ventral to the electrode tip. Calibration bar is 1 mm.

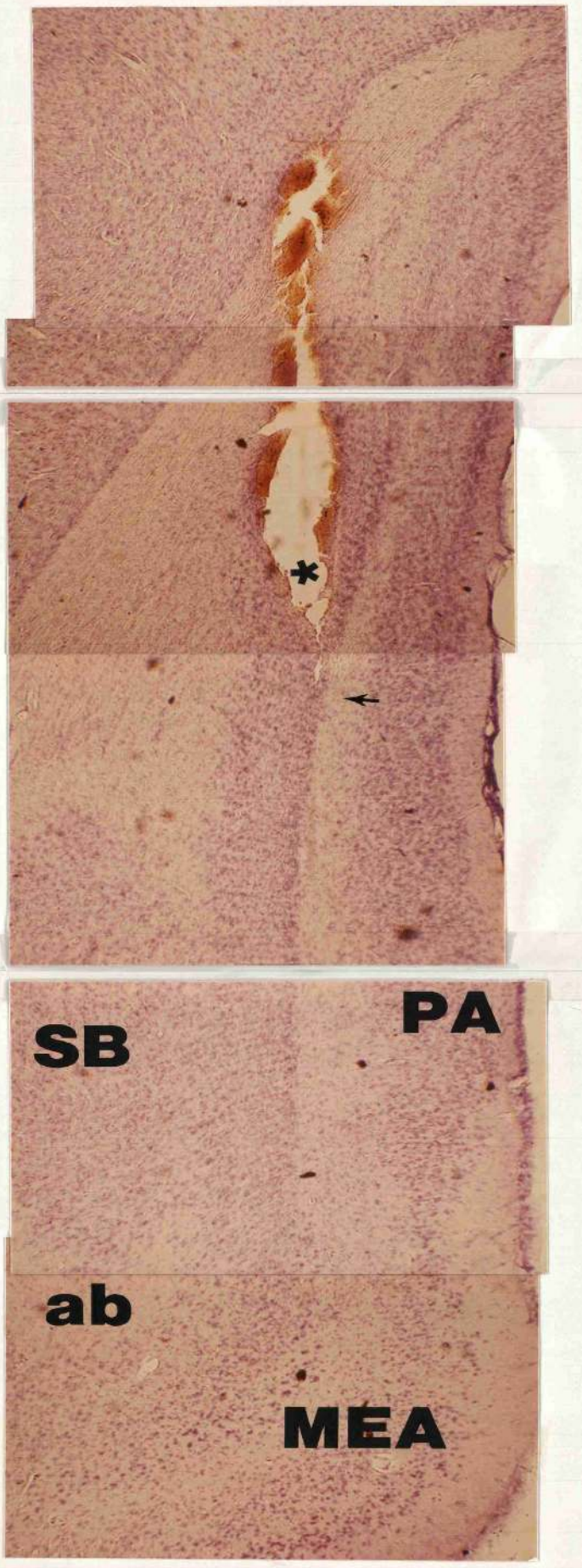
SB
PA
ab
MEA

angular bundle. The potentials generated dorsally, intermediately and ventrally in the bundle were stored on disk.

Results

The angular bundle (ab) on the lateral margin of the subiculum (SB) is heavily stained with solochrome, revealing myelinated fibres. The fibres lying ventral and medial to the subiculum (arrow on figure 6-1), do not appear to be myelinated; or at least less heavily than those occupying the dorsal margin of the subiculum, and can be seen medial to the subiculum in CFV stained tissue (figure 6-2). The angular bundle fibres curve over the dorsal surface of the subiculum forming a 'plume' as they ascend, leaving the section almost perpendicular to the coronal plane.

Electrode placements

In figures 6-1 and 6-2, electrode lesions can be clearly seen in the fibres of the angular bundle, the positions of the electrode tips being marked by asterisks. In figure 6-1, the electrode evoked medial

perforant path type potentials in the dorsal dentate gyrus, while in figure 6-2, lateral perforant path type potentials were produced. Medial perforant path type synaptic potentials are therefore apparently produced by stimulation of the myelinated fibres which course dorsal of the subiculum, while the myelinated fibres must be traversed by the electrode in order to evoke lateral perforant path type potentials by stimulating the more ventral, probably non-myelinated, fibres.

Stimulation of the angular bundle fibres at an optimal position for driving the granule cells, using a weak stimulus (well below population spike threshold), produces population epsp's in the dentate. On differentiation, these epsp's reveal two components, figure 6-3. The onset latency of the components measured from the differential waveforms are $1.09 \pm .07$ and $3.38 \pm .17$ msec, means$\pm$se's, n=10. These latencys are independent of stimulus intensity. Figure 6-4 i shows a population epsp generated by stimulating dorsally in the angular bundle, ie approximately 2.3 mm below brain surface, while 6-4 ii shows an epsp generated by stimulating more ventrally, at 3.5 mm below brain surface. This replicates the result of McNaughton and Barnes (1977) on tranversing the angular bundle with a stimulating electrode. It is probable that the first

Figure 6-3. Upper trace is a typical synaptic evoked potential recorded near to the cell bodies, well below threshold for granule cell discharge. The lower trace is the differential of the upper, clearly revealing two components within the original waveform. The angular bundle was stimulated using monopolar cathodal squarewaves, 6 usec pulse width, 5 V. X-axes are in msec, upper trace Y-axis in mV, lower trace Y-axis in mV/msec.

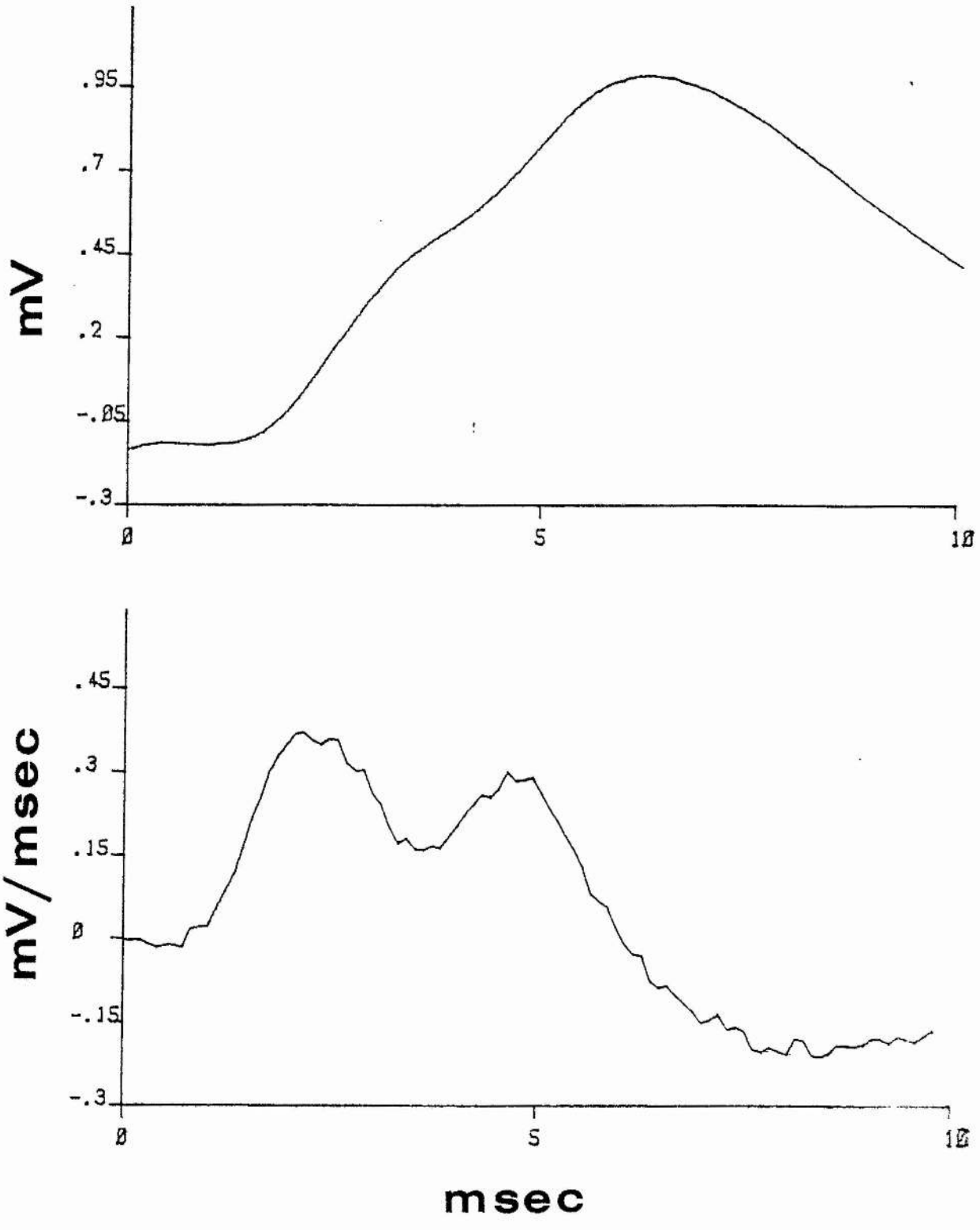
mV
.95
.7
.45
.2
-.05
-.3
0
5
10
mV/msec
.45
.3
.15
0
-.15
-.3
0
5
10
msec

Figure 6-4. i. Typical synaptic potentials recorded near to the granule cell bodies when stimulating at the dorsal extreme of the angular bundle. Bipolar stimulation, 5 usec pulse width, 5 V.

ii. Typical synaptic potentials recorded near to the granule cell bodies when stimulatng ventrally in the angular bundle. Bipolar stimulation, 5 usec pulse width, 5 V.

Frequency of stimulation in both cases was .2 Hz. Calibration bars are 2 mV / 4 msec.

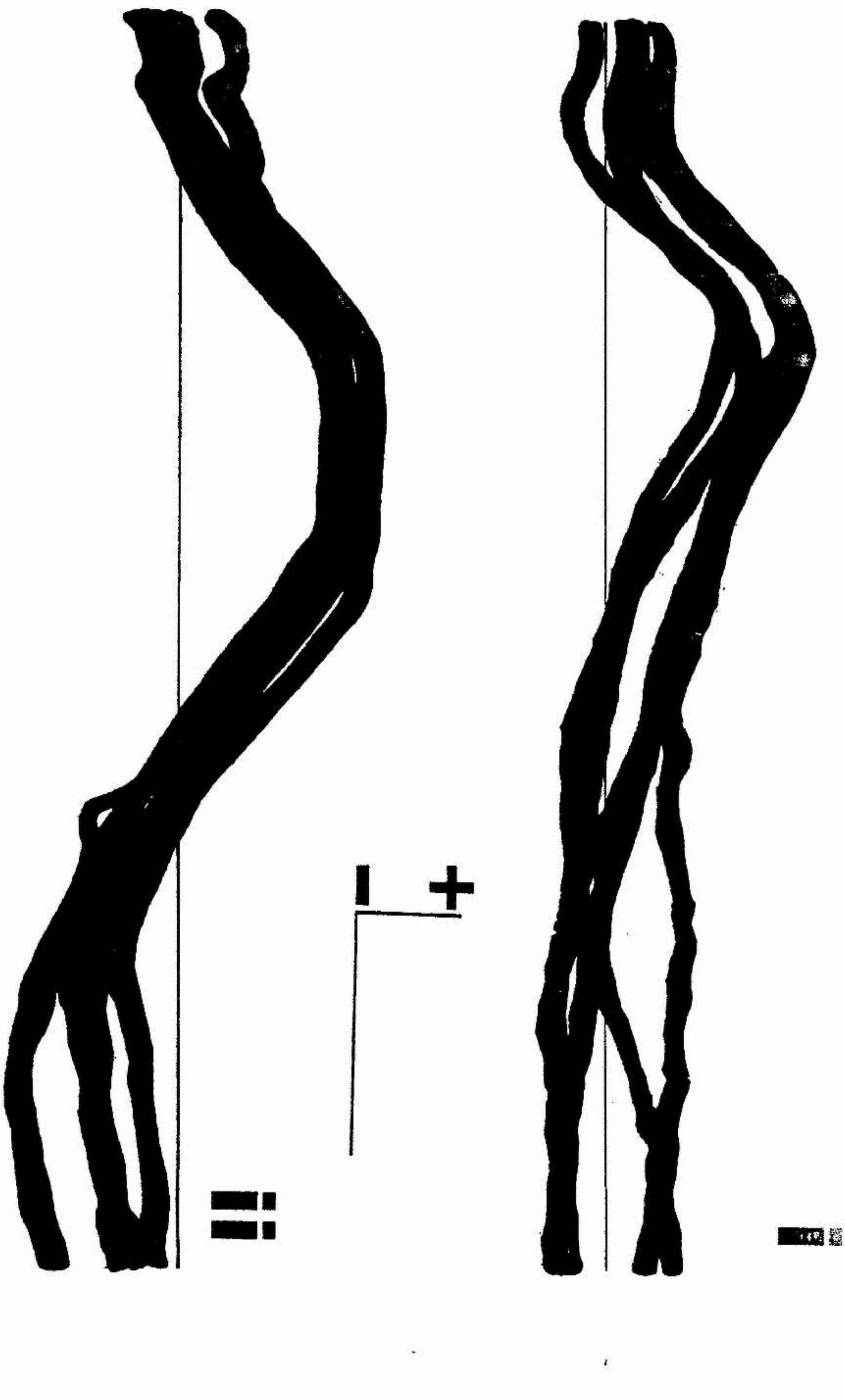

component revealed by differentiation of the compound waveform is due to activation of the medial perforant path, while the second is due to the lateral perforant path. It is probably also significant that when the stimulating electrode is in a position to stimulate both pathways, the medial is activated at stimulus durations below threshold for activation of the lateral, suggesting that the medial perforant path is composed of larger and or more heavily myelinated fibres than the lateral.

Discussion

The differential staining of the angular bundle with solochrome cyanine suggests that meylinated fibres are preferentially activated on stimulating dorsally in the bundle. Stimulating more ventrally activates non-myelinated fibres. This finding is also supported by the population epsp onset latencies recorded in the dentate gyrus. This is an interesting result because in order to be consistent with Tielen et al. (1981), the degree of myelination in the lateral and medial perforant path fibres must be reversed by the time the dentate gyrus is reached. That is to say, the fibres of both lateral and medial perforant paths would be differentially myelinated throughout their lengths.

Further work is required to elucidate whether this is the case.

Taking the triangulated distance between the recording and stimulating electrode tips, ie 4.5 mm, as the perforant path fibre length, the onset latency data suggest significant volume conduction of the population epsp. This volume conduction of preceeding radial current would probably be over 2 mm, as the values for conduction velocity are rather high compared with the results of Tielen et al., especially so when one proposes a 1 msec synaptic delay.

Summary

1. The medial and lateral perforant paths are differentially myelinated at the level of the angular bundle. The medial perforant path is more heavily myelinated than the lateral.

2. This differential myelination reveals itself in the onset latencies of the population epsp's recorded in the dentate gyrus.

CHAPTER 7

PAIR-PULSE STIMULATION

Introduction

Lomo (1971b), Teyler and Alger (1976), and McNaughton (1980), report the effects of paired stimulation of the perforant path on evoked field-potentials recorded in the dentate gyrus.

Lomo (1971b), working on the anaesthetised rabbit, quantified the magnitude and duration of potentiation, both of subthreshold synaptic field potentials, and of the granule cell population spike, which occurred after a conditioning stimulus to the perforant path. He observed an increase in the rate of rise and the maximum amplitude of the molecular layer synaptic potential evoked by a second shock, compared with the first. This potentiation was maximal at 20 msecs after the first stimulus, and decayed with increasing conditioning-test intervals, being completely over after 200

msec. Using stronger stimuli, the granule cell population spike was completely inhibited at 8-10 msec whereas using a 30 msec conditioning-test interval, the population spike amplitude might be 6 times that evoked by the conditioning pulse. Population spike potentiation fell with increasing stimulus intervals and was not present with intervals of about 200 msec. Lomo suggested several possible explanations for the potentiation of test responses including increased transmitter release from each activated terminal, facilitated action potential invasion of synapses dormant during the response to the first stimulus, or perhaps a postsynaptic change such as receptor sensitization, or dendritic spine swelling.

The observation is important because minimal (ie a single pulse) conditioning stimulation is necessary to induce profound changes in evoked activity in the dentate. This stimulation paradigm is perhaps more likely to yield results comparable with data collected from other systems (eg. in the cortex, Baranyi and Feher, 1981),

Teyler and Alger (1976), reported the effect of repetitive suprathreshold stimulation of the perforant

path in rat hippocampal slices, at a frequencies of 1 Hz and below. After stimulating at 1 Hz for 10 seconds, the maximum amplitude of the molecular layer evoked potential had decreased to around 10% of that obtained when stimulating at 30 second intervals. The hilar recorded spike amplitude was similarly depressed. Both the molecular layer potential population spike spontaneously recovered on recommencement of the control stimulation frequency. Fricke and Prince (1984) report that repetitive spiking of granule cells causes an increase in intrasomatic Ca^{2+}, giving rise to an increased gK^{+}, causing hyperpolarization and a cessation of action potential generation. Thus, part of Teyler and Alger's results can be explained. The recovery from repetitive stimulation took about 30 seconds, but by repeating the experiment and altering the interval between the last 1 per second stimulus and the onset of the 1 per 30 second stimuli, the process of recovery could be observed in more detail. Population spike recovery appeared to include a phase of facilitation at an interval of about 16 seconds, where the potential was 30% larger than that obtained at 30 second intervals, then falling to baseline magnitude. The changes in the dynamics and magnitudes of the field potentials were referred to as being a product of 'habituation'.

McNaughton, working on the rat hippocampal slice and the in-vivo rat hippocampus, made the following interesting observation. Depending upon where in the perforant path one stimulates, the evoked synaptic potentials respond differently to the second of a pair of stimuli. The recordings made in the slice studies revealed a facilitation of the molecular layer subthreshold synaptic potential when stimulating in the outer-third region of the granule cell dendritic tree, ie in the lateral entorhinal projection synaptic field, when it has been preceded by a conditioning pulse up to 1 second previously. Conversely, the fibres arising from the medial entorhinal cortex, stimulating in the middle third of the molecular layer, showed a depression of their molecular layer synaptic potential, which lasted over 2 seconds following a conditioning pulse. McNaughton interpreted these observations in terms of transmitter release dynamics. If the medial entorhinal fibres released a greater proportion of their available transmitter per impulse than the lateral entorhinal fibres, then under certain circumstances, the medial fibres might 'run-short' of transmitter when activated at short inter-stimulus intervals. On the other hand the build up of pre-synaptic Ca^{2+} would perhaps be enough to elevate the release of transmitter from the lateral fibre terminals and thus give rise to a facilitation.

During the course of the present experiments a previously unreported phenomenon was observed. If one records simultaneously from the molecular layer and hilus with two adjacent electrodes with vertically displaced tips, the amplitude changes in the molecular layer potential are generally the opposite of those occurring at or near the granular layer when test stimulating after a previous conditioning shock.

Methods

The observations were made in 6 rats (385-530g). Recordings were made using two adjacent platinum-iridium Teflon coated electrodes, one tip in the molecular layer, and the other at or near the hilus. The vertical disparity of the electrode tips was between 300 and 400 um (see materials and methods). A bipolar stimulating electrode was used, in an attempt to minimise current spread in the angular bundle and therefore obtain more homogeneous synaptic potential types. The electrode consisted of two 100 um outer diameter, Teflon coated, steel wires; the tips being separated by less than 1mm. The stimulus voltage varied between 3 and 4.5 volts (.15-.3 mA), while stimulus durations were less than 50 usec.

As the stimulating electrode penetrated the brain, the dorsal edge of the angular bundle was stimulated first; approx 2.5 mm below brain surface. By adjusting the stimulation current and duration, it is possible to obtain an almost pure medial perforant path potential from this region. After collecting all required data from the dorsal stimulation site, the electrode was lowered vertically between 1 - 1.5 mm, such that the electrode tips were now between 3.5 and 4 mm below brain surface. In such a position an almost pure lateral perforant path potential was evoked in the dentate. The stimulus duration in each case was adjusted to give a synaptic potential of low variability.

The perforant path fibres were stimulated using a paired-pulse paradigm, the second shock being identical to the first, delayed between 20 and 200 msecs. The frequency of paired stimulation was .2 Hz, which remained constant throughout. Potentials could be displayed on an oscilloscope and were stored on FM tape, for off-line analysis.

Results

Evoked potential maximum amplitude measurements were made by computer on 5 consecutive pairs of potentials, taking as baseline the potential at 1.8 msec after the first stimulus. Mean amplitudes and mean amplitude differences were then calculated. Data from a typical animal are presented in figures 7-1 and 7-2. Figure 7-1 shows the mean change in the maximum amplitude of hilar and molecular layer recordings when stimulating at the dorsal edge of the angular bundle. Figure 7-2 shows the mean change in the maximum amplitude of hilar and molecular layer potentials when stimulating at the ventral extreme of the angular bundle. Notice that the amplitude of the second potential of the pair recorded in the hilus behaves in a way similar to those recorded by McNaughton. An initial 'facilitation' is produced at 20 msecs after the conditioning pulse when stimulating at the ventral position (fig. 7-2), whereas a depression is observed throughout the 200 msecs when stimulating at the dorsal site (fig. 7-1).

However the polarity of the post-conditioning amplitude changes in the molecular layer, are the same as those in the hilus. As the molecular layer and hilar potentials are of opposite polarity, molecular

Figure 7-1. Results obtained from stimulation at the dorsal edge of the angular bundle. The upper graph is a plot of the difference in the maximum potential (negative going) recorded in the molecular layer (M) against the interstimulus interval.

The lower graph is a plot of the difference in the maximum potential recorded near the granular layer (positive going) against the interstimulus interval (H - hilus).

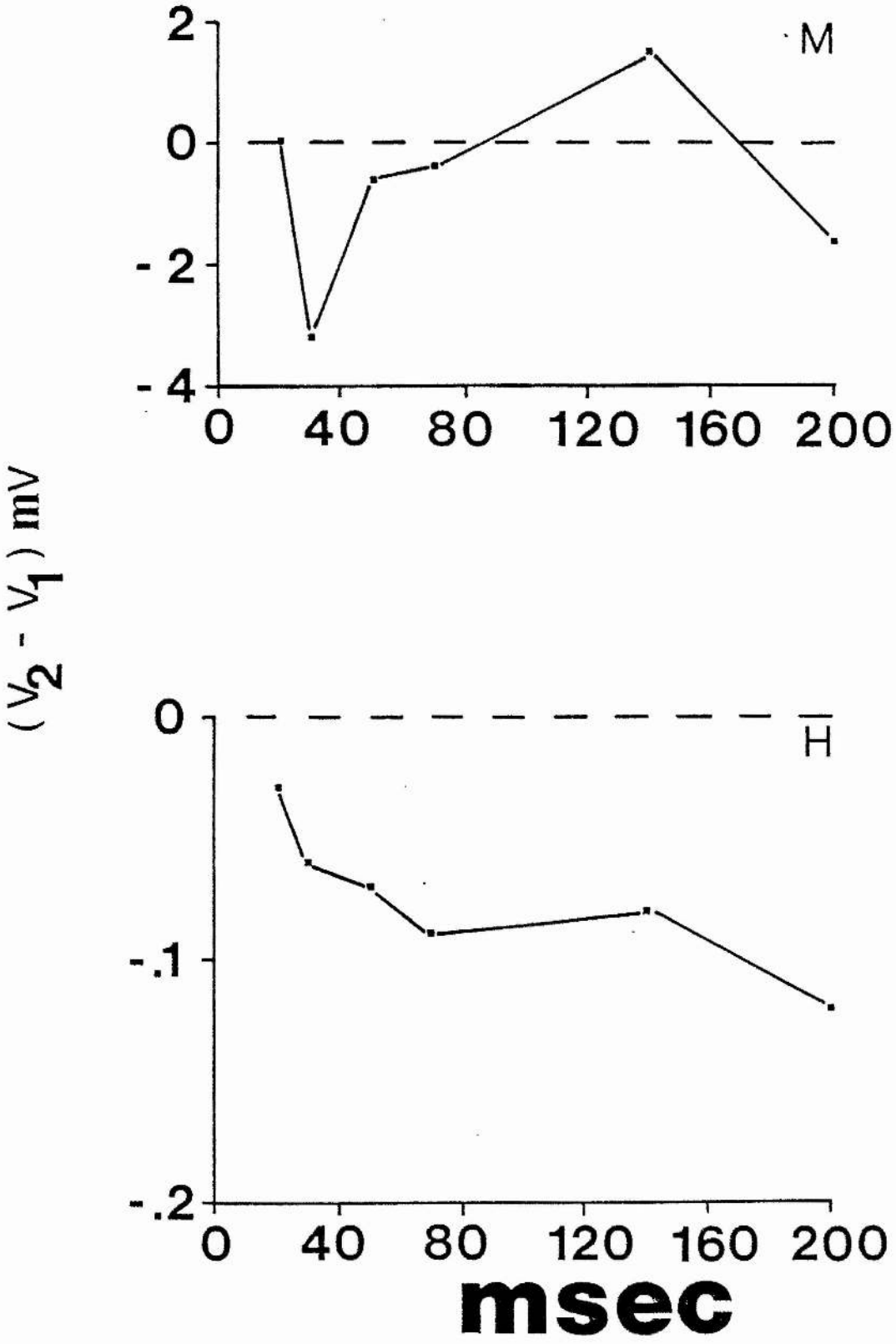
2
0
-2
-4
M
0
40
80
120
160
200
$(V_2 - V_1)$ mV
0
-.1
-.2
H
0
40
80
120
160
200
msec

Figure 7-2. Results obtained from stimulation at a ventral site in the angular bundle. The upper graph is a plot of the difference in the maximum potential (negative going) recorded in the molecular layer (M) on paired stimulation, against interstimulus interval.

The lower graph is a plot of the difference of the maximum potential (positive going) recorded near the granular layer (H - hilus), against interstimulus interval.

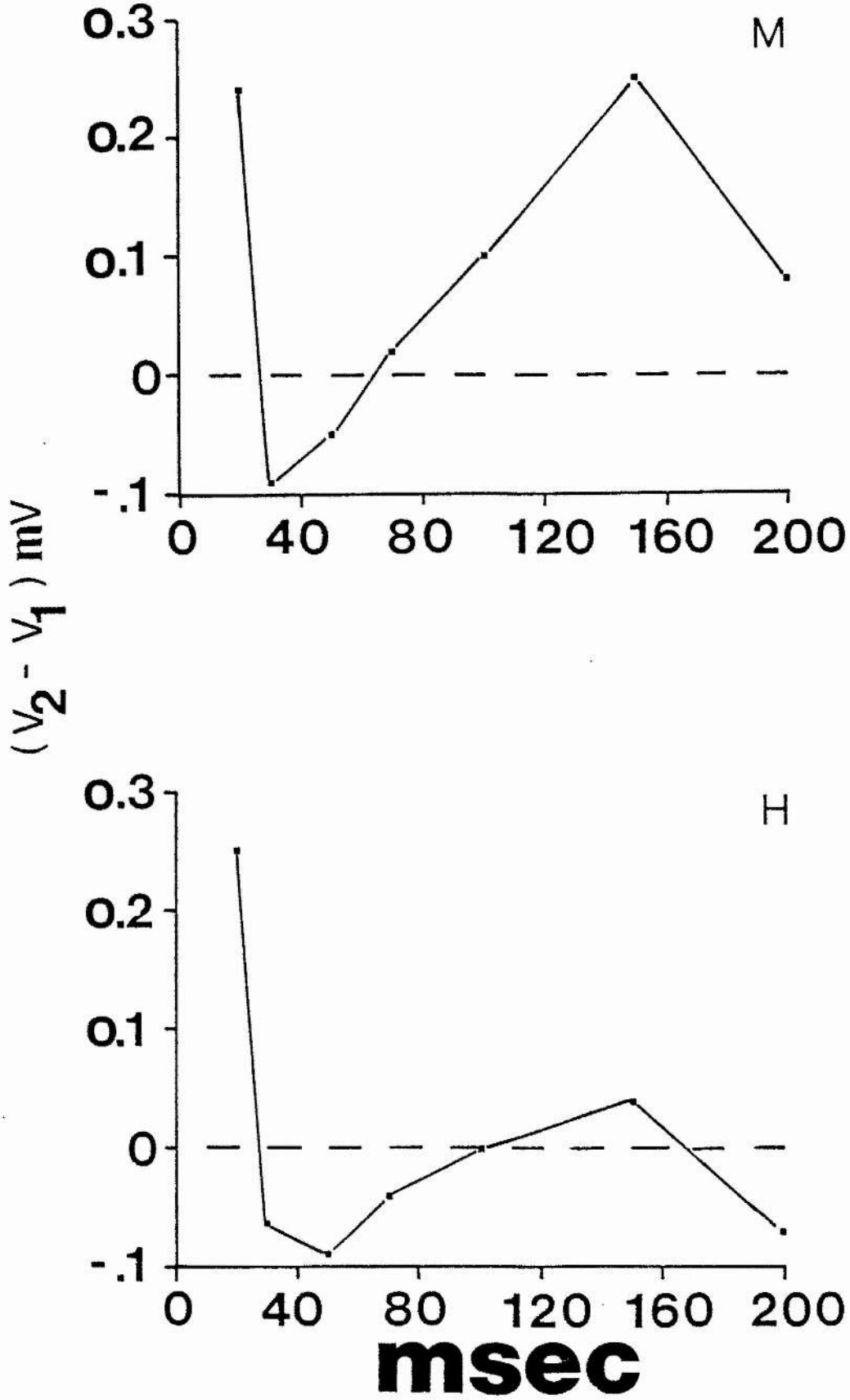
M
H
0.3
0.2
0.1
0
-.1
0
40
80
120
160
200
msec
$(V_2 - V_1)$ mV

changes in amplitude are in the opposite direction of those in the hilus. This observation suggests that one cannot assume increased synaptic conductance accounts for increases in the size of synaptically evoked field potentials in the dentate, where recordings have been made via one electrode only.

Figure 7-3, shows three superimposed consecutive paired-potential traces, where the dorsal edge of the angular bundle is being stimulated. The molecular layer electrode is so close to the potential reversal point that part of the waveform is recorded positive. The second synaptic potential is more negative at both the molecular and granular layer than the first.

Using the interpolation method (given in materials and methods), the fractional potential difference between the most ventral recording electrode and the reversal point, relative to the total potential difference between both recording electrodes, was calculated at that latency at which there was the greatest potential difference between the electrode tips, figure 7-4.

Figure 7-3. Three consecutive paired-potentials, evoked from the dorsal edge of the angular bundle. The interstimulus interval is 20 msec. Upper traces recorded from the molecular layer, lower traces from the hilus. The stimulating electrode is positioned in the dorsal region of the angular bundle, giving rise to short onset/peak latency potentials.

Calibration: upper traces .2 mV / 10 msec; lower traces 1 mV / 10 msec.

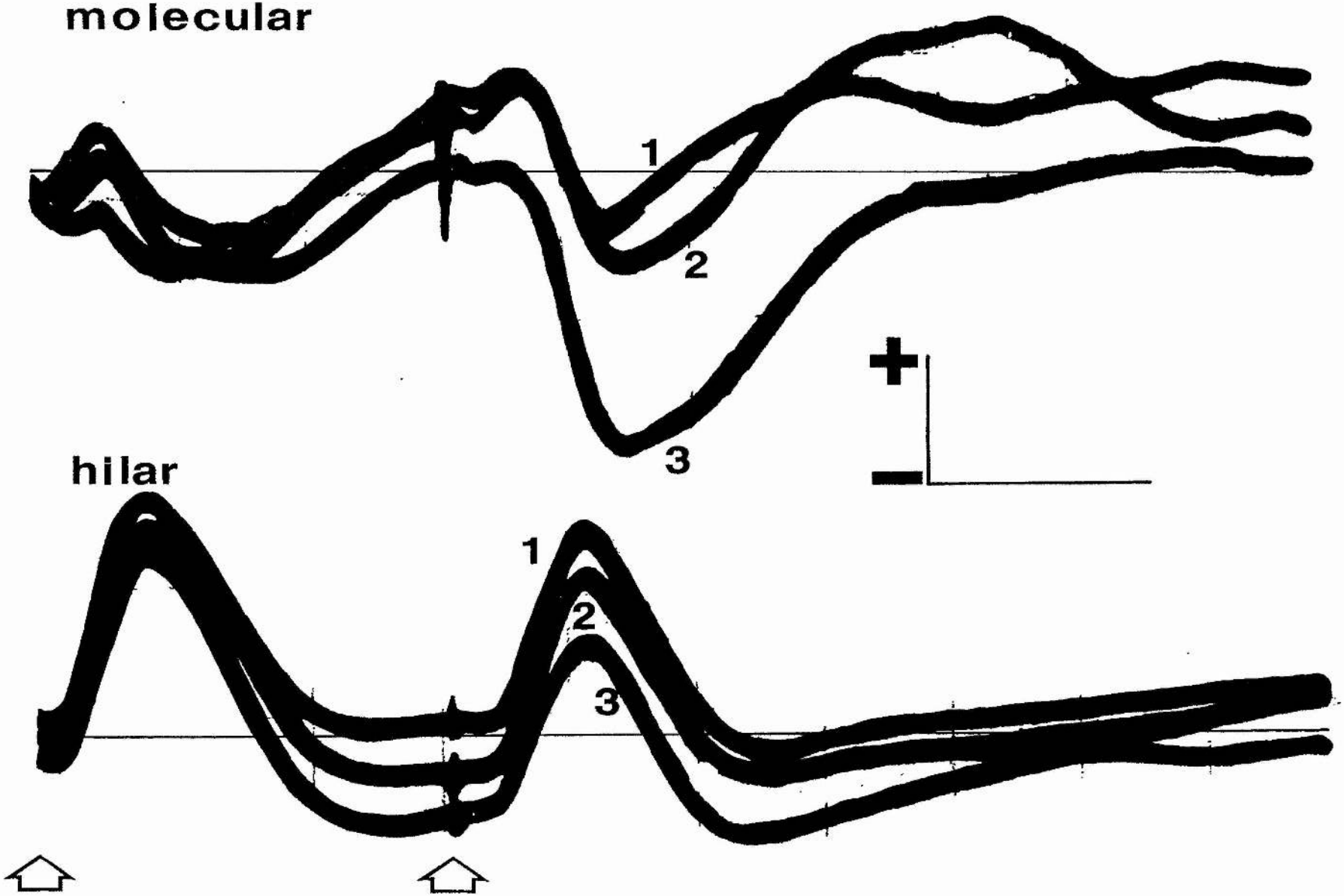
molecular
1
2
3
+
−
hilar
1
2
3

Figure 7-4. Plots of movement of the interpolated reversal point, expressed as a fraction of the total potential difference between the two electrodes at the post-stimulus latency giving the largest difference in inter-electrode potential difference, against inter-stimulus interval.

Upper graph is data obtained from the medial perforant path- dorsal angular bundle stimulation site.

Lower graph is data obtained from the lateral perforant path - ventral stimulation site.

The arrow represents the dorsal (positive) movement of the reversal point, which is characteristic of this pathway at interstimulus intervals of less than 30 msec. X1 is the interpolated reversal point of the first evoked potential, and X2 is that of the second. The brackets indicate the duration of the first evoked potential.

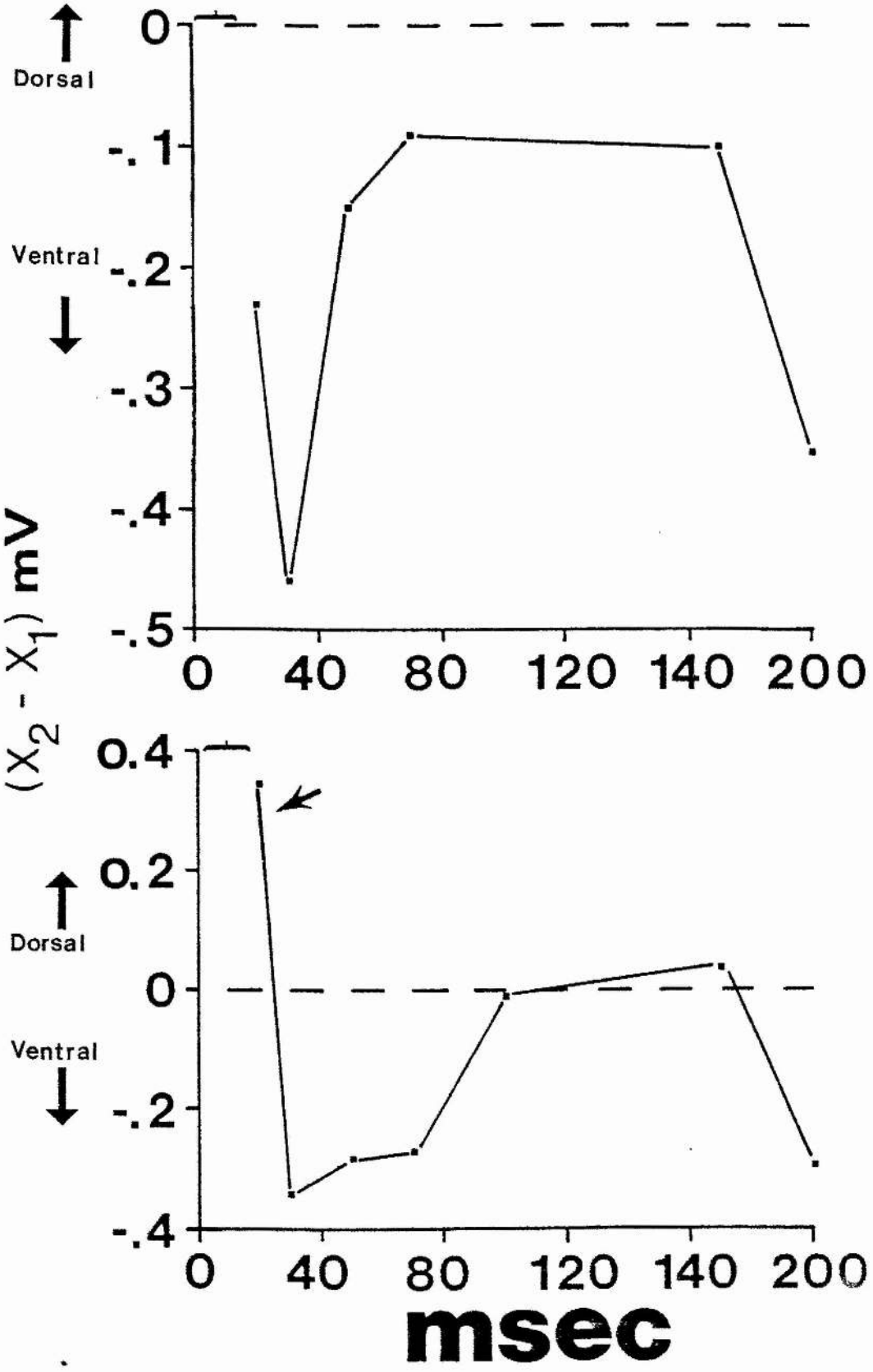
Dorsal
Ventral
0
-.1
-.2
-.3
-.4
-.5
0
40
80
120
140
200
$(X_2 - X_1)$ mV
0.4
0.2
Dorsal
0
Ventral
-.2
-.4
0
40
80
120
140
200
msec

Discussion

Although changes in post-synaptic conductance may be occurring after a conditioning stimulus, clearly the changes in synaptic potential dynamics observed here are caused by primarily alterations in the spatial shape of the field potential, including movement of the reversal point towards and away from the granular layer. The results described here suggest that the synaptic field potential spatial dynamics can change enough to cause large proportional increases or decreases in the amplitude of the potential recorded at a point in the extracellular potential field, and in ways which might be explained by rapid changes in the electrotonic characteristics of the granule cells. Such changes in the electrotonic characteristics of the granule cells, may explain Lomo's (1971b) population spike facilitation, and the facilitation of the population spike observed by Teyler and Alger (1976), on escape from 'habituation'. Alterations of membrane resistance have been reported by Crunelli et al., 1984, on iontophoresis of glutamate, NMDA and quisqualate onto granule cell dendrites in the hippocampal slice.

Although it may be possible to explain movements in the field potential reversal-point in terms of increases in the ventral extent of the sink ie on activation of synapses between the previously activated

terminal region and the soma, it is unlikely this could explain both movement of the reversal-point towards and away from the cell body layer. The following is therefore proposed. On activation of afferent synapses on the granule cells, there is a rapid and prolonged increase in the dendritic membrane resistance (decreasing the electrotonic length of the dendritic tree), lasting longer than 200 msecs (Crunelli et al.'s data suggest such an effect lasts the order of seconds.) This is accompanied by a movement of the synaptic field potential reversal-point towards the granule cell body layer. The transitory movement of the field potential reversal-point away from the cell body layer when stimulating at the ventral extreme of the angular bundle may be explained by feed forward inhibition, associated with the activation of this section of the perforant path, and causing a profound decrease in the membrane resistance of the peripheral dendrites and the soma during the synaptic action of GABA. It should therefore be possible to prevent this effect on the synaptic potentials by pharmacological blockade of GABA receptors. The data suggest that the duration of the synaptic action of GABA in the dentate is of the order of 10's of msecs. Changes in the dendritic membrane resistance will clearly produce inverse changes in the magnitude of synaptic field potentials. For example, increasing dendritic membrane resistance will reduce the size of synaptic evoked potentials, while making the granule cells more excitable.

Evidence for feed-forward inhibition in the perforant path

Lomo (1968; 1971a) recording intracellular synaptic potentials on activation of the perforant path recorded epsp's followed immediately by ipsp's, without a spike being necessarily present during during the epsp. Clearly this might imply surround inhibition, ie neighbouring cells are firing action potentials, or perhaps feed-forward inhibition. Such inhibition is known to take place on activation of commissural fibres (Douglas et al., 1982), the cellular mediator being the basket cell (Seress and Ribak, 1983), synapsing on the peripheral dendrites and the soma of the granule cells.

Apart from the previously described movement of the field potential reversal-point away from the cell body layer, after stimulating at the ventral site in the angular bundle, there is another effect observable from the extracellular synaptic potential which might be due to feed-forward inhibition. As the inhibitory action of GABA is caused primarily by a decrease in membrane resistance, one might expect an increase in the total amount and, or, a rearrangement of current set flowing by simultaneous excitatory synaptic activity. Therefore at the onset of the action of GABA, an increase in magnitude of the excitatory synaptic extracellular dipole should be evident, probably observed as

a transient 'swelling' on a potential waveform recorded at a point near the cell bodies. There should be a threshold for obtaining the inhibitory effect (as presumably the basket cells fire action potentials) and a decrease in the onset latency of the effect with increasing stimulus intensity.

Evidence for the existence of such a potential transient is given in figure 7-5 and 7-6. This potential transient has perhaps mistakenly been attributed to the onset of the granule cell population spike (eg Abraham and Goddard, 1982; McNaughton and Barnes, 1977). It is only present after stimulation at the ventral site in the angular bundle, or when the stimulus strength is sufficient to activate the perforant path non-specifically (figure 7-5A). It is present when the granule cell population spike is refractory, or recurrently inhibited (figure 7-5B), and has a variable onset latency, dependent upon the duration of stimulation, figure 7-5A. Unlike the population spike which is tremendously facilitated by stimulation at intervals of 100 usec, the transient is depressed (figure 7-6), suggesting that there is some interaction between repeated synaptic activation and the mechanism underlying the generation of this transient. The transient is also present at stimulus intensities below that necessary to elicit a population

Figure 7-5 A. Simultaneous recordings from molecular (upper) and hilus (lower) of the dorsal blade of the dentate. Three waveforms are superimposed, each generated at a constant voltage, with varying stimulus widths. Smallest granular layer potential (1), 10 usec stimulus duration clearly shows two 'humps', corresponding to the synaptic current of the medial and lateral perforant paths, and an abrupt change in the rate of de cay of the potential (arrow). The middle amplitude potential (2), 15 usec stimulus duration bears a third convexity (arrow), which is larger still in the largest potential (20 usec stimulus duration). Only the longest stimuli is evoking a population spike on the waveform (3). Calibration: 1 mV / 4 msec (both upper and lower traces).

B. The lower figure comprises 4 superimposed traces, obtained at a stimulus (75 usec duration), capable of discharging granule cells (see spike on upper waveform). The lower three were the product of stimulating at 20 msec inter-stimulus interval. Waveforms presented are consecutive. In the 2 evoked potentials which show no sign of a spike, the third 'hump' (see A) is still present (arrows). Calibration: 3 mV / 2 msec.

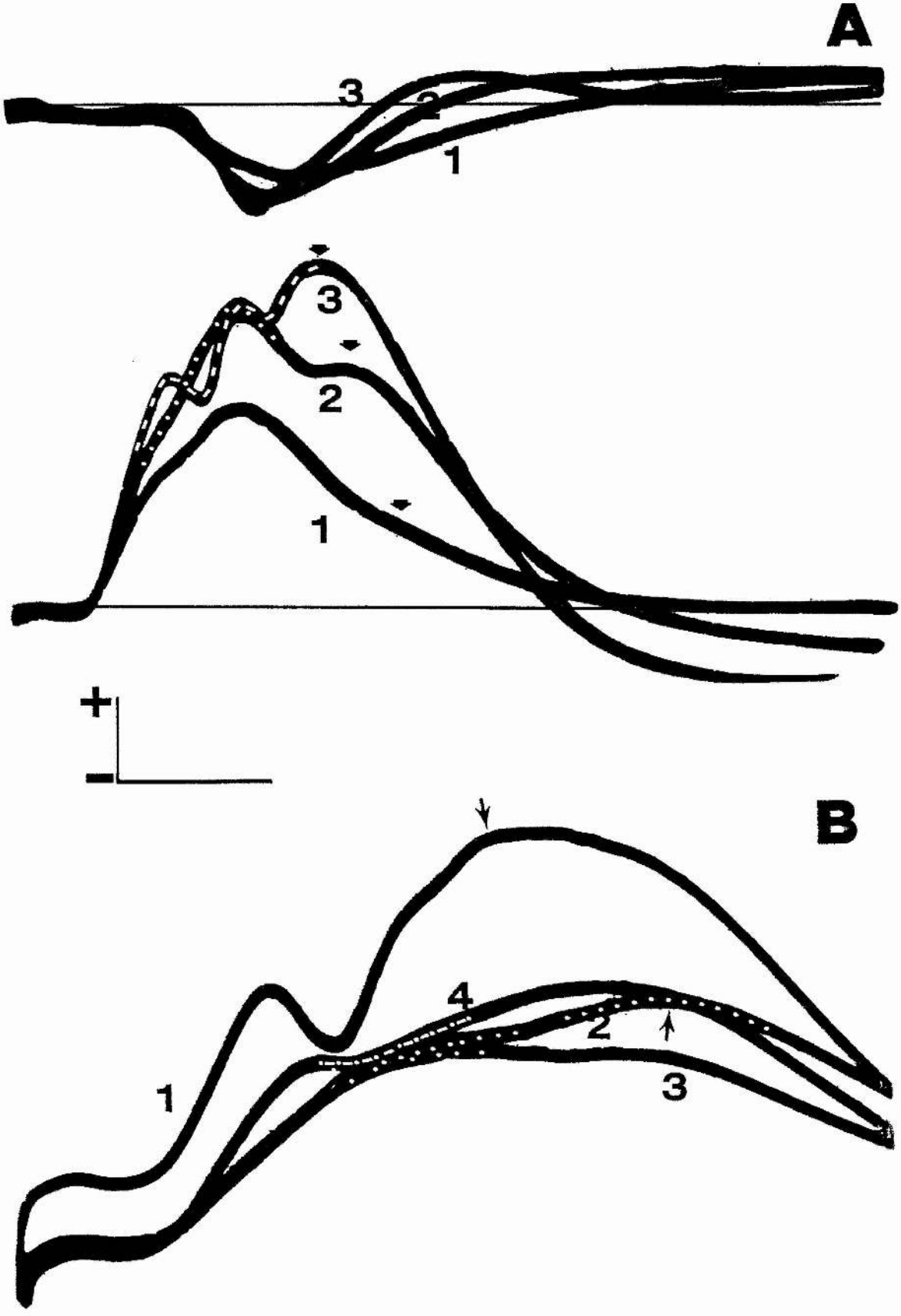
A
3
2
1
3
2
1
+
-
B
1
4
2
3

Figure 7-6. 5 consecutive evoked potentials recorded near the granular layer (8 usec stimulus duration), below the threshold for discharging the granule cells. Interstimulus interval is 100 msec, and with each subsequent stimuli, the amplitude of the evoked potential decreases. Waveforms are numbered in the order of evokation. Notice how the third 'hump' (labelled with arrows) on the potential almost disappears after about 4 stimuli (number 4). Calibration: 2 mV / 4 msec.

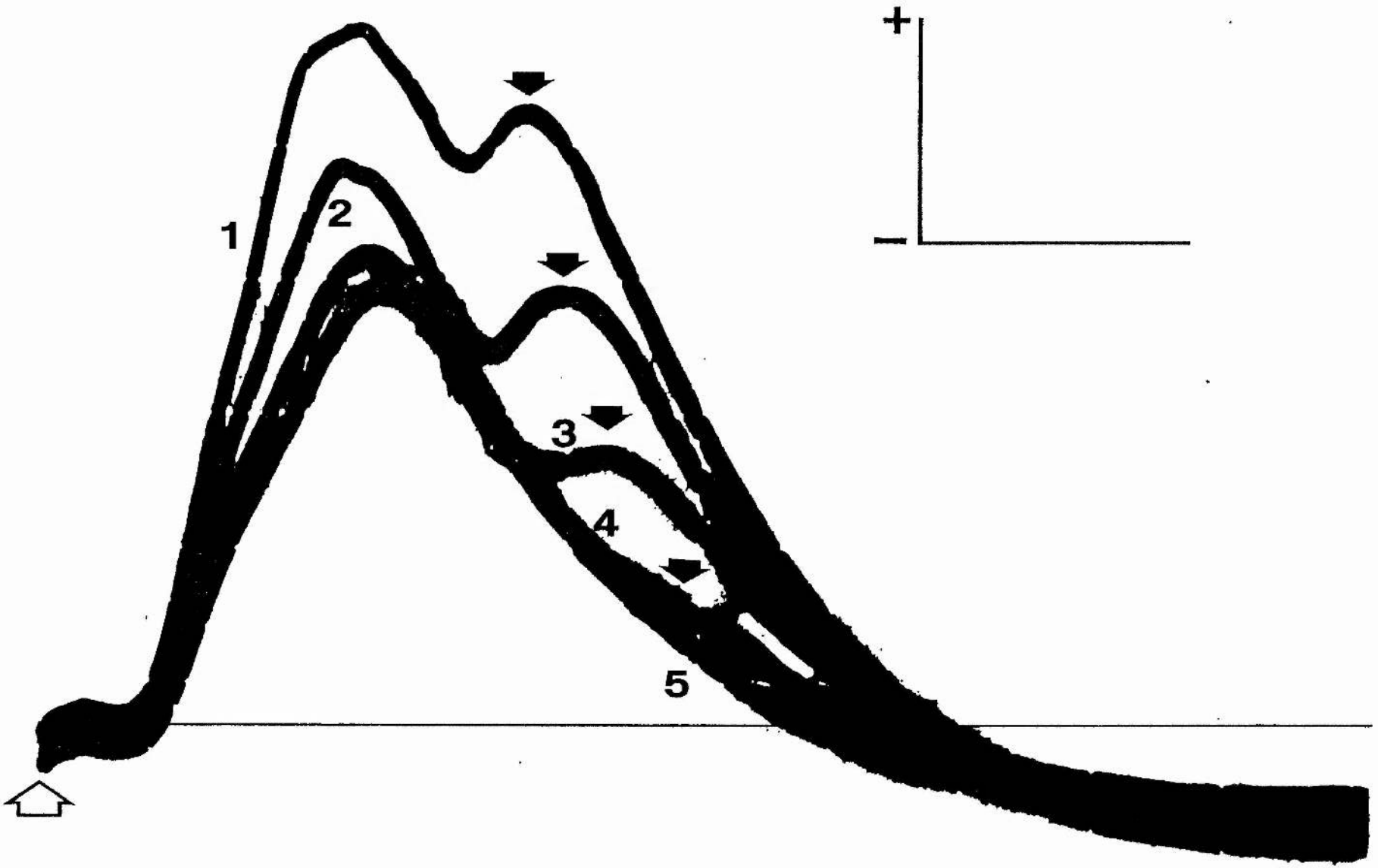
+
−
1
2
3
4
5

spike. Bliss and Gardner-Medwin (1973), provide superb examples of the transient in a rabbit dentate gyrus (J. Physiol. 232, p.361, fig 1a)

Summary

1. Population epsp's were simultaneously recorded from the molecular and granular layer of the dorsal blade of the dentate gyrus.

2. Population epsp amplitude changes at the granular layer, after conditioning stimulation, are in the opposite direction of those in the molecular layer.

3. Alterations in the magnitude of population epsp's recorded at one point in the dentate cannot simply be regarded as caused by changes in synaptic conductance only.

4. A previously unreported potential transient was investigated by altering stimulus duration and frequency. It was suggested that feed-forward inhibition in the dentate may be responsible for the transient.

CHAPTER 8

EXPERIMENTS ON LTP

Dentate Population-spike Dynamics

Introduction

Activation of perforant path fibres in the angular bundle gives rise to evoked potentials in the dentate gyrus, which have been classified as follows (see Lomo, 1966; Lomo, 1971a). Firstly, using stimuli of short duration or low intensity, a population epsp is evoked, caused by the current flow generated by synaptic activation in the local molecular layer. This potential is positive going near the granular layer. Secondly, superimposed on this potential when using stimuli of high intensity or long duration is a population spike, generally regarded as a biphasic, negative-going waveform with a duration of between about 1.5 - 2 msec, generated by the synchronized firing of many granule cells. With a strong enough stimulus, an evoked potential is therefore composed of

both a population epsp and a population spike. The potential preceding the onset of the spike has a variable duration, depending on the population spike onset latency. This section of the suprathreshold waveform is supposed to be produced by the current flow generated on synaptic activation only, and measurements taken from it thought of as indexes of synaptic current (eg Douglas et al., 1982). If it could be shown that the dynamics of the pre-spike potential do not vary independently of the population spike then one might have to regard the pre-spike potential as being produced, in part, by current flowing on cell discharge. This is likely, as radial currents will precede the laminar spread of activity in the dentate

Previous authors (Bliss et al., 1983), have attempted to quantify the response of the dentate granule cell population to perforant path fibre input, by plotting the amplitude of the population spike against the slope of the pre-spike positivity. Such an approach is clearly only a true indication of the effectiveness of synaptic drive if measurements can be made on evoked potentials which are a good index of synaptic current flow. Extracellular potential measuements are dependent upon at least four factors; namely the exact positioning of the electrode tip in the

synaptically generated potential field, the electrotonic characteristics of the granule cells, the synaptic conductance and other simultaneous, local current flow.

Therefore, recording at the dorsal cell layer, the following experiments examine the relationship between the pre-spike positivity, and the spike negativity, using a range of stimulus durations before and after tetanization.

Methods

The experiments were performed on 8 rats weighing between 305 and 370g. Recordings were made close to the dorsal blade granule cells in the dentate, using a teflon coated wire. The stimulating electrode was adjusted to the most effective position in the angular bundle for evoking synaptic field potentials. In such a position, both the medial and lateral perforant path fibres were stimulated at stimulus durations > approx 5 usec. The stimulation depth was 2.2 $\pm$.2 mm (mean$\pm$se) below brain surface, which corresponded to a region of the angular bundle giving rise to predominantly short rise-time and evoked potentials in the dentate when using short stimulus durations. The stimulus voltage

was set at the lowest necessary to elicit a maximal dentate population spike, at 100 usec stimulus duration. This varied from 3 to 4 volts.

The animals were divided into three groups. The first group of 4 animals was stimulated as follows. After obtaining a maximal population spike at 100 usec stimulus duration, 5 evoked potentials were recorded at 16 predetermined stimulus durations (3-100 usec), at a test frequency of .1 Hz, the durations being presented in random order. The second group of 2 animals, which were used as controls, were stimulated in exactly the same way, the random order of stimulus presentation being the same in all animals. In the third group of 2 animals, 5 evoked potentials were recorded at 8 predetermined stimulus durations (3-18 usec), at .1 Hz test frequency.

After completing the first data collection, the data being stored on a magnetic disk, the 4 animals from the 3-100 usec stimulus duration group, and the 2 animals in the 3-18 usec group received 5 high frequency tetani, a single tetanus being 99 waves of 100 usec duration at 400 Hz. The frequency of tetani was .2 Hz. The 2 control animals did not receive tetanic stimula-

tion. Subsequent to tetanization, no stimuli were applied for 30 minutes. Thereafter, a repetition of the data collection began.

Analysis of Data

The dentate evoked potentials were differentiated using Sterling's formula, the maximum differential of the pre-spike positive wave taken as the first positive peak in the differential waveform after stimulation (here called dV/dt component 1). The maximum differential of the spike is taken as the first negative going peak in the differential waveform (called dV/dt component 2), figure 8-1. The maximum differential of the population spike is not always negative, ie the spike potential can be no more than an indentation in the population epsp waveform at stimulus durations close to its threshold. Where the stimulus voltage is set to produce a maximal population spike at 100 usec stimulus duration, the population spike negativity begins to be appear at around 20 usec (figure 8-2).

Figure 8-1. Figure shows evoked potential waveforms, recorded from the hilar region on activation of the perforant path by increasing stimulus durations. The differential of the evoked potential is given beneath each original waveform.

Arrows on the 100 usec differential waveform show component 1 and component 2 dv/dt max; while directly above are the corresponding points on the potential waveform.

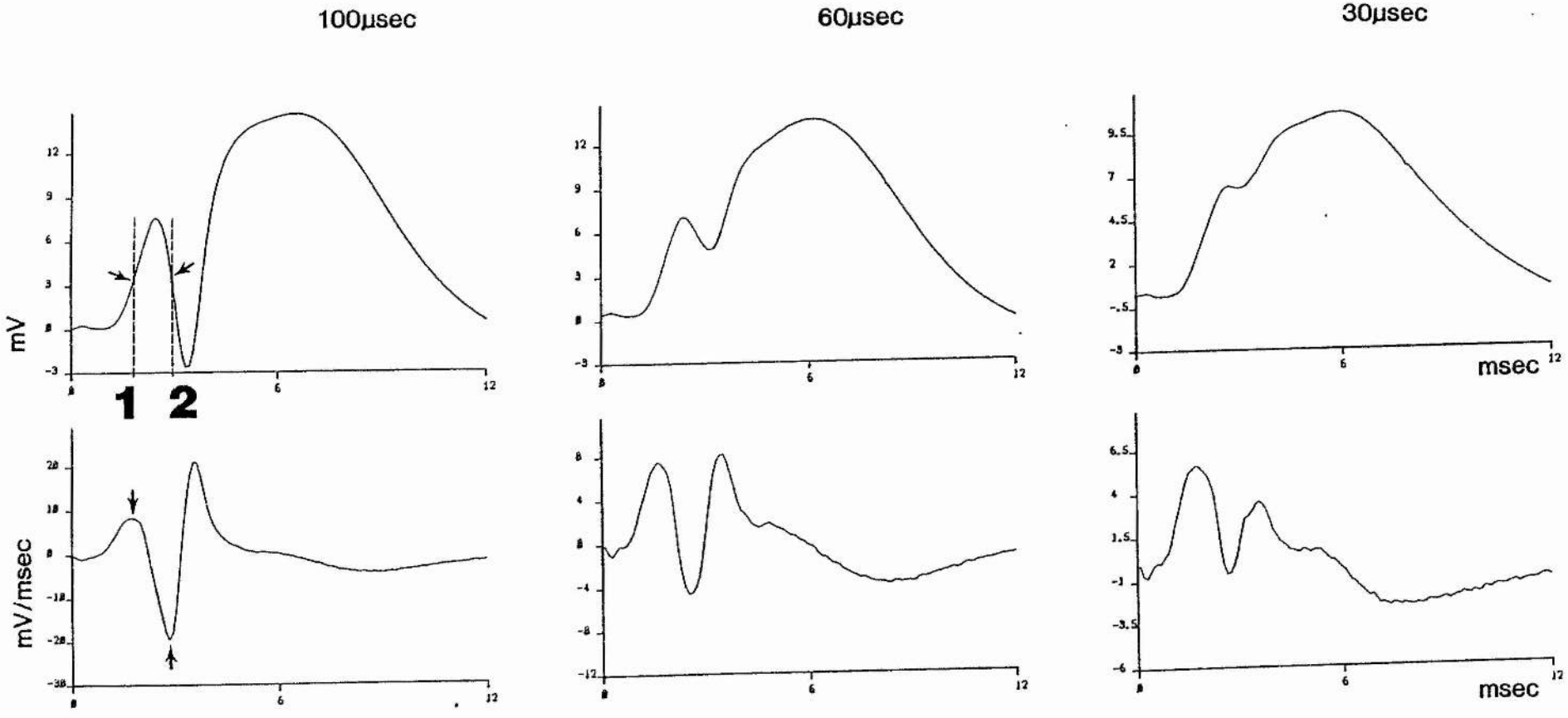
100µsec
60µsec
30µsec
mV
1
2
mV/msec
msec
msec

Figure 8-2. Typical data from an experimental animal (animal 122). Upper graph is a plot of dV/dt component 1 against the test stimulus width in usec. Lower graph is a plot of dV/dt component 2 against test stimulus width in usec. Units of dV/dt are mV/msec.

Squares represent mean data collected before tetanization and stars represent mean data collected after tetanization. Bars are $\pm$sd. Lines on lower graph were fitted by regression.

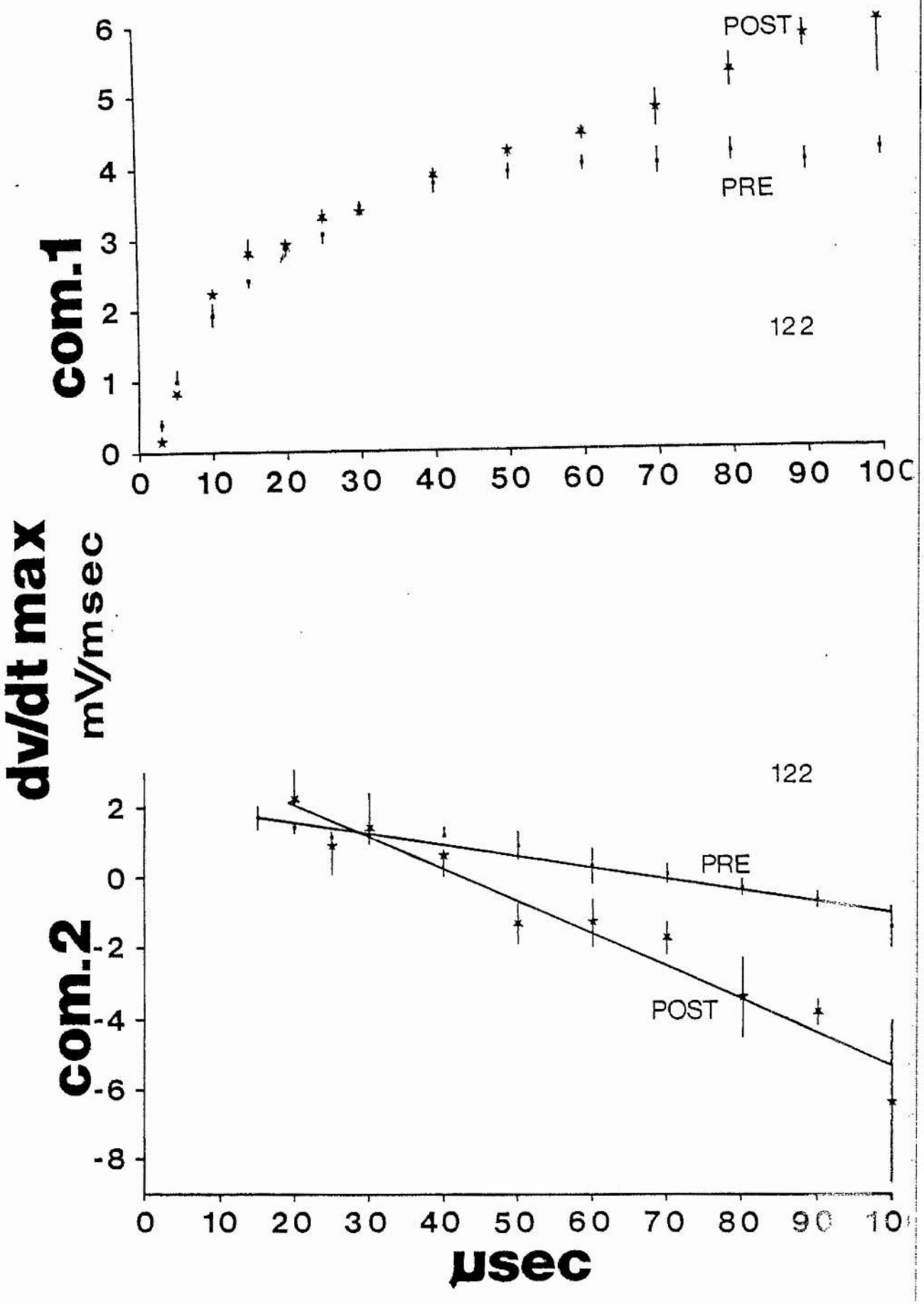
com.1
POST
PRE
122
0
1
2
3
4
5
6
0
10
20
30
40
50
60
70
80
90
100
dv/dt max
mV/msec
com.2
122
PRE
POST
2
0
-2
-4
-6
-8
0
10
20
30
40
50
60
70
80
90
µsec

Results

The effect of increasing stimulus duration on dV/dt components 1 and 2

The upper row of waveforms in figure 8-1 are evoked potentials recorded from the hilar region. Increasing the stimulus duration enhances the amplitude of the potential, and of the superimposed population spike (note change in the scale). Increasing stimulus duration produces an increase in dV/dt component 1, and when suprathreshold for granule cell discharge, increases the negativity of dV/dt component 2, as shown in the lower row of waveforms in figure 8-1.

The effect of afferent tetanization on dV/dt components 1 and 2

A highly significant increase in the magnitude of dV/dt component 1 at stimulus durations greater than 40 usec was observed in all 4 animals in the first group, subsequent to tetanization (Table 8-1). They also showed an increase in dV/dt component 2 at suprathreshold stimulus durations. Figure 8-2 is data from a typical animal. The large increase in the size of dV/dt component 1 is mirrored by the changes in dV/dt component 2. Equivalent effects were not seen in the

two non-tetanized control animals, data from one of them being presented in figure 8-3.

An interesting observation was made at short stimulus durations, namely that none of the tetanized animals showed a significant increase in dV/dt component 1 at very short stimulus durations, around 3 usec. This was true of both the animals which had received test stimulation sub and suprathreshold to granule cell discharge. In fact 3 of the animals show a decrease (Table 8-2), data obtained from animal 130 pre and post-tetanization being presented in figure 8-4.

Figure 8-3. Data obtained in control animal 126. The upper graph is a plot of dV/dt component 1 against the test stimulus width in usec. The lower graph is a plot of dV/dt component 2 against the test stimulus width in usec. Units of dV/dt are mV/msec.

The squares represent mean data collected before the 30 minute period without stimulation. The stars represent mean data collected after the same period. Bars are $\pm$sd.

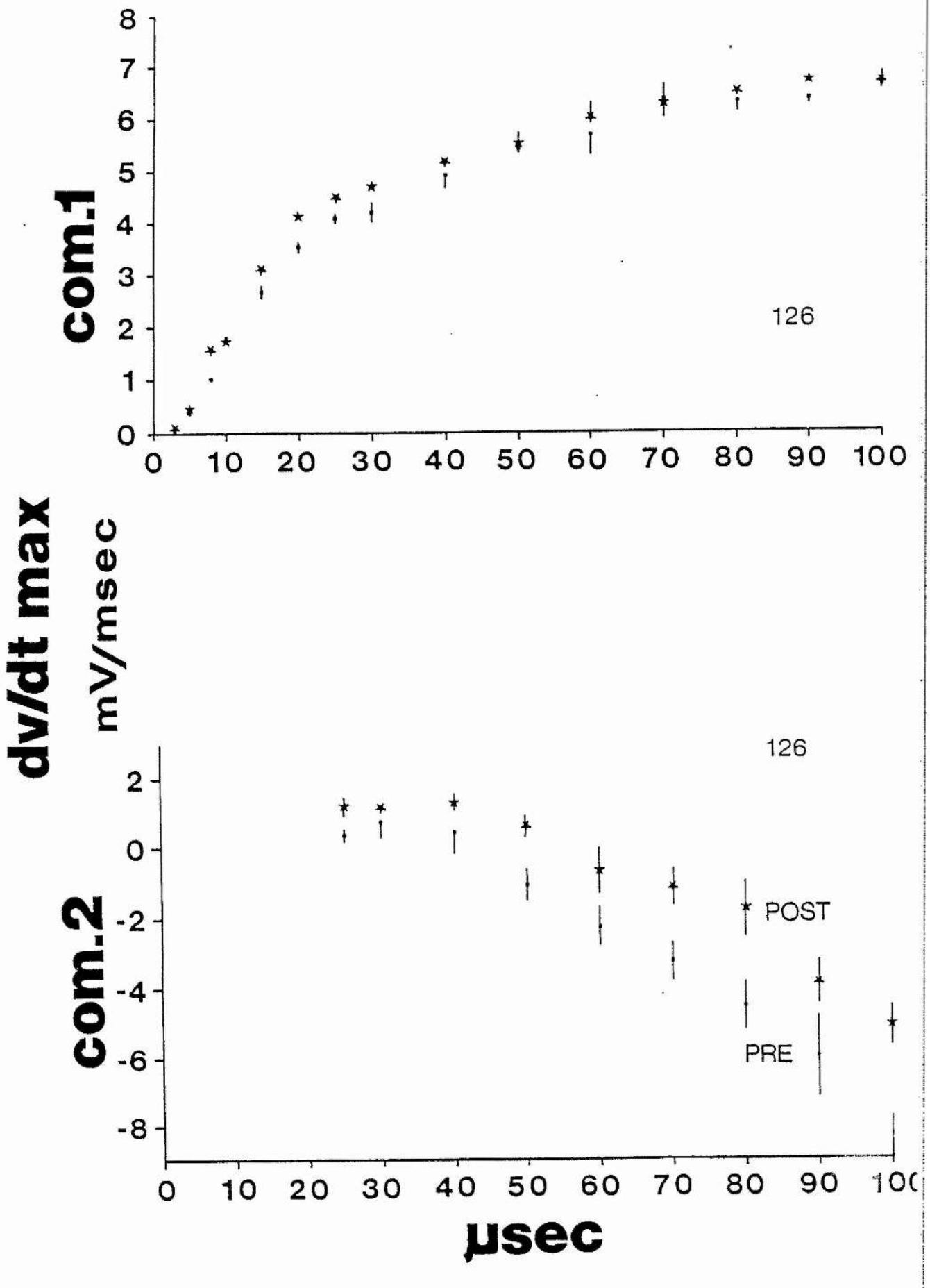
com.1
126
0
1
2
3
4
5
6
7
8
0 10 20 30 40 50 60 70 80 90 100
dv/dt max
mV/msec
com.2
126
POST
PRE
2
0
-2
-4
-6
-8
0 10 20 30 40 50 60 70 80 90 100
µsec

Figure 8-4. Data from animal 130, collected over a subthreshold range of stimulus durations, from 3 to 18 usec. Squares represent data collected before tetanization (means±sd's), while stars represent data collected 30 min after tetanus (means±sd's). Number of waveforms averaged at each stimulus duration was 5. Units of dV/dt max, mV/msec.

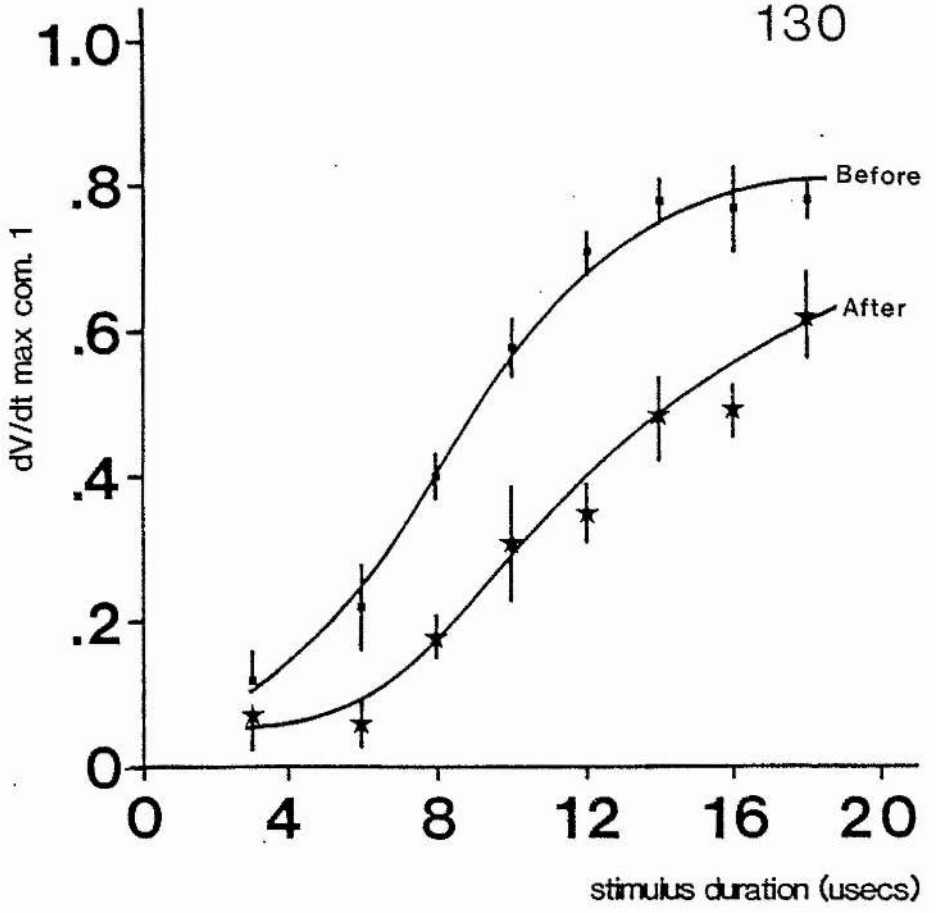
130
1.0
.8
.6
.4
.2
0
dV/dt max com. 1
Before
After
0
4
8
12
16
20
stimulus duration (usecs)

Relationship between the increase in magnitude of dV/dt component 1 and 2, after tetanization.

In 3 of the 4 experimental animals test stimulated above population spike threshold, the following relationship between dV/dt components 1 and 2 was observed. Scanning from high to low stimulus durations, the standard deviations associated with the mean of dV/dt component 2, pre and post-tetanization, start to overlap at the same stimulus duration at which the standard deviations of the mean of dV/dt component 1 begin to overlap figure 8-2. The change in dV/dt component 1 (pre-tetanization value minus post-tetanization value) is highly correlated with the change in dV/dt component 2 ($r=.9$, $P<.001$, calculated for rat 122; and $r=.7$, $P<.05$, for rat 124), over the range of suprathreshold stimuli, figure 8-5.

Figure 8-5. The figure shows data from two experimental animals, where the change in dV/dt in component 1 is plotted against the change in dV/dt in component 2, subsequent to tetanization. Units on both axis are mV/msec.

Left graph. Animal 124 : $r = -.7$, $P < .05$, slope = 9.5 Right graph. Animal 122 : $r = -.9$, $P < .001$, slope = 2.7

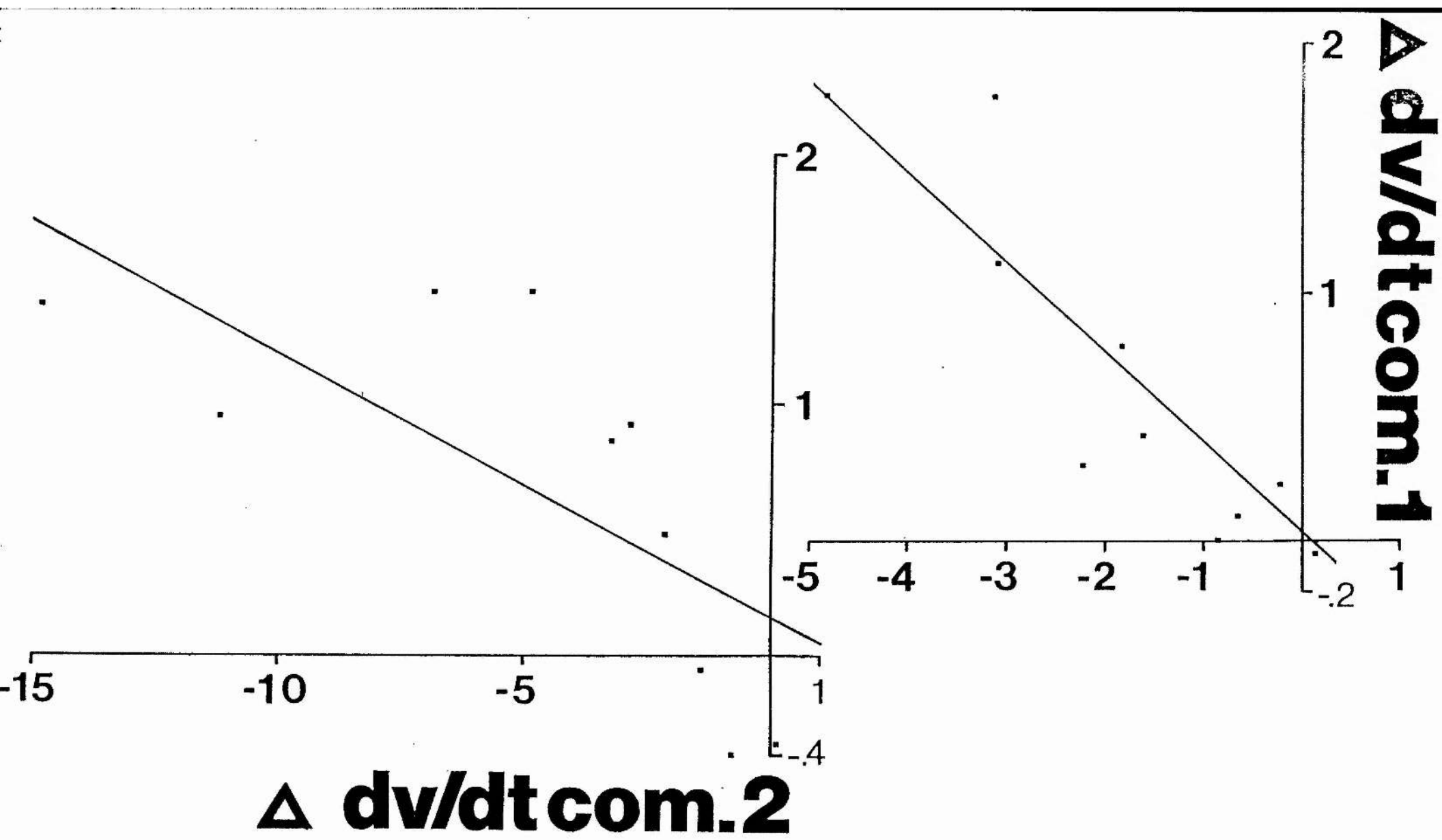
2
1
-.4
-15
-10
-5
1
Δ dv/dt com.2
2
1
-.2
-5
-4
-3
-2
-1
1
Δ dv/dt com.1

TABLE 8-1
=========
dV/dt max component 1, 100 usec stimulus duration : pre and post-tetanization

No	dV/dt comp. 1 pre-	dV/dt comp. 1 post-	t-test
121	9.39 -	9.97 -	-
122	4.13 ± .04	5.91 ± .13	P< .001
123	5.54 ± .13	7.30 ± .02	P< .001
124	7.27 ± .08	8.64 ± .07	P< .001
126	6.79 ± .06	6.78 ± .11	NS
127	4.28 ± .05	3.49 ± .06	P<.001
	mV/msec	mV/msec	

The table shows dV/dt max component 1, before and after tetanization (means ± se's).The significance associated with each pair is given on the right hand side of the table (Student's t-test). Rows 1-4 are experimentals, rows 5 - 6 are non-tetanized controls. Raw data was lost in animal 121, hence only mean data is presented (n=5).

TABLE 8-2

dV/dt max component 1, 3 usec stimulus duration : pre and post-tetanization

No	dV/dt comp. 1 pre-	dV/dt comp. 1 post-	t-test
121	.56 -	.49 -	-
122	.38 ± .04	.14 ± .02	P< .001
123	.12 ± .03	.15 ± .02	NS
124	1.32 ± .05	.59 ± .03	P< .001
130	.12 ± .02	.07 ± .02	NS
132	.17 ± .01	.19 ± .02	NS
126	.02 ± .01	.04 ± .02	NS
127	.14 ± .12	.12 ± .05	NS
	mV/msec	mV/msec	

The table shows dV/dt max component 1, before and after tetanization (means ± se's). The significance associated with each pair is given on the right hand side of the table (Student's t-test). Rows 1-6 are experimentals, rows 7-8 are non-tetanized controls (n=5).

Discussion

The results suggest that the dentate population spike is a triphasic, positive-negative-positive potential when recorded at the dorsal blade granule cell bodies. This is because the correlation between the LTP of the population spike and the LTP of the pre-spike potential is so high. Also when stimulating at the dorsal edge of the angular bundle the subthreshold population epsp is not potentiated 30 minutes after tetanization, whereas the suprathreshold epsp is potentiated. Therefore the positivity recorded preceding a spike negativity on a supra-threshold evoked waveform recorded near the hilus, is probably not caused by current flow generated on synaptic activation alone.

The conclusion that the population spike is triphasic might be avoided if one suggested that potentiation of synaptic transmission was either only occurring, or is only observable, when a relatively large number of afferents are being activated together. This would be quite contrary to previously obtained results from intracellular recording. Small populations of repeatedly activated synapses can produce

potentiated epsp's (Andersen, 1978; Yamamoto and Chujo, 1978; Haas and Rose, 1982; Lynch et al., 1983).

Explanation of the triphasic population spike

Typically, the extracellularly recorded action potentials of central neurones are triphasic (Terzuolo and Araki, 1961), and may be as large as extracellular somatic spike potentials. The triphasic nature of the population spike measured here may perhaps be explained as follows. Assuming the entry of perforant path fibres into a single lamina of the dentate gyrus at the dentate crest, taking the distance from the crest to the electrode tip as .75 mm, and the conduction velocity of perforant fibres as 2 m/sec , if the number of synapses activated are sufficient to elicit granule cell action potentials, the cells at the dentate crest will fire .4 msec before the cells adjacent to the electrode tip. This means that the region of the dentate at the electrode tip may be positive, with respect to the indifferent, the instant that the crest cells activate (ie about .4 msec before the neurones adjacent to the electrode discharge, figure 8-6i). The potential recorded will depend on how much axonal transmembrane current there is within the region near

Figure 8-6. i. The electrode tip is situated in the hilus of the dentate gyrus. Granule cells at the dentate crest are firing action potentials, and the potential recorded at the electrode tip is +ve, due to axonal transmembrane current and transmembrane current from horizontal dendrites.

ii. About .4 msec later, the cells adjacent to the electrode tip are depolarized. The electrode is recording a negativity.

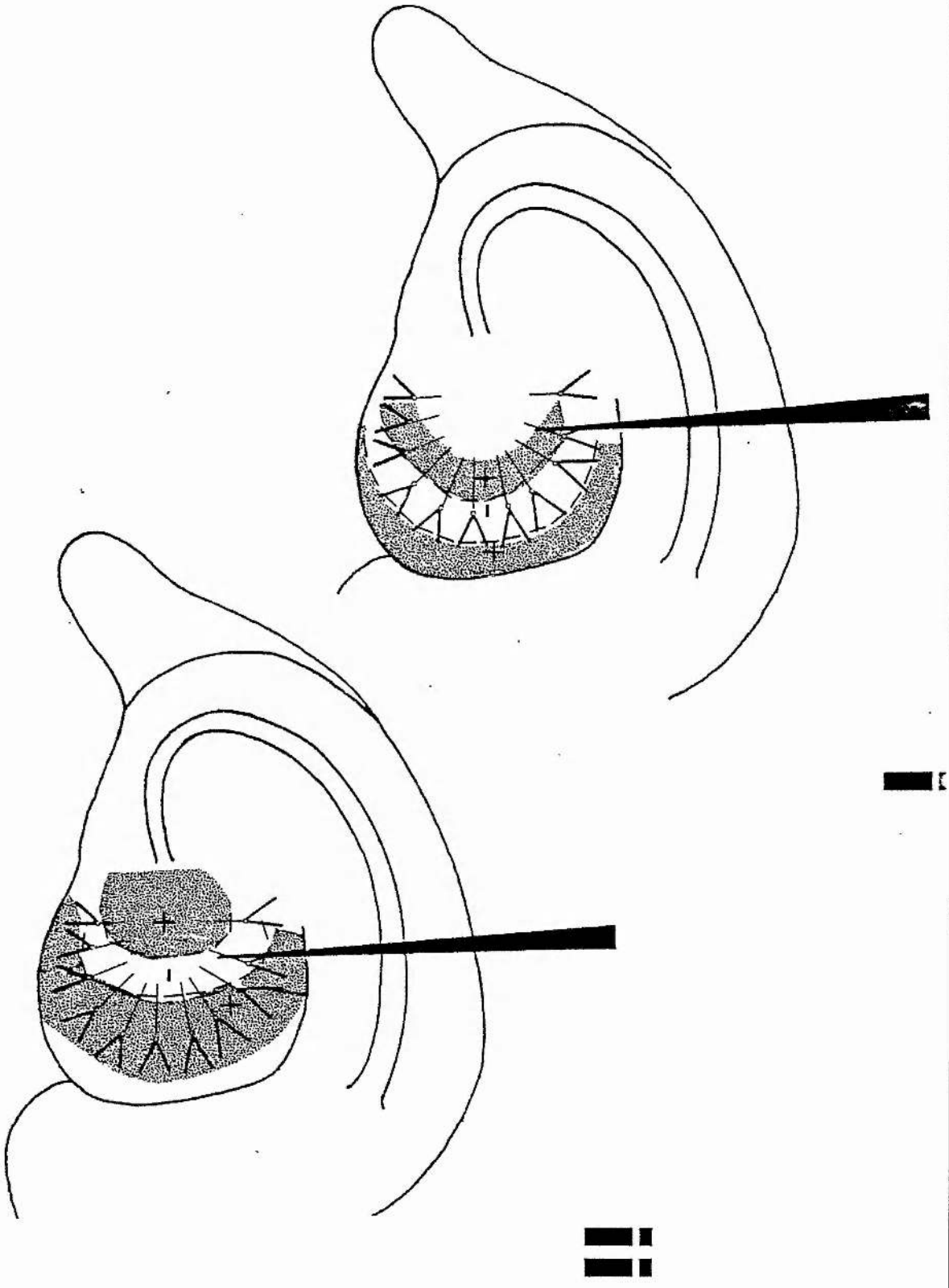

the electrode, and the potential divide. After cells at the crest have been activated, a triphasic, part cellular, part axonal action potential could traverse the recording region, figure 8-6ii.

It has been previously noted that synaptic field potentials can be recorded over distances of at least 2 mm. If we accept that the amplitude of the population spike potential is roughly the same order as a synaptic potential, the spatial extent of the extracellular potential field will also be similar. This being the case, it is likely that the recorded spike positivity begins around 1 msec before the onset of the spike negativity. This is because the dentate lamina are probably sequentially activated. As the perforant path action potentials approach the recording lamina, the hilus becomes positive in each lamina through axonal transmembrane current and transmembrane current from horizontally lying dendrites of already activated cells. The hilus in the adjacent, nearer lamina will then have become positive, and so on. The observed potential at the recording site will therefore increase in positivity, until the near-by granule cells discharge action potentials, figure 8-7a (NB Synaptic potentials have been ignored in the accompanying figures).

Figure 8-7a. Diagram of a row of granule cells located at the crest of the dorsal dentate gyrus, in several adjacent segments. Lateral perforant path (perf) fibres are shown innervating each cell sequentially, in a simplified manner. The granule cell closest to the reader has yet to activate, while the cells further away have already initiated action potentials, which are travelling as a triphasic wave away from the cell bodies. The position of the electrode tip is given by the asterisk. Note that until the neighbouring neurones activate, the electrode will record the approaching positivity.

M. Molecular layer.

G. Granule cell body.

H. Hilus.

b. Diagram is a simplified scheme of the dorsal blade of the dentate gyrus, the perforant path entering on the right, carrying action potentials (AP). The stippled line indicates the possible track of an electrode, where the two circles on the line represent two recording sites, ie a molecular site, and a hilar/granular site. It is possible that when the cells near the dentate crest are activating (arrows), the molecular electrode site would record a negativity, while the hilar/granular electrode a positivity.

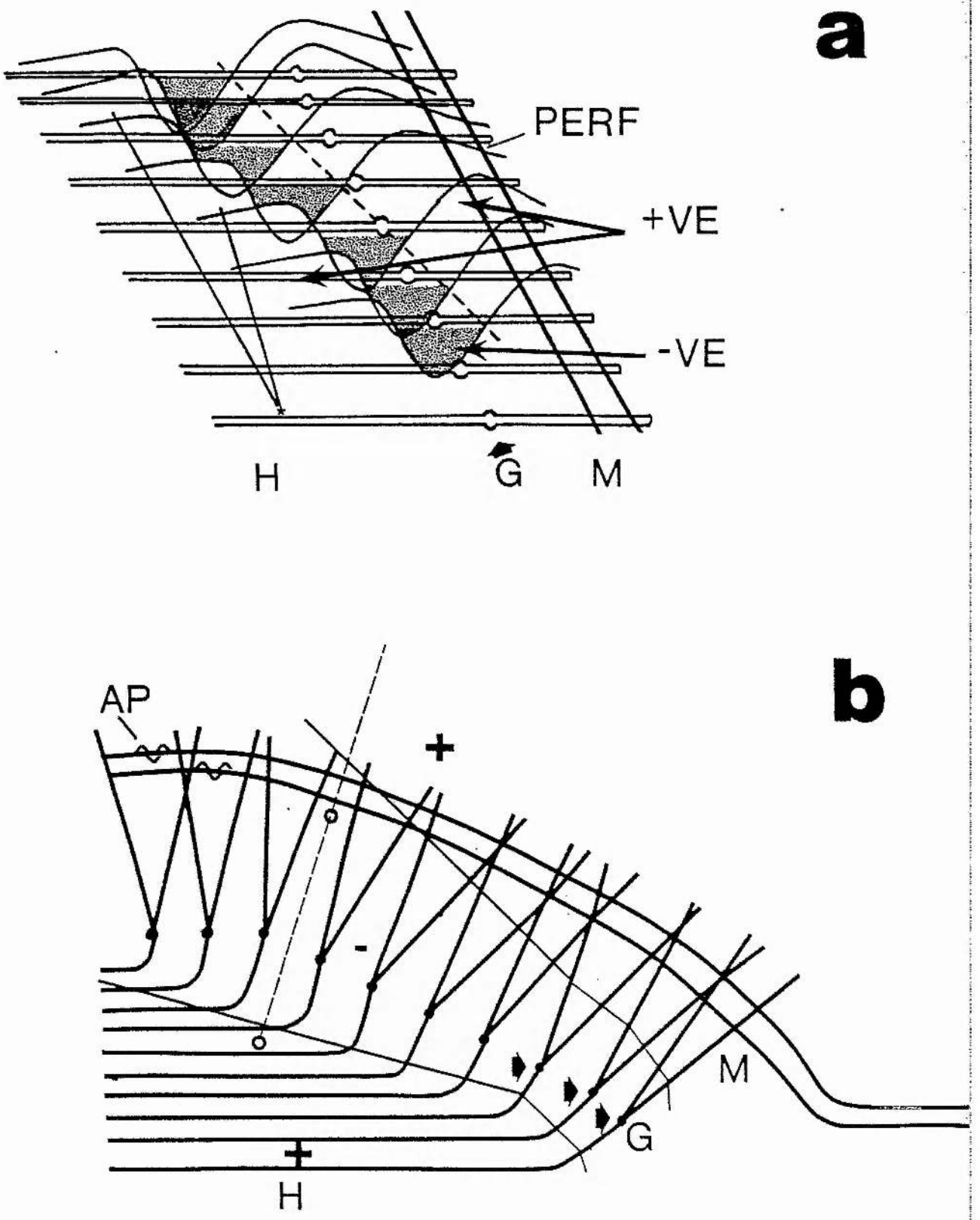
a
PERF
+VE
-VE
H
G
M
b
AP
+
-
M
G
H

Implications of triphasic dentate population spike

The data presented here suggests that the potentiation of the pre-negative spike positivity can proportionally co-vary with the potentiation of the spike negativity. The constant of proportionality is greater than 1, and will depend on the exact positioning of the electrode tip, (figure 8-6 and 8-7). Therefore, for a given increase in the slope of the pre-negative spike positivity, one might expect a proportionally greater increase in the slope of the spike negativity. If one believed that the two evoked potential components varied independently, this might lead one to conclude that because a given population epsp is associated with a larger negative population spike, the excitability of the granule cells had increased after tetanization, and could be quantified by such measurements. Undoubtedly the input/output activity ratio for the granule cells decreases after tetanization, but the validity of plotting excitability curves using such data recorded extracellularly must be called into question.

Synaptic evoked potentials

It is therefore crucial to consider the complication arising from the use of hilar recorded suprathreshold evoked potentials. Depending on the pre-tetanus magnitude and latency of the granule cell population spike, in the suprathreshold potential, part of the post-tetanic epsp potentiation will be caused by an increase in population spike magnitude, and a decrease in spike latency. Such potentiation of the pre-negative spike positivity would have the same duration as that of the population spike and may therefore account, at least in part, for long-lasting epsp potentiation in the suprathreshold waveform. No such complication exists with synaptic potential data. Other authors measure the extracellular epsp, when recording from the molecular layer, eg Lomo, 1971a; 1971b; Dolphin et al., 1982), although, unfortunately the molecular layer suprathreshold waveform may be similarly affected by the volume conduction of spike potentials generated by neurones some distance from the recording site (figure 8-7b).

The observation of the differential potentiation of the population epsp above and below population spike threshold needs further comment. Some workers, in particular McNaughton et al. (1978) and McNaughton (1982)

have shown that the amplitude of hilar recorded synaptic potentials (stimulus intensity well below that necessary to elicit granule cell discharge) can be increased after tetanization, with a duration certainly greater than 30 minutes. The data presented here suggest that there is no statistically significant increase in dV/dt of the synaptic potentials evoked by 3 usec stimulus durations, but rather a tendency to decrease, not seen in two untetanized animals. The explanation for this may be methodological, were McNaughton (1982), is stimulating ventrally in the angular bundle, and here, the dorsal edge of the bundle is preferentially stimulated. The synaptic potentials generated from the two sites may not therefore respond to tetanic stimulation in exactly the same way, particularly at post-tetanization latencies of > 30 minutes.

Dentate Population epsp Dynamics

Introduction

It has been reported many times previously, that high frequency activation of the perforant path can significantly enhance the evoked response from the granule cells in the dentate to test stimuli in the previously activated pathway. (Bliss and Lomo, 1973; Bliss and Gardner-Medwin, 1973; Douglas and Goddard, 1975; McNaughton et al., 1978). The mechanisms proposed as mediating this long-term potentiation have been discussed previously, but in summary, most involve an increase in synaptic conductance, eg increased numbers of post-synaptic receptors or elevated transmitter release (Dolphin et al., 1982; Lynch and Baudry, 1984). One would therefore expect to record a larger synaptic potential anywhere along the z-axis of the cell layer, except at the potential reversal-point.

An alternative mechanism, namely increased dendritic membrane resistance, has also been discussed which is attractive both as a candidate for LTP and for memory, (Bindman and Prince, 1984; Baryani and Feher, 1981; Alkon, 1982), and might be expected to have the

following effects on a synaptically generated field potential. Accompanied by no changes in synaptic conductance, increased r_m would reduce the maximum size of the synaptic potential recorded along the z-axis of the cell layer, and also alter the spatial dynamics of the potential such that the reversal-point is brought closer to the granular layer. If the reduction in size of the synaptic potential is counteracted by a simultaneous increase in synaptic conductance, the effect on the shape of the potential profile should still remain.

The following series of experiments were therefore performed in order to assess whether the synaptic potential reveals any changes after afferent tetanization which might be attributable to increases in dendritic r_m. After finding stimulation parameters which elicit reliable LTP, the form of the synaptic potential profile was assessed by recording simultaneously from the molecular and the granular layer of the dorsal blade, and also by generating complete profiles at a fixed post-stimulus latency by systematically changing the position of a glass microelectrode.

Methods

Experiments were performed on male rats (280-455g), and will be reported in three sections. The experimental arrangement has been described previously (materials and methods). The stimulus intensity was set to the minimum voltage necessary for eliciting a maximal population spike at 100 usec stimulus duration, which was always less than 5 volts.

Experiment 1

The potentiating effect of a single 400 Hz train comprising 99 impulses at 100 usec stimulus duration was assessed on population epsp's recorded at the dorsal blade granular layer. The potentials were generated on stimulation at a dorsal site in the angular bundle. Observations were made on 8 experimental and 8 control animals. Single teflon coated 70 um diameter platinum-iridium wires were used to record evoked potentials near the dorsal blade granule cells. The stimulating electrode tip was placed in a dorsal position in the angular bundle where an obvious population spike was attainable at long (ie around 100 usec) stimulus widths (2.38$\pm$.11 mm below brain surface, mean$\pm$se). Stimulation was monopolar cathodal, at a test frequency of .2 Hz. At short stimulus widths ie <

5 usec, almost pure short-onset latency potentials were obtained in the dentate from this stimulating position.

Evoked potentials were analysed on-line, average amplitudes were calculated, and average waveforms stored on disk (n=5). In experimental animals, recordings were made at short stimulus widths (3-4 usec) and at a long stimulus width (100 usec), immediately before high intensity tetanus of the perforant path. At 2 min, 5 min, 10 min, 20 min and 40 min after tetanization, recordings were made of synaptic potentials evoked by 3-4 usec stimulation. At 40 minutes post-tetanization, potentials evoked 100 usec duration stimuli were also recorded. The animals were not stimulated between recording sessions. Recordings of potentials evoked by 100 usec duration stimuli (at .2 Hz), were made in controls, before and after a 40 minute period during which the animals were not stimulated.

Activation of an increasing proportion of perforant path fibres is also bound to alter the shape of the potential profile, and in particular extend the limit of sink current ventrally, by activating medial perforant path synapses on the middle third of the granule cell dendrites. Therefore, in the 8 control

animals, after making the above recordings, the position of the potential reversal point was estimated at 5 msec post-stimulus latency for 3, 4, 5, 6, 8, 10 and 15 usec stimulus durations, in 5 consecutive evoked potentials, .2 Hz test stimulus frequency. The average value at each duration was calculated on-line by computer.

Experiment 2

In 6 experimental and 6 non-tetanized control animals, the potential reversal point was interpolated between the tips of 2, 70 um diameter teflon coated platinum-iridium wires, the tips being separated by 400 um. The stimulation site was at a dorsal position in the angular bundle (see above), with the stimulus voltage at the lowest necessary to elicit a maximal population spike at 100 usec duration. Experimental animals were test stimulated at .2Hz, with a 5 usec stimulus, receiving high frequency tetani at 5 minutes and 10 minutes after the start of recording. Test stimulation then continued for a further 25 minutes.

The experimental animals were then tetanized at 150, 200 and 250 usec duration at 5, 15 and 25 minutes

after the onset of recording. After the final tetanizing train the animals received test stimulation for a further 15 minutes.

Experiment 3

Using 10 experimental and 10 non-tetanized control animals, after penetrating the hippocampus, and finding the region of granule cell multiple unit discharge using a Na^+-acetate (2M) filled glass micropipette, the electrode was manipulated in 20 um steps dorsally from the granule cell layer, for 400 um. It was then moved back, in 20 um steps, to the cell layer. At each point, the electrode was allowed to settle for 30 seconds, before the average amplitude of 5 potentials, evoked at .2 Hz, was calculated at 3 msec post-stimulus. The stimulating electrode was positioned dorsally in the angular bundle exactly as above. The reversal point was estimated using linear interpolation between points, off-line.

Results

Experiment 1.The potentiating effect of a single 99 stimuli, 400 Hz train

Comparing data from 7 experimentals (data from one

animal was lost), and 7 controls (I could not elicit a population spike in one animal), the mean change in the size of the population spike in controls was -.25±.26 mV mean±se (ie the spike amplitude was reduced), and in experimentals the mean change was +1.68±.58 mV (t=2.83, P<.02 Students' t-test). The average increase of the population spike (measured from the peak of the pre-negative positivity, to the peak negativity) relative to pre-tetanus values at 100 usec stimulus duration, was 10.2±5.1 (means±se, n=7), range *26.5 to *.97; ie on average over 1000% of the pre-tetanization amplitude. Such a statistic has very limited meaning, as the fractional increase in amplitude attained with LTP clearly depends on the size of the spike to begin with. However, it is clear that a single 99 stimuli, 400 Hz tetanus normally elicits LTP, with a duration of more than 40 minutes.

The data obtained from the subthreshold stimulation shows an elevation in the amplitude of the granular layer recorded positivity after tetanization, which decays by 20 minutes post-tetanus, to be replaced (on average) by a depression. This was precisely what was found in the population spike dynamics experiments. This trend is clearly not statistically significant at

40 minutes post-tetanus. The results for the subthreshold potentials, evoked by short stimulus widths, are presented graphically in figure 8-8.

Figure 8-9 is a plot of the average position of the estimated reversal point relative to the granular layer electrode tip for all 8 control animals. The data shows that on average, increasing the test stimulus duration from 3 to 15 usec, with constant stimulus voltage causes a ventral movement of the estimated reversal point of 4 %.

Experiment 2. Estimation of the synaptic potential reversal-point

The results of the experiment are presented graphically in figure 8-10 and 8-11. Comparing the mean difference of the estimated reversal-point position, during the 5 minutes before and between 5 and 10 minutes after the first high frequency tetanus, with the difference over the same time periods in the control animals, there was a significant ventral movement of the reversal point after tetanization: 7±2% of the total potential difference between the electrode tips, relative to the control value of 2±1% ventral

Figure 8-8. i. Graph is a plot of mean fractional change in amplitude of subthreshold synaptic potentials, in 8 experimental animals, estimated at a fixed latency of 5 msec post-stimulus latency, against time in minutes. tetanization occurs at time 0. Bars are ±se's.

ii. Plot of mean fractional change in amplitude of subthreshold synaptic potentials, in 8 experimental animals, estimated at 2.5 msec post-stimulus latency (same waveforms as above), against time in minutes. Tetanization as above. Note that the two latencies give slightly different results - the short latency measurement shows greater initial potentiation, but also greater depression (on average) at 40 minutes. This may reflect the differing synaptic populations active during evoked potential production.

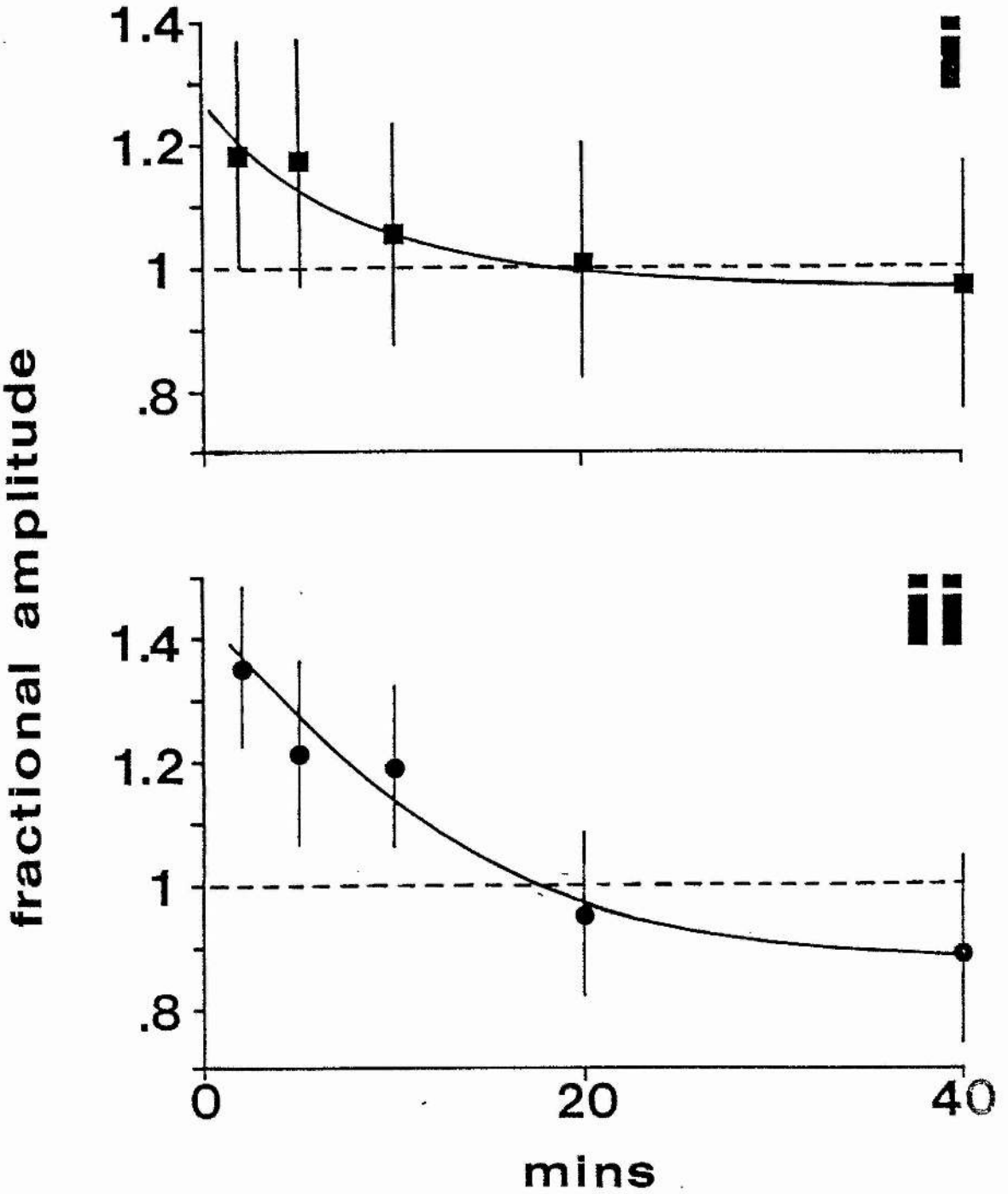
1.4
1.2
1
.8
i
1.4
1.2
1
.8
ii
fractional amplitude
0
20
40
mins

Figure 8-9 . Plot of average interpolated reversal point position, as a function of increasing stimulus width, at a constant voltage. Data from 8 control animals (PD is percentage difference).

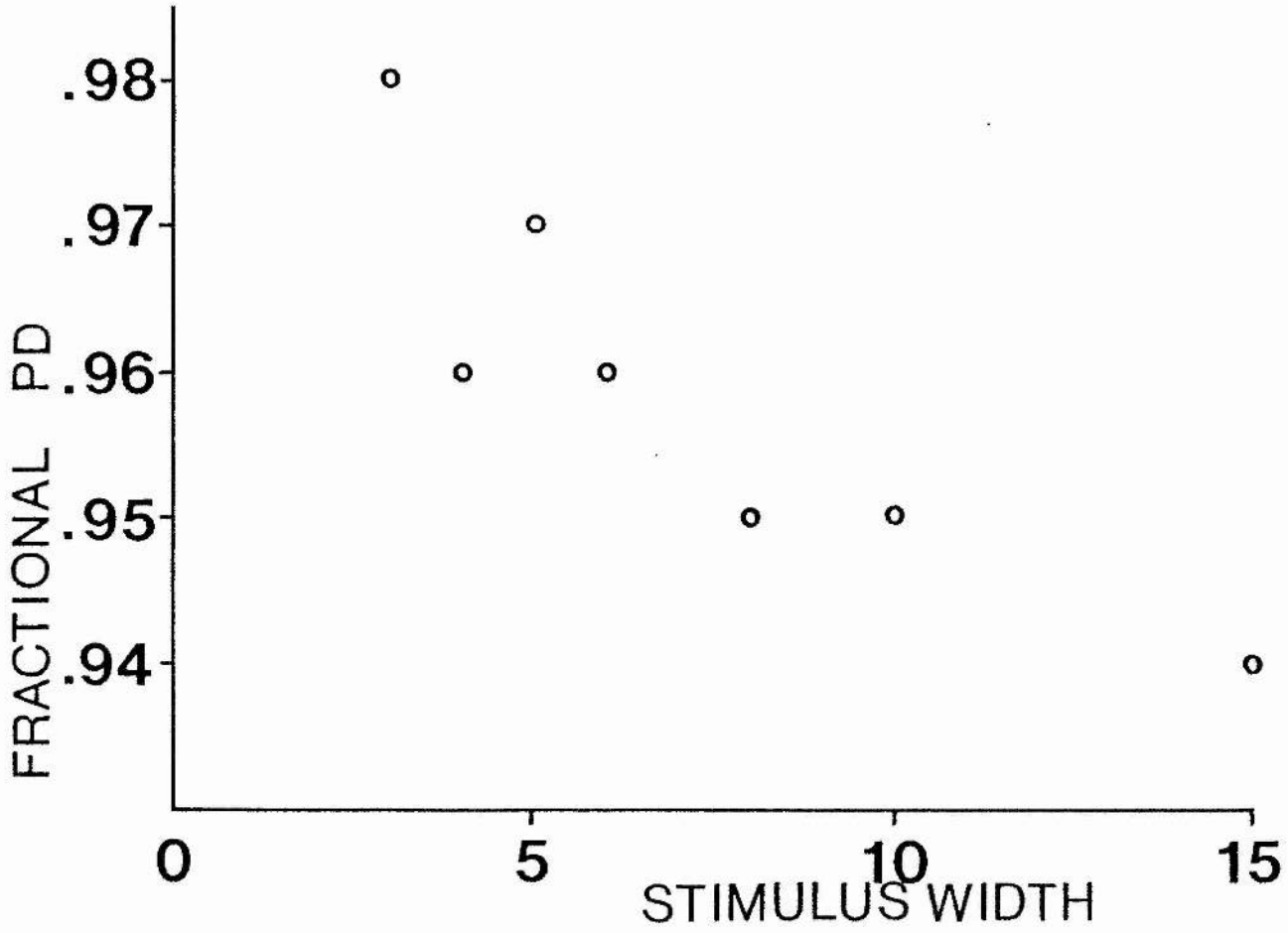
.98
.97
.96
.95
.94
FRACTIONAL PD
0
5
10
15
STIMULUS WIDTH

Figure 8-10. Plot of interpolated reversal point position against time in 5 second intervals. At 5 minutes and 15 minutes after the start of recording the perforant path was tetanized using two 400 Hz tetani, times indicated by chevrons (see text).

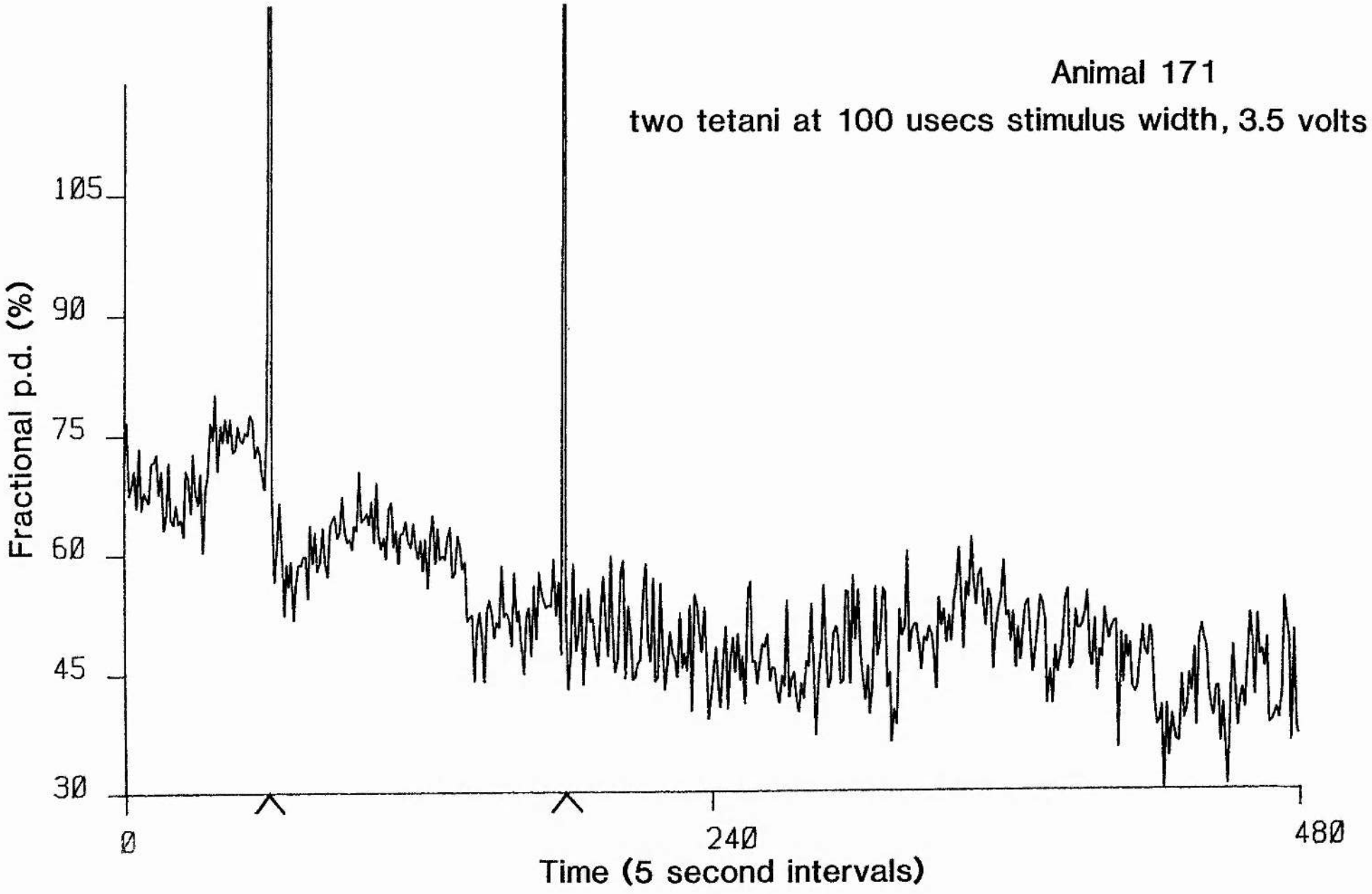
Animal 171
two tetani at 100 usecs stimulus width, 3.5 volts
105
90
75
60
45
30
Fractional p.d. (%)
0
240
480
Time (5 second intervals)

Figure 8-11. Plot of interpolated potential reversal point position against time, as previous figure. Data is the mean for 6 animals. Hash mark indicates a value of $P<.05$, comparing the mean position during the control period and between 5 and 10 minutes after tetanization.

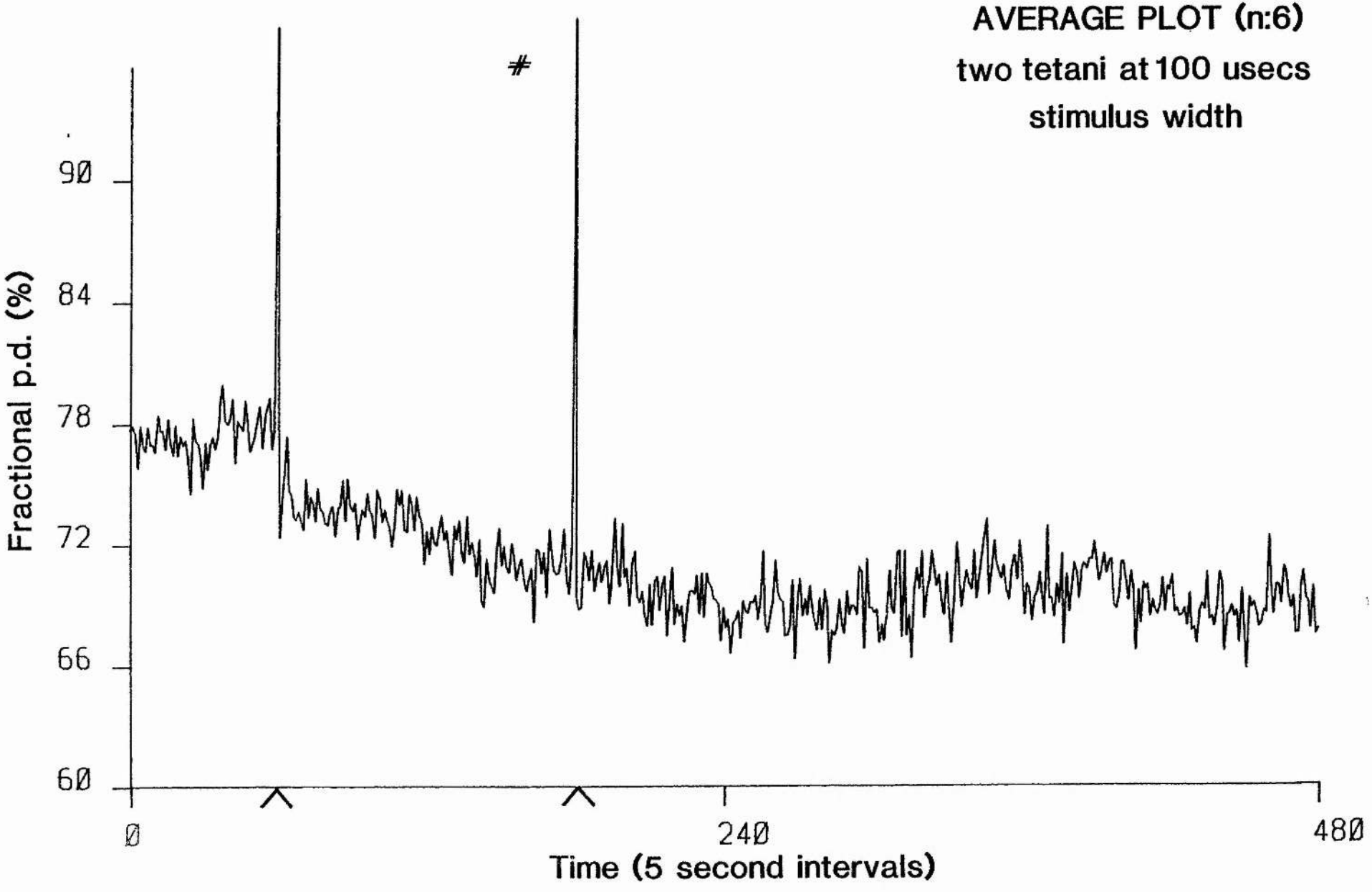
AVERAGE PLOT (n:6)
two tetani at 100 usecs
stimulus width
#
90
84
78
72
66
60
Fractional p.d. (%)
0
240
480
Time (5 second intervals)

(means±se, p<.05, Student's t-test). This suggests that there is a step-like change in the spatial shape of the synaptic potential. A second identical tetanus did not appear to enhance the effect.

The results of increasing the the tetanizing stimulus duration are presented graphically in figure 8-12. Comparisons were made between the mean interpolated reversal-point position during the 5 minutes before the first high frequency train and between 5 and 10 minutes after each tetanus. The results and significance in Student's t-tests are given in table 8-3.

Table 8-3
=========
Potential reversal point movement after increasing tetanizing stimulus duration.

Stimulus duration	Experimentals	Controls	t-test
150 usec	-3.6± 1.0%	-.32 ± .3%	P< .02
200 usec	-6.1± 1.1%	-1.2 ± .7%	P< .01
250 usec	-8.2± 1.6%	-2.3 ± .8%	P< .01

(- indicates ventral movement)

The experimental animals showed fairly sharp, step-like movements of the interpolated reversal-point, immediately after each tetanus, whereas the control animals

Figure 8-12. Plot of the interpolated potential reversal point against time in 5 second intervals. Chevrons on the x-axis indicate times of tetanic activation of the perforant path. Hash marks refer to the result of Student's t-tests comparing experimental and contol data. 2 hash marks indicate P<.02, 3 hash marks indicate P<.01 . See text for details.

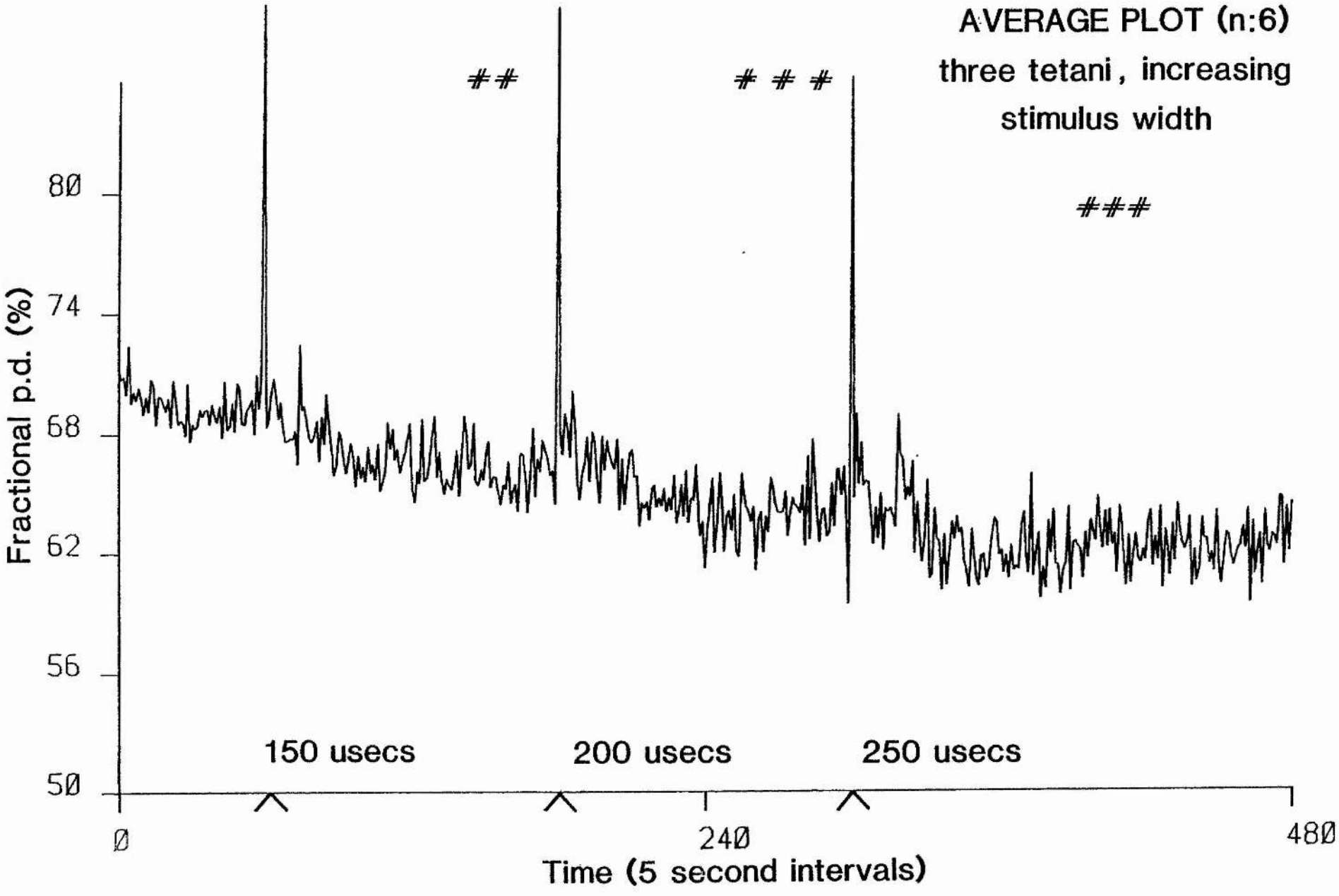
AVERAGE PLOT (n:6)
three tetani, increasing
stimulus width
##
# # #
###
80
74
68
62
56
50
Fractional p.d. (%)
150 usecs
200 usecs
250 usecs
0
240
480
Time (5 second intervals)

showed some degree of drift in the same direction.

Using analysis of variance, the mean reversal-point movement after the three tetani differed significantly between experimentals and controls ($F=14.04$, $P=.0038$). However, the passage of time effect in controls caused a significant ventral movement in the reversal point ($F=7.49$, $P=.01$) over equivalent periods. This had the effect of producing a non-significant groups by tetanizing stimulus duration interaction. Some of the ventral movement of the reversal point in experimentals could therefore have been due to a passage of time effect.

Experiment 3. Depth-profile potential reversal

A typical depth profile generated by passing through the molecular layer of the granule cells is shown in figure 8-13. The current source density (CSD) profile is shown adjacent. The second derivative waveform covers less distance than the original potential, as data is lost when using a differentiating algorithm.

Despite the length of time it takes to complete

Figure 8-13. a. Second differential of the synaptic potential profile (equivalent to CSD), g enerated by stimulation at the dorsal edge of the angular bundle (electrode placement shown in histology, figure 9-1). Section of CSD profile above zero is a region of sink current maximal at around 310 um from the granule cell layer. Note that the profile starts at 80 um from the cell layer - which is inevitable, data is 'lost' in order to differentiate.

b. Original synaptic potential depth profile - amplitude of the potential being measured at the fixed post-stimulus latency of 3 msec. This is a pure short-onset/peak potential, and appears to be generated by synapses occupying the medial entorhinal fibre terminal field. 0 um was the point of maximal multiple-unit discharge, and is taken as the granule cell layer.

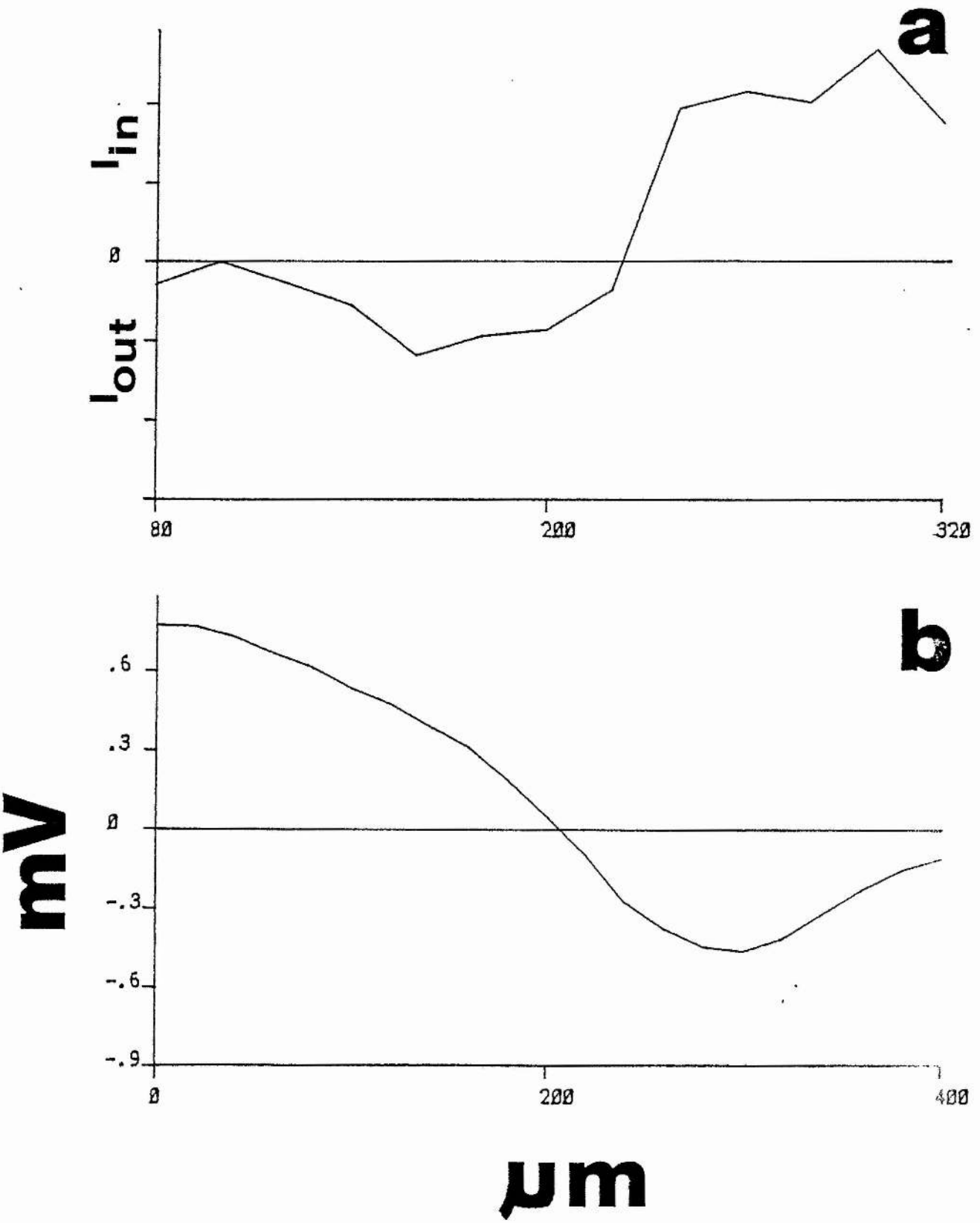
a
I_{in}
0
I_{out}
80
200
320
b
.6
.3
0
-.3
-.6
-.9
0
200
400
mV
µm

the depth-profile data collection, ie 30 minutes - a statistically significant ventral movement of the reversal point was found in tetanized animals relative to controls. Using linear interpolation between data points, the average distance from the starting point (ie at the point of maximum granule cell discharge), to the point of potential reversal was calculated from the upward and downward passes of the electrode, before and after tetanization. Data is presented in table 8-4.

Table 8-4

Depth profile reversal-point movement after afferent tetanization

post - pre-tetanus	group
-12.6 ± 6.6 um	experimentals
+7.9 ± 7.0 um	controls

- indicates ventral movement (t=2.13, P< .05, Students' t-test)

Discussion

The data suggests that the 99 stimuli, 400 Hz tetanus train employed can induce long-lasting (> 40 min) potentiation of the granule cell population spike on perforant path activation. High frequency afferent

activation can induce long-lasting (> 30 minutes) changes in the spatial dynamics of subthreshold synaptic potentials which may be the result of a long-lasting increase in dendritic r_m. The magnitude of the change measured by interpolating the position of the reversal point, may be directly related to the duration of the tetanizing stimuli, and hence to the number of simultaneously activated perforant path fibres. The depth profile generated by activation of the fibres lying in the dorsal r egion of the angular bundle before and after tetanic stimulation reveals a ventral movement of the position at which the synaptic potential reverses polarity.

The apparent movement of the potential reversal-point might be explained by several mechanisms. Tetanization may alter the excitability of the perforant path fibres, thus extending the region of sink current in the granule cell dendrites towards the cell body layer. The membrane resistance of the granule cell bodies might be reduced, or the granule cell dendritic $r_m$could be increased. The dendritic axial resistance could be reduced by dendritic swelling. As there is much evidence suggesting that there is no change in the excitability of hippocampal afferents subsequent to tetanus (eg Andersen, 1978), and the

movement in the estimated reversal point at a fixed post-stimulus latency with increasing stimulus duration is small, it seems unlikely that ventral extension of the sink could account for the effect. Long-lasting decreases in the somatic membrane resistance would tend to decrease the cellular excitabiltiy, so would be an unlikely mechanism. As dendritic swelling (as opposed to dendritic spine swelling) has not been reported, Increasing dendritic r_m is perhaps the most attractive hypothesis.

Changes of the synaptic field potential in the dentate subsequent to perforant path tetanization can be explained as being caused by, i) an increase in the conductance of the postsynaptic region of active synapses, which have previously been activated at high frequency, and ii) a simultaneous increase in the membrane resistance of the granule cells. A prediction which is implicit in the hypothesis is that where some fraction of the afferent input to a granule cell has been activated at high frequency, non-tetanized afferents when subsequently activated would elicit an evoked potential smaller in amplitude, slope etc. than before. This is explained diagrammatically in fig 8-14. The hypothesis can therefore account for the observations of Abraham and Goddard (1983), McNaughton

Figure 8-14. Simplified circuit diagram of the dorsal blade of the dentate, incorporating lateral and medial perforant path inputs, and the recording circuit (subsidiary circuit on r_o). r_i is the intradendritic resistance, r_o is the parallel extracellular resistance, r_m is the granule cell dendritic membrane resistance, and r_{sy} is the synaptic resistance. The batteries represent the electrochemical gradient for Na^+ which crosses the postsynaptic membrane on receptor activation.

The input resistance at the synaptic region of both lateral and medial perforant paths is variable, and therefore shown as a rheostat. It can be altered by the amount of transmitter released at a synapse, the number of receptors, or the diameter of dendritic spines etc. Where there is no synaptic activity, r_{sy} is very great, and little or no current flows in the circuit. Synaptic activation induces current flow in the circuit (ie reduces r_{sy}), which is recorded at the potentiometer in the subsidiary circuit as a potential - which can be positive or negative depending on the position of the electrode along resistor r_o. The present theoretical discussion confers r_m with the properties of a rheostat.

Therefore, if on the separate tetanic activation of either lateral or medial perforant paths, the resulting effects are a decrease of r_{sy}, specific to that pathway, and to increase r_m, where shortly after tetanization (eg < 40 minutes), the overall effect is to decrease the total resistance in the circuit specific to that pathway, then at the same time, subsequent activation of the other pathway would induce a current flow less than that induced before the tetanization. This is because r_m has increased. Extracellular potentials will therefore inevitably be smaller for this pathway. However, intracellular potentials will be potentiated from both pathways, because of the increase in r_m. Therefore it may not be true to say that as the magnitude of an extracellular synaptic potential is reduced, the effectiveness of the group of afferent synapses generating the potential are either 'depressed' in efficacy, or 'de-potentiated' (see eg Levy and Steward, 1979).

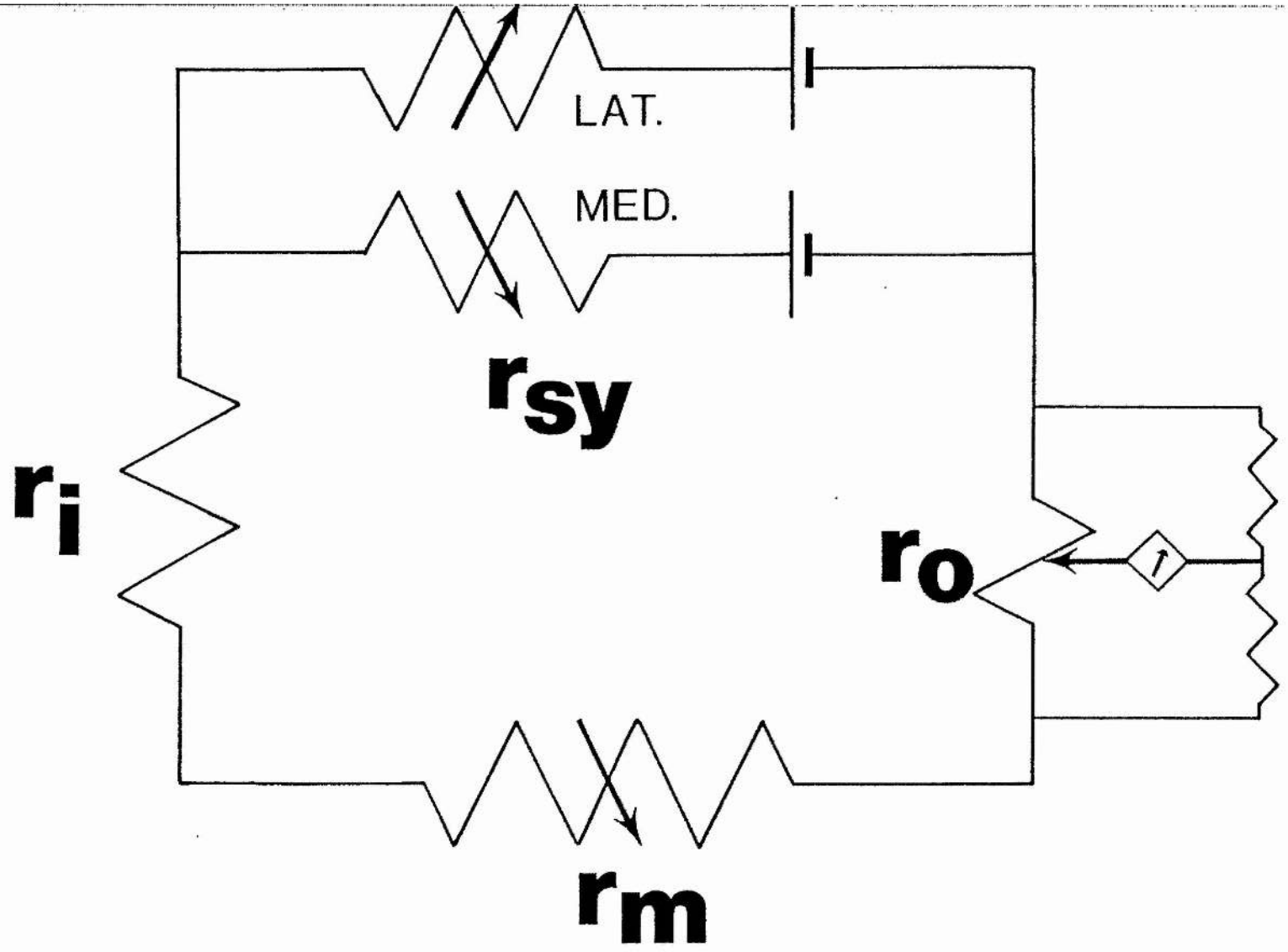
LAT.
MED.
r_{sy}
r_i
r_o
1
r_m

(1983), Levy and Steward (1979), of heterosynaptic 'depression'. Abraham and Goddard reported that after tetanic activation of the medial perforant path, the synaptic potential elicited on stimulation of the lateral path was depressed and vice-verca. The effect could last up to 3 hours, but could be prevented by prior tetanic activation of the test pathway.

The changes in the magnitude of the synaptic potential might therefore be thought of as the result of the interaction of increased membrane resistance and increased synaptic conductance.

Summary

1. Stimulating at a dorsal site in the angular bundle, LTP of the granule cell population spike was induced by tetanic activation.

2. The in vivo granule cell population spike is probably a triphasic positive, negative, then positive going waveform (as measured near the granular layer). This is a complicating factor when measuring the pre-spike population epsp.

3. LTP of the population epsp, induced by minimal

stimulation in the angular bundle, had decayed in about 20 minutes (on average) after a single 400 Hz tetanus. LTP of the population spike, induced by stronger stimulation, was still highly significant at this time.

4. The spatial shape of a synaptic potential changes after tetanization, including a ventral movement of the reversal point. The degree of change is dependent on the duration of the tetanizing stimuli.

5. The observations may be explained by an increase in granule cell dendritic membrane resistance, although several alternative explanations were discussed.

CHAPTER 9

FINAL DISCUSSION

Increased membrane resistance on repeated synaptic activation has been implicated in heterosynaptic facilitation observed in the neocortex (Baranyi and Feher, 1981), and is suspected as the mechanism of increased cortical responsiveness to antidromic stimulation of the pyramidal tract subsequent to high frequency antidromic activation (Bindman and Prince, 1984). Decreasing the electrotonic length of the dendrites by increasing dendritic r_m, is an attractive memory mechanism as it offers the dendritic tree of a cell as an 'associative surface'. Heterosynaptic facilitation is the key. Baranyi and Feher show, in a very elegent demonstration in the motor cortex of the cat, that pairing a weak synaptic input with a strong one progressively enhances the strength of the weaker input. During paired stimulation the weak input is activated some 10's of msec before the strong. This causes the postsynaptic cell membrane resistance to increase (recorded in the soma), until the weak input can discharge the cell, which formerly it was unable to do. The

effect occurs after 60 to 90 stimulus pairings, and lasts up to 40 minutes. They also showed that subsequent activation of the weaker input on its own at .5 Hz for 34 minutes caused the effect to be abolished, with a corresponding reversion to the pre-stimulation $r_m$values. Baranyi and Feher suggested the changes in $r_m$may be due to alterations in membrane K^+conductance.

It seems that increasing the amount of Ca^{2+} inside a hippocampal neurone is a necessary factor in eliciting LTP (see Eccles, 1983 for a review) although this is not proven (Sastry and Goh, 1984). If the concentration of intracellular Ca^{2+}could be raised locally, giving rise to local membrane phosphorylation close to an activated synapse, then one might have a highly specific way of changing the effectiveness of synapses. Only synapses distal of that region would feel any effect. Perhaps the ionophores activated by transmitter binding at the NMDA type receptor primarily admit $Ca^{2+}$to the post-synaptic locality.

Given the discrete laminar organization of afferents synapsing in the granule cell dendrites, it is tempting to postulate that, as a general principle, those afferents synapsing on the proximal dendrites can

modulate the effectiveness of more distal terminating afferents. It is possible that the electrotonic distance of a distal synapse on a dendritic branch, is regulated by synapses lying between that synapse and the cell body. One might suggest that activation of a single, or perhaps a few medial entorhinal axons, could regulate the effectiveness of lateral entorhinal axons synapsing on the same dendrite; the activity of the former acting as a gating mechanism for the later. Viewing the dentate gyrus as a whole, the medial entorhinal cortex might set up a pattern of spatial and temporal synaptic activity, which acts as a 'sieve' for lateral entorhinal afferent activity. Thus the dentate would act to filter an input (carried by the lateral entorhinal fibres), only passing-on salient information to Ammon's horn.

A scenario which includes much of the discussed and presented data is as follows. Tetanic activation of the perforant path gives rise to increases in transmitter release, by elevating the number of quanta released from synapses operational before tetanization, and by elevating the probability of transmission from any given synapse - so that previously dormant synapses become functional. This effect must last at least 30-40 minutes, but will depend on the tetanizing

stimulus characteristics. The cause would probably be elevated pre-synaptic [Ca^{2+}] increasing the number of vesicles released per stimulus.

Repeated synaptic activation probably also causes an increase in post-synaptic [Ca^{2+}]. Perhaps the influx of Ca^{2+} is primarily due to NMDA receptor activation by glutamate. This elevation of post-synaptic [Ca^{2+}] might give rise to an increase in the number of post-synaptic receptors, or perhaps to the phosphorylation of K^+-channels in the dendritic membrane, decreasing the electrotonic distance between the synapse and the soma. An appropriate K^+-conductance is the so called I_m current (Adams et al., 1981; review: Adams, 1982). Such a phosphorylation process could be modulated, via cyclic nucleotides, by monoamines and Ach. Increases in r_m are associated with the action of Ach in the cortex (Krnjevic et al., 1971) and the actions of dopamine and noradrenaline in the hippocampus (Herrling, 1981). As the ascending activity from the brain stem modulates the gross functioning of the brain, and hence the behavioural state of the whole animal, eg awake or asleep (Winson and Abzug, 1978; Barnes, McNaughton, Goddard, Douglas and Adamec , 1977), so the monoamines and Ach modulate the responsiveness of hippocampal cells. One might postulate

that the synaptic inputs from brain stem nuclei have widespread effects on the electrotonic characteristics of the granule cell directly, or by regulating the efficacy of other synaptic inputs.

Long-term potentiation and memory

Electrophysiological synaptic plasticity in the form of heterosynaptic facilitation, must be viewed within the whole information processing mechanisms of the brain, and not simply referred to as 'memory'. An up-regulation of synaptic efficacy could not account for memory formation and storage, and cannot be divorced from myriad other integrative mechanisms existing within anatomically defined neural systems, and between those systems, in the vertebrate brain, all of which are involved in the interaction of an organism with its environment. Memory can only be defined in behavioural terms. It reveals itself as alterations in the behaviour of an organism as a result of experience. Particular learning paradigms have been developed in order to quantify the degree of task acquisition, and at the same time offering an insight to the corresponding neural mechanisms (Baranyi and Feher, 1981; Alkon, 1982). Such paradigms include classical, or Pavlovian conditioning, and operant conditioning. The suggestion that learning may be thought of as the establishment of excitation chains in neuronal populations by an up-regulation of synaptic efficacy - linking a sensory input to a motor output by some tortuous neural circuit, is hopelessly naive. Undoubtedly learning must

involve the differential inhibition of neural systems output as much as the enhanced relay of excitation from one neurone to another. An example of this would be the finding by Thompson and his colleges that an ipsi-lateral cerebellar lesion is necessary and sufficient to abolish classical conditioning of the nictitating membrane conditioned reflex in rabbits (see Thompson, 1983). The function of the cerebellar folia is to inhibit (via the Purkinjie cells) the cells of the intracerebellar nuclei, which act to modulate motor activity. Without the integrity of the system, the association between a tone (conditioned stimulus) and an air puff, directed at the cornea (unconditioned stimulus) cannot be made. It is only to be expected that learning involves the enhancement of information transmission between one cell and another, while, simultaneously involving a decrement of information transfer elsewhere, even perhaps up and down-regulation of synapses on the same post-synaptic neurone. It has recently been shown, for example, that long term potentiation of synaptic transmission can be controlled by inhibitory interneurones (Douglas et al., 1982; Wigstrom and Gustafsson, 1982).

Anatomical regions of the brain can be easily classified when there is some distinct sensory input,

eg from the retina, or some distinct motor output, eg to the motoneurones of the spinal cord. It is much harder to elucidate the function of poly-modal association areas, such as the hippocampus. Indeed it is not yet clear in what terms 'psychological-function', as distinct from the physiological mechanisms of impulse transmission and synaptic transduction, should be couched. There seem to be two ways forward, both of which are complementary although perhaps the former description will prove both harder to attain but more generally applicable across species than the later.

Examination of both the information entering the hippocampus (eg frequency and synchrony of granule cell action potentials), and the output, namely the characteristics of action potential generation in cell field CA1, may reveal the principles of the transformation of information effected by the hippocampus. It may be possible to describe the input/output relationship of the hippocampus as a series of algorithms. Such an approach may allow extrapolation of function between species, and in particular, to man. Alternatively, we may seek neural correlates of behaviour in the whole animal, by lesion, recording and stimulation in the hippocampus. Here we must be aware that the sensory environment in which cells are active,

and the behaviour which is impaired by lesion may be in no sense 'what the hippocampus is doing'; rather it is a task or an environment which calls into action the neural mechanisms available in that brain region. For instance, it is yet to be demonstrated whether the primary task of the hippocampus is in the production of a 'cognitive map' (O'Keefe and Nadel, 1978) - indeed there is much evidence, certainly in humans and rodents, that the neural networks of the hippocampus are involved in a more generalizable learning function. This of course will be an involvement shared with other regions of the brain.

References

Abraham, W.C. and McNaughton, N. (1984). Differences in synaptic transmission between medial and lateral components of the perforant path. Brain Res. 303, 251-260.

Adams, P.R. (1982). Voltage-dependent conductances of vertebrate neurones. TINS 5, 116-119.

Adams, P.R., Brown, D.A. and Halliwell, J.V. (1981). Cholinergic regulation of M-current in hippocampal pyramidal cells. J. Physiol. 317, 29-30P.

Alger, B.E. and Nicoll, R.A. (1979). GABA-mediated biphasic inhibitory responses in the hippocampus. Nature 281, 315-317.

Alger, B.E. and Nicoll, R.A. (1982). Pharmacalogical evidence for two kinds of GABA receptor on rat hippocampal pyramidal cells studied in vitro. J. Physiol. 328, 125-141.

Alkon, D.L. (1982). A biophysical basis for molluscan associative learning. In Conditioning, representation of involved neural functions (ed C.D. Woody), 147-170. Plenum press, NY.

Andersen, P. (1978). Long-lasting facilitation of synaptic transmission. In Functions of the septo-hippocampal system (eds K. Elliott and J. Whelan). Ciba Foundation, Elsevier.

Andersen, P., Bliss, T.V.P. and Skrede, K.K. (1971). Lamellar organization of hippocampal excitatory pathways. Exp. Brain Res. 13, 222-238.

Andersen, P., Dingledine, R., Gjerstad, L., Langmoen, I.A., and Mosfeldt Laursen, A. (1980). Two different responses of hippocampal pyramidal cells to application of gamma-amino butyric acid. J.Physiol. 305, 279-296.

Andersen, P., Eccles, J.C. and Loyning, Y. (1964a). Location of post-synaptic inhibitory synapses on hippocampal pyramids. J. Neurophysiol. 27, 592-607.

Andersen, P., Eccles, J.C. and Loyning, Y. (1964b). Pathway of post-synaptic inhibition in the hippocampus. J. Neurophysiol. 27, 608-619.

Andersen, P., Holmqvist, B. and Voorhoeve, P.E. (1966). Excitatory synapses on hippocampal apical dendrites activated by entorhinal stimulation. Acta Physiol. Scand. 66, 461-472.

Andersen, P., Sundberg, S.H., Sveen, O. and Wigstrom, H. (1977). Specific long-lasting potentiation of synaptic transmission in hippocampal slices. Nature 266, 736-737.

Amissiann, V.E. (1961). Microelectrode studies of the cerebral cortex. Int. Rev. Neurobiol. 3, 67-136.

Assaf, S.Y., Crunelli, V. and Kelly, J.S. (1981) Electrophysiology of the rat dentate gyrus. In The electrophysiology of isolated mammalian C.N.S. preparations. (eds G.A. Kerkut and H.V. Wheal). Academic press. NY and London.

Assaf, S.Y., Mason, S.T. and Miller, J.J. (1979). Noradrenergic modulation of neuronal transmission between the entorhinal cortex and the dentate gyrus of the rat. J. Physiol. 292, 52 P.

Baranyi, A. and Feher, O. (1981). Synaptic facilitation requires paired activation of convergent pathways in the neocortex. Nature 290, 413-415.

Barnes, C., McNaughton, B.L., Goddard, G., Douglas, R. and Academic, R. (1977). Circadian rhythm of synaptic excitability in rat and monkey central nervous system. Science 197, 91-92.

Barrett, J.N. and Crill, W.E. (1974). Specific membrane properties of cat motoneurones. J. Physiol. 239, 301-324.

Baudry, M., Arst, D., Oliver, M. and Lynch, G. (1981). Development of glutamate binding sites and their regulation by calcium in rat hippocampus. Brain Res. 227, 37-48.

Baudry, M., Kramer, K., Fagni, L., Recasens, M. and Lynch G. (1983). Classificaton and properties of acidic amino acid receptors in hippocampus. II. Biochemical studies using a sodium efflux assay. Mol. Pharmacol. 24, 222-228.

Baudry, M. and Lynch, G. (1979). Regulation of glutamate receptors by cations. Nature 282, 748-750.

Baudry, M. and Lynch, G. (1982). Possible mechanisms of L.T.P.: role of glutamate receptors. In Hippocampal L.T.P. mechanisms and implications for memory. (eds L.W. Swanson, T.J. Teyler and R.F. Thompson). Neuro. Res. Prog. Bull. 20, no. 5.

Baudry, M., Oliver, M., Creager, R., Wieraszko, A. and Lynch, G. (1980). Increase in glutamate receptors following repetative electrical stimulation in hippocampal slices. Life Sci. 27, 325-330.

Berger, T.W. (1984). Long-term potentiation of hippocampal synaptic transmission affects rate of behavioural learning. Science 224, 627-630.

Berger, T.W. and Thompson, R.F. (1978a). Neuronal plasticity in the limbic system during classical conditioning of the rabbit nictitating membrane response. I. The hippocampus. Brain Res. 145, 323-346.

Berger, T.W. and Thompson, R.F. (1978b). Identification of pyramidal cells as the critical elements in hippocampal neuronal plasticity during learning. Proc. Natl. Acad. Sci. 75, 1572-1576.

Bindman, L.J., Lippold, O.C.J. and Milne, A.R. (1982). A post-synaptic mechanism underlying long-lasting changes in the excitability of pyramidal tract neurones in the anaesthetized cat. In Conditioning, representation of involved neural functions (ed C.D. Woody), 171-178. Plenum press, NY.

Bindman, L.J. and Prince, C.A. (1984). Intracellular current stimulation producing prolonged changes in excitability and input resistance of cortical neurones in the anaesthetized rat. J. Physiol. In press, Cambridge meeting, 40P.

Blackstad, T.W. (1967). Cortical gray matter. A correlation of light and electron microscopic data. In The neuron. (ed H.Hyden). Elsevier. Amsterdam.

Blackstad, T.W., and Kjaerheim, A. (1961). Special axo-dendritic synapses in the hippocampal cortex. Electron and light microscopic studies on the e layer of mossy fibres. J. Comp. Neurol. 117, 133-159.

Bliss, T.V.P. and Gardner-Medwin, A. (1973). Long-lasting potentiation of synaptic transmission in the dentate area of unanaesthetized rabbit following stimulation of the perforant path. J. Physiol. 232, 357-374.

Bliss, T.V.P., Goddard, G.V. and Riives, M. (1983). Reduction of long-term potentiation in the dentate gyrus of the rat following selective depletion of monoamines. J. Physiol. 334, 475-491.

Bliss, T.V.P. and Lomo, T. (1973). Long-lasting potentiation of synaptic transmission in the dentate area of the anaesthetized rabbit following stimulation of the perforant path. J. Physiol. 232, 331-356.

Brindley, F.R. Jr (1974). Volume conductor theory. In Medical Physiology (ed V.B. Mountcastle). C.V. Mosby, Saint Louis.

Browning, M., Dunwiddie, T., Bennett, W., Gispen, W. and Lynch G. (1979). Synaptic phosphoproteins : specific changes after repetitive stimulation of the hippocampal slice. Science 203, 60-62.

Brunelli, M., Castellucci, V. and Kandel, E.R. (1976). Synaptic facilitation and behavioral sensitization in Aplysia: possible role of serotonin and cyclic AMP. Science 194, 1178-1181.

Burke, R.E. and Ten-Bruggencate, G.T. (1971). Electronic characteristics of motoneurones of varying size. J. Physiol. 212, 1-20.

Butters, N. and Cermak, L.S., (1980). Alcoholic Korsakoff's syndrome: an information processing approach to amnesia. Academic press, NY and London.

Buszaki, G. and Eidelberg, E. (1982). Convergence of associational and commissural pathways on CA1 pyramidal cells of the rat hippocampus. Brain Res. 237, 283-295.

Christensen, B.N. and Teubl, W.P. (1979). Estimates of cable parameters in lamprey spinal cord neurones. J. Physiol. 297, 299-318.

Cohen, P. (1982). The role of protein phosphorylation in neural and hormonal control of cellular activity. Nature 296, 613-620.

Collingridge, G.L., Kehl, S.J. and McLennan, H. (1983). Excitatory amino acid in synaptic transmission in the Schaffer collateral-commissural pathway of the rat hippocampus. J. Physiol. 334, 33-46.

Coombs, J.S., Curtis, D.R. and Eccles, J.C. (1957). The interpretation of spike potentials of motoneurones. J. Physiol. 139, 198-231.

Costa, E. (1981). The role of gamma-aminobutyric acid in the action of 1,4-benzodiazepines. In Towards understanding receptors. (ed J.W. Lamble). Current reviews in biomedicine 1. Elsevier.

Cowan, W.M., Gottlieb, D.I., Hendrickson, A.E., Price, J.L. and T.A. Woolsey. (1972). The autoradiographic demonstration of axonal connections in the central nervous system. Brain Res. 37, 21-51.

Cox, G. (1982). Neuropathological techniques. In Theory and practice of histological techniques (eds J.D. Bancroft and A. Stevens) 2nd ed. Churchill Livingstone. Edinburgh.

Crunelli, V., Forda, S. and Kelly, J.S. (1984). The reversal potential of excitatory amino acid action on granule cells of the rat dentate gyrus. J. Physiol. 351, 327-342.

Deadwyler, S.A., West, J.R., Cotman, C.W. and Lynch, G.S. (1975). A neurophysiological analysis of commissural projections to dentate gyrus of the rat. J. Neurophysiol. 38, 167-184.

Desmond, N.L. and Levy , W.B. (1981). Ultrastructural and numerical alterations in dendritic spines as a consequence of long-term potentiation. Anat. Rec. 199, 68A.

Desmond, N.L. and Levy, W.B. (1982). A quantitative anatomical study of the granule cell dendritic fields of the rat dentate gyrus using a novel probabilistic method. J. Comp. Neurol. 212, 131-145.

Dolphin, A.C., Errington, M.L. and Bliss, T.V.P. (1982). Long-term potentiation of the perforant path in vivo is associated with increased glutamate release. Nature 297, 496-498.

Douglas, R.M. (1978). Heterosynaptic control over synaptic modification in the dentate gyrus. Neurosci. Abstr. 4, 470.

Douglas, R.M. and Goddard, G.V. (1975). Long-lasting potentiation of the perforant path-granule cell synapses in the rat hippocampus. Brain Res. 86, 205-215.

Douglas, R.M., Goddard, G.V. and Riives, M. (1982). Inhibitory modulation of long-term potentiation: evidence for a post-synaptic locus of control. Brain Res. 240, 259-272.

Douglas, R.M., McNaughton, B.L. and Goddard, G.V. (1983). Commissural inhibition and facilitation of granule cell discharge in fascia dentata. J. Comp. Neurol. 219, 285-294.

Dunwiddie, T.V. and Lynch, G. (1979). The relationship between extracellular calcium concentrations and the induction of hippocampal long-term potentiation. Brain Res. 169, 103-110.

Dunwiddie, T.V., Madison, D. and Lynch, G. (1978). Synaptic transmission is required for initiation of Long-term potentiation. Brain Res. 150, 413-417.

Durand, D., Carlen, C.L., Gurevich, N., Ho, A. and Kunov, H. (1983). Electrotonic parameters of rat dentate granule cells, measured using short current pulses

and HRP staining. J. Neurophysiol. 50, 1080-1097.

Eccles, J.C. (1983). Calcium in long-term potentiation as a model for memory. Neuroscience 10, 1071-1081.

Edinger, L. (1908). Voriesungen uber den ban der nervosen zentralorgane, Bd. 2, Vergieichende Anatomie des Gehirns, Leipzig.

Edwards, D.H. and Mulloney, B. (1984). Compartmental models of electrotonic structure and synaptic integration in an identified neurone. J. Physiol. 348, 89-113.

Fifkova, E. and Van Harreveld, A. (1975). Long-lasting morphological changes in dendritic spines of dentate granule cells following stimulation of the entorhinal area. J. Neurocytol. 6, 211-230.

Finn, R.C., Browning, M. and Lynch, G. (1980). Trifuoperazine inhibits hippocampal long-term potentiation and the phosphorylation of a 40000 dalton protein. Neurosci. Lett. 19, 103-108.

Fox, S.E. and Ranck, J.B. Jr. (1975). Localization and identification of theta and complex-spike cells in the dorsal hippocampal formation of rats. Exp. Neurol. 49, 299-313.

Fricke, R.A. and Prince, D.A. (1984). Electrophysiology of dentate gyrus granule cells. J. Neurophysiol. 51, 192-209.

Gloor, P., Vera, C.L. and Sperti, L. (1963). Configuration and laminar analysis of the "resting" potential gradient, of the main-transient response to perforant path, fimbrial and mossy fibre volleys and of "spontaneous" activity. Electroenceph. Clin. Neurophysiol. 15, 353-378.

Gottlieb, D.I. and Cowan, W.M. (1972). Evidence for a temporal factor in the occupation of available synaptic sites during the development of the dentate gyrus. Brain Res. 41, 452-456.

Gottlieb, D.I. and Cowan, W.M. (1973). Autoradiographic studies of the commissural and ipsilateral association connections of the hippocampus and dentate gyrus of the rat. I. The commissural connections. J. Comp. Neurol. 149, 393-422.

Gray, E.G. (1969). Electron microscopy of excitatory and inhibitory synapses: a brief review. In Mechanisms of synaptic transmission (eds K.Akert and P.G. Waser). Prog. Brain Res. 31, 141-155. Elsevier, Amsterdam.

Greengard, P. (1976). Possible role for cyclic nucleotides and phosphorylated membrane proteins in postsynaptic actions of transmitters. Nature 260, 101-108.

Haas, H.L. and Rose, G. (1982). Long-term potentiation of excitatory synaptic transmission in the rat hippocampus: the role of inhibitory processes. J. Physiol. 329, 541-552.

Halgren, E., Squires, N.K., Wilson, C.L., Rohrbaugh, J.W., Babb, T.L. and Crandall, P.H. (1980). Endogenous potentials generated in the human hippocampal formation and amygdala by infrequent events. Science 210, 803-805.

Halgren, E., Wilson, C.L., Squires, N.K., Engel, J., Walter, R.D., and Crandall, P.H. (1983). Dynamics of the hippocampal contribution to memory: stimulation and recording studies in humans. In Neurobiology of the hippocampus (ed W.Seifert). Academic Press, London.

Handelmann, G.E. and Olton, D.S. (1981). Spatial memory following damage to hippocampal CA3 pyramidal cells with kainic acid: impairment and recovery of function. Brain Res. 217, 41-58.

Harley, C. and Neuman, R. (1980). Iontophoretic application of adrenergic agonists potentiates angular bundle evoked field potentials in the dentate gyrus. Neuroscience abst. 152.1, 447.

Harris, E.W., Ganong, A.H. and Cotman, C.W. (1984). Long-term potentiation in the hippocampus involves

activation of N-methyl-D-aspartate receptors. Brain Res. in press.

Harris, E.W., Lasher, S.S. and Sherwood, O. (1978). Habituation like decrements in transmission along the normal and lesion-induced temporo-dentate pathways in the rat. Brain Res. 151, 623-631.

Hebb, D.O. (1949). The organization of behavior. J.Wiley, NY.

Herrling, P.L. (1981) The membrane potential of cat hippocampal neurons recorded in vivo displays four different reaction-mechanisms to iontophoretically applied transmitter agonists. Brain Res. 212, 331-343.

Hirst, G.D.S., Redman, S.J. and Wong, K. (1981). Post-tetanic potentiation and facilitation of synaptic potentials evoked in cat spinal motoneurones. J. Physiol. 321, 97-109.

Hjorth-Simonsen, A. (1970). Fink-Heimer silver impregnation of degenerating axons and terminals in mounted cryostat sections of fresh and fixed brains. Stain Techn. 45, 199-204.

Hjorth-Simonsen, A. (1972). Projection of the lateral part of the entorhinal area to the hippocampus and fascia dentate. J. Comp. Neurol. 146, 219-232.

Hjorth-Simonsen, A. (1973). Some intrinsic connections of the hippocampus in the rat: an experimental analysis. J. Comp. Neurol. 147, 145-162.

Hjorth-Simonsen, A. and June, B. (1972). Origin and termination of the hippocampal perforant path in the rat studied by silver impregnation. J. Comp. Neurol. 144, 215-232.

Hjorth-Simonsen, A. and Zimmer, J. (1975). Crossed pathways from the entorhinal area to the fascia dentata. I. In normal rabbits. J. Comp. Neurol. 161, 57-70.

Hodgkin, A.L. (1938). The subthreshold potentials in

a crustacean nerve fibre. Proc. R. Soc. B 126, 87-121.

Hodgkin, A.L. and Rushton, W.A.H. (1946). The electrical constants of a crustacean nerve fibre. Proc. R. Soc. B 133, 444-479.

Hubbard, J.I., Llinas, R. and Quastel, D.M.J. (1969). Electrophysiological analysis of synaptic transmission. Edward Arnold. London.

Iansek, R. and Redman, S.J. (1973). An analysis of the cable properties of spinal motoneurones using a brief intracellular current pulse. J. Physiol. 284, 613-636.

Jack, J.J.B., Noble, D and Tsien, R.W. (1983). Electric current flow in excitable cells. 2nd edition, OUP.

Jack, J.J.B. and Redman, S.J. (1971). An electrical description of the motoneurone, and its application to the analysis of synaptic potentials. J. Physiol. 215, 321-352.

Jack, J.J.B., Redman, S.J. and Wong, K. (1981). The components of synaptic potentials evoked in cat spinal motoneurones by impulses in single group Ia Afferents. J. Physiol. 321, 65-96.

Jefferys, J.G.R. (1979). Initiation and spread of action potentials in granule cells maintained in vitro in slices of guinea-pig hippocampus. J. Physiol. 289, 375-388.

Kluver, H. and Bucy, P.C., (1939). Preliminary analysis of functions of the temporal lobes in monkeys. Arch. Neurol. Psychiat. 38, 725-743.

Koch, C. and Poggio, T. (1983). Electrical properties of dendritic spines. TINS 6, 80-83.

Krnjevic, K., Pumain, R. and Renaud, L. (1971). The mechanism of excitation by acetylcholine in the cerebral cortex. J. Physiol. 215, 247-268.

Kujtan, P.W. and Carlen, P.L. (1982). Phencyclidine effects measured intracellularly in hippocampal CA1 cells are dose dependent. Neurosci. Abst. 8, 102.1.

Laatsch R.H. and Cowan, W.M. (1966). Electron microscopic studies of the dentata gyrus of the rat. I. Normal structure with special reference to synaptic organization. J. Comp. Neurol. 128, 359-396.

Lacey, M.G. and Henderson, G. (1983). Antagonism of N-methyl-D-aspartic acid excitation of rat hippocampal pyramidal neurons in vitro by phencyclidine applied in known concentrations. Soc. Neurosci. Abstr. 9, 260.

La Fara, R.L. (1973). Computer methods for science and engineering. Hayden Book company. New Jersey.

Laroche, S. and Bloch, V. (1981). Conditioning of hippocampal cells and long-term potentiation: an approach to mechanisms of post-trial memory facilitation. In Biological basis of learning and memory formation. IBRO monograph series, vol. 9, (eds C. Ajmone-Marson and H. Matthies) Raven, London.

Laurberg, S. (1979). Commissural and intrinsic connections of the rat hippocampus. J. Comp. Neurol. 184, 685-708.

Lee, K., Oliver, M., Schottler, F. and Lynch, G. (1981). Electron microscopic studies of brain slices: the effects of high frequency stimulation on dendritic ultastructure. In The electrophysiology of isolated mammalian CNS preparations (eds G.A. Kerkut and H.N. Wheal). Academic press, NY.

Lee, K., Schottler, F., Oliver, M. and Lynch, G. (1980). Brief bursts of high frequency stimulation produce two types of structural change in rat hippocampus. J. Neurophysiol. 44, 247-258.

Levy , W.B. and Steward, O. (1979). Synapses as associative memory elements in the hippocampal formation. Brain Res. 175, 233-245.

Linden, R.J. and Snow, H.M. (1974). The inotropic state of the heart. In Recent advances in physiology 9

(ed R.J. Linden).

Lomo, T. (1966). Frequency potentiation of excitatory synaptic activity in the dentate area of the hippocampal formation. Acta physiol. scand. 68, suppl. 277, 128.

Lomo, T. (1968). Nature and distribution of inhibition in a simple cortex (dentate area). Acta Physiol. Scand. 74, 8-9A.

Lomo, T. (1969). Synaptic mechanisms and organization of the dentate area of the hippocampal formation. Thesis, University of Oslo, Norway.

Lomo, T. (1971a). Patterns of activation in a monosynaptic cortical pathway: the perforant path input to the dentate area of the hippocampal formation. Exp. Brain Res. 12, 18-45.

Lomo, T. (1971b). Potentiation of monosynaptic epsp's in the perforant path - dentate granule cell synapse. Exp. Brain Res. 12, 46-63.

Lorente de No, R. (1939). Transmission of impulses through cranial motor nuclei. J. Neurophysiol. 2, 402-464.

Lorente de No, R. (1947). A study of nerve physiology. Studies from the Rockefeller Institute, Vol. 132, Ch. 16.

Loy, R., Koziell, D.A., Lindsey, J.D. and Moore, R.Y. (1980). Noradrenergic innervation of the adult rat hippocampal formation. J. Comp. Neurol. 189, 699-710.

Lynch, G.S. and Baudry, M. (1984). The biochemistry of memory : a new and specific hypothesis. Science 224, 1057-1063.

Lynch, G.S., Dunwiddie, T. and Gribkoff, V. (1977). Heterosynaptic depression: a postsynaptic correlate of long-term potentiation. Nature 266, 737-739.

Lynch, G.S., Gribkoff, V.K. and Deadwyler, S.A. (1976). Long term potentiation by a reduction in dendritic responsiveness to glutamic acid. Nature 263, 151-153.

Lynch, G.S., Kelso, S., Barrionuevo, G. and Schottler, F. (1983). Intracellular injections of EGTA block the induction of long-term potentiation. Nature 305, 719-721.

Mahut, H., Moss, M. and Zola-Morgan, S. (1981). Retention deficits after combined amygdalo-hippocampal and selective hippocampal resections in the monkey. Neuropsychologia. 19, 201-225.

Mahut, H., Zola-Morgan, S. and Moss, M. (1982). Hippocampal resections impair associative learning and recognition memory in the monkey. J. Neurosci. 2, 1214-1229.

Mair, W.G.P., Warrington, E.K. and Weiskrantz, L. (1979). Memory disorder in Korsakoff's psychosis. A neuropathological and neuropsychological investigation of two cases. Brain. 102, 749-783.

Matthews, D.A., Cotman, C. and Lynch G. (1976). An electronmicroscopic study of lesion induced synaptogenesis in the dentate gyrus of the adult rat. I. Magnitude and time course of degeneration. Brain Res. 115, 1-21.

McCarthy, G. (1984). Intra-cerebral evoked potential recording in man. Brain research association lecture, 25th May, University of St.Andrews.

McLean, P. (1952). Some psychiatric implications of physiological studies on the frontotemporal portions of limbic system (visceral brain). Electroenceph. Clin. Neurophysiol. 4, 407-418.

McNaughton, B.L. (1980). Evidence for two physiologically distinct perforant pathways to the fascia dentata. Brain Res. 199, 1-19.

McNaughton, B.L. (1982). Long-term synaptic enhancement and short-term potentiation in rat fascia dentata

act through different mechanisms. J. Physiol. 324, 249-262.

McNaughton, B.L. (1983). Activity dependent modulation of hippocampal synaptic efficacy: some implications for memory processes. In Neurobiology of the hippocampus. (ed. W. Seifert). Academic press, London.

McNaughton, B.L. and Barnes, C.A. (1977). Physiological identification and analysis of dentate granule cell responses to stimulation of the medial and lateral perforant pathways in the rat. J. Comp. Neurol. 175, 439-454.

McNaughton, B.L., Barnes, C.A. and Andersen, P. (1981). Synaptic efficacy and epsp summation in granule cell of rat fascia dentata studied in vitro. J. Neurophysiol. 46, 952-966.

McNaughton, B.L., Douglas, R.M. and Goddard, G.V. (1978). Synaptic enhancement in fascia dentata: cooperativity among coactive afferents. Brain Res. 157, 277-293.

Milner, B. (1966). Amnesia following operation on the temporal lobes. In Amnesia (eds C.W.M. Whitty and O.L. Zangwill). Butterworths, London.

Milner, B. (1972). Disorders of learning and memory after temporal lobe lesions in man. Clin. Neurosurg. 19, 421-446.

Morris, R.G.M., Garrard, P. and Woodhouse, I.Q. (1980). Fornix lesions disrupt location learning by the rat. Behav. Brain Res. 2, 266.

Morris, R.G.M., Garrard, P., Rawlins, J.N.P. and O'Keefe, J. (1982). Place navigation impared in rats with hippocampal lesions. Nature. 297, 681-683.

Nadler, J.V., Vaca, K.W., White, F.W., Lynch, G.S. and Cotman, C.W. (1976). Aspartate and glutamate as possible transmitters of excitatory hippocampal afferents. Nature. 260, 538-540.

Nafstad, P.H.J. (1967). An electronmicroscope study of the termination of the perforant path fibres in the hippocampus and the fascia dentata. Z. Zellforsch. 76, 532-542.

Nicholson, C. and Freeman, J.A. (1975). Theory of current source-density analysis and determination of conductivity tensor for anuran cerebellum. J. Neurophysiol. 38, 356-368.

Nicholson, C. and Llinas, R. (1971). Field potentials in the alligator cerebellum and theory of their relationship to Purkinje cell dendritic spikes. J. Neurophysiol. 34, 509-531.

O'Keefe, J. (1976). Place units in the hippocampus of the freely moving rat. Exp. Neurol. 51, 78-109.

O'Keefe, J. and Nadel, L. (1978). The hippocampus as a cognitive map. Clarendon press, Oxford.

Olpe, H.R., Barrionuevo, G, and Lynch, G. (1982). Vincamine: a psychogeriatric agent blocking synaptic potentiation in hippocampus. Life Science 31, 1947-1953.

Olton, D.S. (1983). Memory functions and the hippocampus. In Neurobiology of the hippocampus (ed W.Seifert). Academic press, London.

Pandya, D.N., Van Hoesen, G.W. and Mesulam, M.-M. (1981). Efferent connections of the cingulate gyrus in the rhesus monkey. Exp. Brain Res. 42, 319-330

Papez, J.W. (1937). A proposed mechanism of emotion. Arch. Neurol. Psychiat. 38, 725-743.

Perkel, D.H. and Mulloney, B. (1978). Electrotonic properties of neurones: steady-state compartmental model. J. Neurophysiol. 41, 621-639.

Perkel, D.H., Mulloney, B. and Budelli, R.W. (1981). Quantitative methods for predicting neuronal behavior. Neuroscience 6, 823-837.

Raisman, G., Cowan, W.M. and Powell, T.P.S. (1965). The extrinsic afferent, commissural and association fibres of the hippocampus. Brain 88, 963-996.

Rall, W. (1959). Branching dendritic trees and motoneuron membrane resistivity. Exp. Neurol. 1, 491-527.

Rall, W. (1962). Theory of physiological properties of dendrites. Ann. N.Y. Acad. Sci. 96, 1071-1092.

Rall, W. (1970). Cable properties of dendrites and effects of synaptic location. In Excitatory synaptic mechanisms. (eds P. Andersen and J.K.S. Jansen). Universiteforlaget, Oslo.

Rall, W., Burke, R.E., Smith, T.G., Nelson, P.G. and Frank, K. (1967). Dendritic location of synapses and possible mechanisms for the monosynaptic epsp in motoneurons. J. Neurophysiol. 30, 1169-1193.

Rall, W. and Shepherd, G.M. (1968). Theoretical reconstruction of field potentials and dendro-dendritic synaptic interactions in olfactory bulb. J. Neurophysiol. 31, 884-915.

Ranck, J.B. Jr (1973). Studies on single neurons in dorsal hippocampal formation and septum in unrestrained rats. I. Behavioural correlates and firing repertoires. Exp. Neurol. 41, 461-555.

Redman, S. and Walmsley, B. (1983). The time course of synaptic potentials evoked in cat spinal motoneurones at identified group Ia synapses. J. Physiol. 343, 117-133.

Rose, G. (1983) Physiological and behavioral characteristics of dentate granule cells. In Neurobiology of the hippocampus (ed W.Seifert). Academic press. London.

Schwartzkroin, P.A. and Andersen, P. (1978). Discussion in Functions of the septo-hippocampal system. (eds K. Elliott and J. Whelan). Ciba Foundation, Elsivier.

Sastry, B.R. and Goh, J.W. (1984). Long-lasting potentiation in hippocampus is not due to an increase in glutamate receptors. Life Sciences 34, 1497-1501.

Scoville, W.B. and Milner, B. (1957). Loss of recent memory after bilateral hippocampal lesions. J. Neurol. Neurosurg. Psychiat. 20, 11-21.

Segal, M. (1980). The action of serotonin in the rat hippocampal slice preparation. J. Physiol. 303, 423-439.

Segal, M. (1981). The action of norepinephrine in the rat hippocampus: intracellular studies in the slice preparation. Brain Res. 206, 107-128.

Segal, M. and Bloom, F.E. (1974a). The action of norepinephrine in the rat hippocampus. I. Iontophoretic studies. Brain Res. 72, 79-97.

Segal, M. and Bloom, F.E. (1974b). The action of norepinephrine in the rat hippocampus. II. Activation of the input pathway. Brain Res. 72, 98-114.

Seress, L. and Ribak, C.E. (1983). Five types of basket cell in the hippocampal dentate gyrus: a combined Golgi and electron microscopic study. J. Neurocytol. 12, 577-597.

Shimahara, T. and Tauc, L. (1977). Cyclic AMP induced by serotonin modulates the activity of an identified synapses in Aplysia by facilitating the active permeability to calcium. Brain Res. 127, 168-172.

Siegelbaum, S.A., Camardo, J.S. and Kandel, E.R. (1982). Serotonin and cyclic AMP close single K channels in Aplysia sensory neurones. Nature 299, 413-417.

Skrede, K.K. and Malthe-Sorenssen (1981). Increased resting and evoked release of transmitter following repetitive electrical tetanization in hippocampus: a biochemical correlate to long-lasting synaptic potentiation. Brain Res. 208, 436-441.

Squire, L.R. (1982). The neuropsychology of human memory. Ann. Rev. Neurosci. 5, 241-273.

Squire, L.R. (1983). The hippocampus and the neuropsychology of memory. In Neurobiology of the hippocampus (ed W.Seifert). Academic press, London.

Steward, O. (1976). Topographic organization of the projections from the entorhinal area to the hippocampal formation of the rat. J. Comp. Neurol. 167, 285-314.

Stone, T.W., Taylor, D.A. and Bloom, F.E. (1975). Cyclic AMP and cyclic GMP may mediate opposite neuronal responses in the rat cerebral cortex. Science 187, 845-847.

Storm-Mathisen, J. (1977). Localization of transmitter candidates in the brain. Prog. Neurobiol. 8, 119-181.

Storm-Mathisen, J., Leknes, A.K., Bore, A.T., Vaaland, J.L., Edminson, P., Haug, F.-M.S. and Ottersen, O.P. (1983). First visualization of glutamate and GABA in neurones in immunocytochemistry. Nature 301, 517-520.

Stringer, J.L., Hackett, J.T. and Guyenet, P.G. (1984). Long-term potentiation blocked by phencyclidine and cyclazocine in vitro. European J. Pharmacol. 98, 381-388.

Swanson, L.W. (1982). Normal hippocampal circuitry. In Hippocampal LTP: mechanisms and implications for memory. (eds. L.W. Swanson, T.J. Teyler, R.F. Thompson) Neuro. Res. Prog. Bull. 20, no. 5.

Swanson, L.W. (1983). The hippocampus and the concept of the limbic system. In Neurobiology of the hippocampus (ed W.Seifert). Academic press, London.

Swanson, L.W. and Cowan, W.M. (1977). An autoradiographic study of the organization of the efferent connections of the hippocampal formation in the rat. J. Comp. Neurol. 172, 49-84.

Swanson, L.W., Sawchenko, P.E. and Cowan, W.M. (1981). Evidence for collateral projections by neurons in Ammon's horn, the dentate gyrus and the subiculum: a multiple retrograde labelling study in the rat. J. Neurosci. 1, 548-559.

Swanson, L.W., Wyss, J.M. and Cowan, W.M. (1978). An autoradiographic study of the organization of intrahippocampal association pathways in the rat. J. Comp. Neurol. 181, 681-716.

Talland, G.A. (1965). Deranged memory. Academic press, NY and London.

Terzuolo, C.A. and Araki, T. (1961). An analysis of intra-versus extracellular potential changes associated with activity of single spinal motoneurones. Ann. N.Y. Acad. 94, 547-558.

Teyler, T.J., Goddard, G.V., Lynch, G. and Andersen, P. (1982). Properties and mechanisms of L.T.P. In Hippocampal L.T.P. mechanisms and implications for memory (eds. L.W. Swanson, T.J. Teyler and R.F. Thompson). Neuro. Res. Prog. Bull. 20, no.5.

Toffano, G., Guidotti, A. and Costa, E. (1978). Purification of an endogenous protein inhibitor of the high affinity binding of gama-aminobutyric acid to synaptic membranes of the rat brain. Proc. Natl. Acad. Sci. U.S.A. 75, 4024-4028.

Thompson, R.F. (1983). Neuronal substrates of simple associative learning: classical conditioning. TINS 6, 270-275.

Thompson, R.F., Berger, T.W., Cegavske, C.F., Patterson, M.M., Roemer, R.A., Teyler, T.J. and Young, R.A. (1976). The search for the engram. Ammer. Psychol. 31, 209-227.

Tielen, A.M., Lopes da Silva, F.H. and Mollevanger, W.J. (1981). Differential conduction velocities in the perforant path fibres in guinea pig. Exp. Brain Res. 42, 231-233.

Turner, B.H., Mishkin, M. and Knapp, M. (1980).

Organization of the amygdalo- petal projections from modality-specific cortical association areas in the monkey. J. Comp. Neurol. 191, 515-549.

Turner, D.A. and Schwartzkroin, P.A. (1980). Steady-state electrotonic analysis of intracellularly stained hippocampal neurons. J. Neurophysiol. 44, 184-199.

Turner, R.W., Baimbridge, K.G. and Miller, J.J. (1982). Calcium-induced long-term potentiation in the hippocampus. Neuroscience 7, 1411-1416.

Vanderwolf, C.H. (1969). Hippocampal Electrical activity and voluntary movement in the rat. Electroenceph. Clin. Neurophysiol. 26, 407-418.

Victor, M., Adams, R.D. and Collins, G.H. (1971). The Wernicke-Korsakoff Syndrome. F.A. Davis, Philadelphia, Pennsylvania.

Vincent, J.P., Kartalovski, B., Geneste, P., Kamenka, J.M. and Lazdunski, M. (1979). Interaction of phencyclidine with a specific receptor in rat brain membranes. Proc. Natl. Acad. Sci. U.S.A. 76, 4678-4682.

Whishaw, I.Q. and Vanderwolf, C.H. (1973). Hippocampal EEG and behavior : changes in the amplitude and frequency of RSA (theta rhythm) associated with spontaneous and learned movement patterns in rats and cats. Behav. Biol. 8, 461-484.

White, W.F., Nadler, J.V., Hamberger, A., Cotman, C.W. and Cummins, J.T. (1977). Glutamate as transmitter of hippocampal perforant path. Nature 270, 356-357.

Wieraszko, A. (1983) Glutamic and aspartic acid as putative neurotransmitters: release and uptake studies on hippocampal slices. In Neurobiology of the hippocampus (ed W.Seifert) Academic press, London.

Winson, J. and Abzug, C. (1978). Neuronal transmission through hippocampal pathways dependent on behavior. J. Neurophysiol. 41, 716-732.

Wigstrom, H. and Gustafsson, B. (1983). Facilitated induction of hippocampal long-lasting potentiation during blockade of inhibition. Nature 301, 603-604.

Wyss, J.M. (1981). An autoradiographic study of the efferent connections of the entorhinal cortex in the rat. J. Comp. Neurol. 199, 495-512.

Yamamoto, C. and Chujo, T. (1978). Long term potentiation in thin hippocampal sections studied by intracellular and extracellular recordings. Exp. Neurol. 58, 242-250.

Young, J.Z. (1938). The evolution of the nervous system and the relationship of the organism and the environment. In Evolution. Essays presented to E.S. Goodrich (ed G.R. de Beer). Clarendon Press, Oxford.

Zimmerman, H., Stadler, H. and Whittaker, V.P. (1981). Structure and function of cholinergic synaptic vesicles. In Chemical neurotransmission 75 years. (eds L. Stjarne, P. Hedqvist, H. Lagercrantz and A. Wennmalm). Academic press, London.

Zukin, S.R. and Zukin, R.S. (1979). Specific H-phencyclidine binding in rat central nervous system. Proc. Natl. Acad. Sci. 76, 5372-5376.